

---

8-2014

## Multiple Myeloma And Its Treatment Alter Peripheral Nervous System Structure And Function

Alyssa K. Kosturakis

Follow this and additional works at: [https://digitalcommons.library.tmc.edu/utgsbs\\_dissertations](https://digitalcommons.library.tmc.edu/utgsbs_dissertations)



Part of the [Medical Neurobiology Commons](#)

---

### Recommended Citation

Kosturakis, Alyssa K., "Multiple Myeloma And Its Treatment Alter Peripheral Nervous System Structure And Function" (2014). *Dissertations and Theses (Open Access)*. 475.  
[https://digitalcommons.library.tmc.edu/utgsbs\\_dissertations/475](https://digitalcommons.library.tmc.edu/utgsbs_dissertations/475)

This Thesis (MS) is brought to you for free and open access by the MD Anderson UTHealth Houston Graduate School at DigitalCommons@TMC. It has been accepted for inclusion in Dissertations and Theses (Open Access) by an authorized administrator of DigitalCommons@TMC. For more information, please contact [digcommons@library.tmc.edu](mailto:digcommons@library.tmc.edu).

**MULTIPLE MYELOMA AND ITS TREATMENT ALTER PERIPHERAL NERVOUS  
SYSTEM STRUCTURE AND FUNCTION**

by

Alyssa Katarina Kosturakis, BA

APPROVED:

---

Patrick M. Dougherty, PhD  
Supervisory Professor

---

James M. Reuben, PhD, MBA

---

Edgar T. Walters, PhD

---

M. Neal Waxham, PhD

---

Jack C. Waymire, PhD

APPROVED:

---

Dean, the University of Texas  
Graduate School of Biomedical Sciences at Houston

**MULTIPLE MYELOMA AND ITS TREATMENT ALTER PERIPHERAL NERVOUS  
SYSTEM STRUCTURE AND FUNCTION**

A

THESIS

Presented to the Faculty of  
The University of Texas  
Health Science Center at Houston  
and  
The University of Texas  
M.D. Anderson Cancer Center  
Graduate School of Biomedical Sciences  
in Partial Fulfillment

of the Requirements

for the Degree of

MASTER OF SCIENCE

by

Alyssa Katarina Kosturakis, BA  
Houston, Texas

August, 2014

## **Dedication**

To my mother, Irene, for her continual support in all aspects of my life. Her constant curiosity and love of learning has inspired my academic pursuits and wish to be a life-long learner.



## **Acknowledgements**

First and foremost, I would like to acknowledge my advisor, Dr. Patrick M. Dougherty, who has forever changed the course of my life and career. It is through his kindness, mentorship, and encouragement that I have had the opportunity to pursue this degree. His love of neuroscience and research is infectious and has inspired in me an immense appreciation for the field and an admiration of those who work in it. I aspire to one day be as knowledgeable and as valuable a researcher as he is.

I would like to thank my committee members, Dr. Edgar T. Walters, Dr. Neal M. Waxham, Dr. Jack C. Waymire, and Dr. James M. Reuben for their service on my committee. I appreciate the time they have spent providing advice and shaping my project.

I am incredibly grateful to my postdoctoral mentor, Dr. Courtney Donica. She has been a true mentor and has spent a significant amount of time discussing my project and providing her input. It is thanks to her encouragement and willingness to help that I have been able to complete this thesis. Special thanks also goes to postdoctoral fellows, Dr. Stephanie Puig and Dr. Martin Smith for their helpful feedback regarding my project, providing intellectually-stimulating conversation and pushing me to question my assumptions.

I would also like to acknowledge the past and present postdoctoral fellows and instructors in my laboratory who have taken their time to train me despite having their own projects. These include Dr. Jessica Boyette-Davis, Dr. Haijun Zhang, Dr. Yan Li, Dr. Hongmei Zhang and Dr. Seo Yeon Yoon.

Jun Ying in the Department of Biostatistics at UT MD Anderson Cancer Center performed a separate analysis, which was referenced in Appendix A and deserves

recognition. I would also like to thank post-doctoral fellow, Dr. Robyn Crooke in the Walters lab for her statistical expertise and guidance.

Last, but not least, I would like to thank my family and friends for their unending support throughout this process.

# **MULTIPLE MYELOMA AND ITS TREATMENT ALTER PERIPHERAL NERVOUS SYSTEM STRUCTURE AND FUNCTION**

Alyssa Katarina Kosturakis, BA

Supervisory Professor: Patrick M. Dougherty, PhD

Peripheral neuropathy is among the most deleterious side effects of frontline chemotherapeutics used to treat prevalent cancers. Chemotherapy-induced peripheral neuropathy (CIPN) refers to the collection of symptoms (e.g. pain, paresthesias and dysesthesias) that develop in distal, glabrous (non-hairy) skin of 20 to 100% of patients treated with chemotherapy. Peripheral neuropathy negatively impacts quality of life in cancer patients and survivors, is refractory to treatment, and is the impetus for dose-reduction and/or cessation of chemotherapy, thereby limiting treatment. Proteasome inhibitor, bortezomib (Velcade<sup>®</sup>) is an effective treatment of multiple myeloma (MM), but often provokes the development of small fiber, sensory, distal neuropathy in patients. MM is caused by malignancy of plasma cells, which indirectly compromises multiple organ systems. Therefore, the contribution of underlying disease versus chemotherapeutic treatment on the development of sensory deficits in MM patients remains unclear.

This study determined the incidence of subclinical neuropathy in multiple myeloma patients prior to receiving chemotherapy. MM patients underwent quantitative sensory testing (QST), which is a non-invasive battery of tests that provides information about the function of discrete sensory fiber types. Patients exhibited a high incidence (>80%) of one or more subclinical QST deficits, including

mechanical stimulation, fine tactile discrimination, and warmth detection thresholds, compared to healthy volunteers. QST also demonstrated enhanced cold pain, sensorimotor deficits, and higher overall neuropathy scores in MM patients. The peripheral innervation of the skin was visualized with non-invasive confocal microscopy and revealed a reduction in the density of touch receptors (Meissner's corpuscles) that negatively correlated with performance on the Bumps detection task. Therefore, MM patients commonly present with sensory and sensorimotor deficits prior to undergoing treatment, and these deficits appear to be due to disease-related decreases in peripheral innervation density.

This study subsequently evaluated the efficacy of minocycline in the prevention of treatment-emergent bortezomib-induced peripheral neuropathy in a double-blind, placebo-controlled, randomized phase I clinical trial by assessing QST and patient reports. The placebo group did not show changes in sensory thresholds after bortezomib treatment, making it difficult to assess the impact of minocycline on sensory deficits. The minocycline group reported lower rates of tingling that approached statistical significance ( $P=0.11$ ). Although statistical significance was not reached in patient reports of symptoms, several limitations inherent in the study design and data collection likely impacted the result. Therefore, the use of minocycline to prevent chemotherapy-induced peripheral neuropathy warrants further investigation in a follow-up trial.

## Table of Contents

Approvals.....	i
Title Page.....	ii
Dedication.....	iii
Acknowledgements.....	iv
Abstract.....	vi
Table of Contents .....	viii
List of Figures .....	xi
List of Tables .....	xiii
Abbreviations.....	xiv
1. Introduction.....	1
1.1. Peripheral Nervous System.....	2
1.1.1 Structure and Conduction Velocity of Primary Afferents .....	3
1.1.2 Modality Specificity of Primary Afferents .....	4
1.1.3 Threshold for Activation and Adaptation of Primary Afferents.....	4
1.1.4 Receptor Expression and Cell Content of Primary Afferents.....	5
1.1.5 Skin Morphology and Sensory Transduction.....	6
1.1.6 Mechanosensation .....	9
1.1.7 Thermosensation .....	13
1.2. Pain, Pain Processing, and Neuropathic Pain .....	14
1.2.1 Pain Classifications and Definitions .....	14
1.2.2 Neuropathic Pain.....	15
1.2.3 Peripheral Mechanisms of Neuropathic Pain .....	16
1.2.4 Central Mechanisms of Neuropathic Pain .....	17
1.2.5 Inflammatory Mechanisms of Neuropathic Pain .....	18
1.3. Multiple Myeloma Pathophysiology, Diagnosis and Staging.....	20
1.4. Treatment of Multiple Myeloma .....	25
1.4.1 Bortezomib: Clinical Overview.....	25
1.4.2 Bortezomib-Induced Neuropathy: Pre-Clinical Studies .....	27
1.4.3 Other Therapies .....	28
1.4.4 Overview CIPN Symptoms and Grading Scales .....	28
1.5. Hypothesis and Specific Aims .....	31
2. Subclinical peripheral neuropathy in multiple myeloma patients prior to chemotherapy is correlated with decreased fingertip innervation density .....	34
2.1. Introduction.....	34

2.2.	Subjects and Methods .....	36
2.2.1	Patients and Volunteers .....	36
2.2.2	Quantitative Sensory Analysis.....	36
2.2.3	Touch Detection Thresholds and Grooved Pegboard Test .....	37
2.2.4	Sharpness Detection Threshold .....	40
2.2.5	Heat and Cold Detection Thresholds .....	42
2.2.6	Skin Temperature.....	42
2.2.7	Imaging and Meissner’s Corpuscle Quantification .....	44
2.2.8	Statistical Analysis .....	46
2.3.	Results .....	46
2.3.1	Study group.....	46
2.3.2	Touch Detection Thresholds and Grooved Pegboard Times.....	48
2.3.3	Sharpness Detection Thresholds .....	48
2.3.4	Skin Temperature and Thermal Detection Thresholds.....	50
2.3.5	General Neuropathy Score.....	52
2.3.6	Quantification of Meissner’s Corpuscles .....	54
2.4.	Discussion .....	56
3.	Preliminary analysis of a phase I study of minocycline vs. placebo to prevent treatment-induced neuropathy in multiple myeloma .....	61
3.1.	Introduction.....	61
3.2.	Subjects and Methods .....	64
3.2.1	Study Site.....	64
3.2.2	Study Design.....	64
3.2.3	Randomization and Blinding.....	64
3.2.4	Inclusion and Exclusion Criteria .....	65
3.2.5	Protocol Deviations .....	65
3.2.6	Clinical Outcome Measures and Methods.....	66
3.2.7	Safety and Tolerability.....	66
3.2.8	Statistics.....	66
3.2.9	Ethics .....	67
3.3.	Results .....	67
3.3.1	Patient Population Analyzed .....	67
3.3.2	Analysis #1 .....	69
3.3.2.1	Patient Demographics .....	69
3.3.2.2	Touch Detection .....	72

3.3.2.3	Peg Board Completion, Sharpness Detection and Skin Temperature 74	
3.3.2.4	Temperature Detection.....	76
3.3.2.5	Rationale for Performing Analysis #2 .....	80
3.3.3	Analysis # 2.....	83
3.3.3.1	Patient Demographics .....	83
3.3.3.2	Touch Detection .....	84
3.3.3.3	Peg Board Completion, Sharpness Detection and Skin Temperature 86	
3.3.3.4	Temperature Detection.....	88
3.3.3.5	Patient Reported Symptom Descriptors .....	91
3.4.	Discussion .....	93
4.	Overall Discussion and Future Directions.....	101
5.	Appendices.....	105
5.1.	Appendix A: Central Processing of Pain.....	105
5.2.	Appendix B: Additional Statistical Analysis for Chapter 3 .....	111
5.3.	Appendix C: Related Preclinical Studies .....	113
	References .....	124
	Vita.....	139

## List of Figures

Figure 1 Mechano-Transduction .....	8
Figure 2 Cutaneous Mechanoreceptors.....	12
Figure 3 Touch Detection Assessed With Von Frey Monofilaments .....	39
Figure 4 Fine Tactile Discrimination Assessed With the Bumps Detection Plate.....	39
Figure 5 Manual Dexterity Assessed with Grooved Pegboard Test.....	40
Figure 6 Weighted, Blunted Needle Assessed Sharpness Detection .....	41
Figure 7 Peltier Thermode Probe Assessed Temperature Thresholds .....	43
Figure 8 Skin Temperature Radiometer.....	43
Figure 9 Lucid Vivascope 1500 Non-Invasive Confocal Scanner .....	45
Figure 10 MM Patients Show Differences in Touch Detection and Peg Board Performance, But Not Sharpness Detection .....	49
Figure 11 MM Patients Show Differences in Skin Temperature and Thermal Detection Thresholds .....	51
Figure 12 Greater Numbers of MM Patients Displayed Out-of-Range Measures Compared to Volunteers .....	53
Figure 13 Inverse Correlation Between Meissner’s Corpuscle Density and Touch Detection.....	55
Figure 14 Study Design .....	69
Figure 15 Touch and Bumps Detection Thresholds Showed Few Differences Between Minocycline and Placebo Groups .....	73
Figure 16 Minocycline Group Showed Faster Dominant Hand Peg Board Completion, but No Differences in Sharpness Detection and Skin Temperature.....	75
Figure 17 Minocycline and Placebo Groups Exhibit Differences in Cool Detection, and Minocycline Does not Attenuate Increases in Cold Pain Thresholds.....	78
Figure 18 Warmth and Heat Pain Thresholds Were Not Different Between Minocycline and Placebo Groups .....	79
Figure 19 Bumps Detection and Age of Placebo Groups Approach, But Do Not Reach Statistical Significance Between Placebo 0mg Versus Low-Dose Bortezomib .....	82
Figure 20 Touch Detection at Volar Forearm Improved and Bumps Detection at the Fingertip Worsened in the Minocycline-Follow-Up Group.....	85
Figure 21 Peg Board Completion, Sharpness Detection, and Skin Temperature .....	87
Figure 22 Fingertip Cool and Cold Pain Thresholds .....	89
Figure 23 Warm and Heat Pain Thresholds.....	90
Figure 24 Patient Descriptors .....	92
Figure 25 Primary Afferent Neuron Synapses in Dorsal Spinal Cord.....	107
Figure 26 Central Pain Processing .....	110
Figure 27 Intraepidermal Nerve Fibers in Rodent Skin .....	115
Figure 28 Blockade of MCP-1 Prevents the Loss of IENFs Induced by Paclitaxel....	116
Figure 29 PGP9.5 and CGRP are Co-Localized in Intraepidermal Nerve Fibers .....	118
Figure 30 Some CGRP Positive Fibers Do Not Appear to Express PGP9.5.....	118
Figure 31 CCR2-KO Mice Showed No Difference in Formalin-Induced Spontaneous Pain.....	121
Figure 32 CCR2-KO Mice Showed No Difference in CFA-Induced Allodynia.....	121
Figure 33 CCR2-KO Mice Showed Less Mechanical Hypersensitivity after Spared Nerve Injury .....	122



Figure 34 CCR2- KO Mice Showed Less Mechanical Hypersensitivity after Paclitaxel Treatment .....	122
Figure 35 CCR2-KO Mice Showed No Reduction in Oxaliplatin-Induced Mechanical Hypersensitivity.....	123

## List of Tables

Table 1 Durie-Salmon Staging for Multiple Myeloma <sup>78</sup> .....	23
Table 2 International Staging System for Multiple Myeloma <sup>79</sup> .....	24
Table 3 Patient Demographics.....	47
Table 4 Patient Demographics: Analysis #1 .....	71
Table 5 Patient Demographics: Analysis #2 .....	83

## Abbreviations

°C: degrees Celsius

μl: microliters

μm: micrometers

AL: light-chain amyloidosis

APs: actions potentials

BIPN: bortezomib-induced peripheral neuropathy

β<sub>2</sub>M: β<sup>2</sup> Microglobulin

CCR2: chemokine receptor 2

CFA: complete Freund's adjuvant

CGRP: calcitonin gene-related peptide

CIPN: chemotherapy-induced peripheral neuropathy

C-MC: mechano-cold primary afferent

CNS: central nervous system

DRG: dorsal root ganglia

ECOG: Eastern Cooperative Oncology Group

fMRI: functional magnetic resonance imaging

GABA: γ-aminobutyric acid

GPCRs: G-protein coupled receptors

HT: high threshold

HTM: high threshold mechanoreceptors

IENFs: intraepidermal nerve fibers

IκB: inhibitor of nuclear factor-κB

IL-1: Interleukin-1

IL-6: Interleukin-6

KCC2: potassium-chloride exporter

LT: low threshold

LTM: Low threshold mechanoreceptors

MAPK: mitogen-activated protein kinase system

MCP-1: monocyte chemoattractant protein-1

MCs: Meissner's corpuscles

MEG: magneto-encephalography

MGUS: monoclonal gammopathy of undetermined significance

MIAs: mechanically insensitive afferents

MM: multiple myeloma

$\text{m}\cdot\text{s}^{-1}$ : meters/second

NCI: National Cancer Institute

NF- $\kappa$ B: nuclear factor  $\kappa$ B

NMDA: N-methyl-D-aspartate

PET: positron emission tomography

PGP 9.5: protein-gene product 9.5

PNS: peripheral nervous system

POEMS: polyneuropathy, organomegaly, endocrinopathy, M-protein, skin abnormalities

QST: quantitative sensory testing

RA: rapidly adapting

SA: slowly adapting

SNI: spared nerve injury

SNL: spinal nerve ligation

TNF- $\alpha$ : tumor necrosis factor- $\alpha$

TNS: total neuropathy score

TRPV1: transient vanilloid receptor 1

VEGF: vascular endothelial growth factor

vs.: versus

WDRs: wide-dynamic-range neurons

WHO: World Health Organization

## 1. Introduction

Cancer currently affects over 1.6 million people in the United States and by 2030, this number is estimated to increase to 2.3 million <sup>1,2</sup>. Cancer claims 1 in 4 American lives and is the second most common cause of death. In less than 20 years, cancer is expected to be the biggest killer of any single disease <sup>3</sup>. However, with increasingly-sensitive tests for detecting cancer and the administration of frontline chemotherapeutic agents, the number of cancer survivors is expected to increase 35% from 13.7 in 2012 to 18 million by the year 2022 <sup>4</sup>. Chemotherapeutics are effective in stopping the progression of cancer because they are often designed to differentially target and eliminate rapidly dividing cancer cells. Despite their advantages in the cancer-fighting arena, they are also associated with deleterious side effects (e.g. anemia, appetite changes, constipation, diarrhea, nausea, vomiting, neurological changes, infection, fluid retention, fatigue, hair loss, infertility, pain and peripheral neuropathy) that negatively affect normal cells and structures of the body <sup>5</sup>. Given the potential longevity of biochemical and cellular changes induced by cancer and chemotherapy, cancer survivors will require a life-time of medical monitoring and treatment for cancer and/or drug-induced health problems and comorbidities <sup>3</sup>. Of the adverse effects induced by cancer treatment, 20 to 100% of patients (depending on the study design and agent) develop a condition known as chemotherapy-induced peripheral neuropathy (CIPN) <sup>6,7</sup>. CIPN occurs when peripheral nerves are damaged, resulting in abnormal sensory function, and pain or loss of motor control. This condition sometimes leads to chemotherapy dose decrease or cessation, thereby limiting the efficacy of cancer treatment. The investigations conducted focus on the

neuropathy multiple myeloma (MM) patients develop from underlying malignancy as well as frontline chemotherapeutic agent, Bortezomib (Velcade<sup>®</sup>). The following sections provide a review of the peripheral nervous system, neuropathic pain conditions, CIPN, MM and treatment agent bortezomib and may be relevant background information for the reader.

### **1.1. Peripheral Nervous System**

CIPN is a condition that develops due to insult to the peripheral nervous system (PNS). The PNS is the network of nerves and ganglia that reside outside of the brain and spinal cord and is divided into the somatic and autonomic nervous systems. The autonomic nervous system involuntarily modulates the functioning of the viscera such as heart rate, respiration rate, perspiration, digestion, sexual arousal and swallowing. The somatic nervous system is comprised of the nerves that relay sensory and motor information to and from the central nervous system (CNS). These nerves provide communication between the skin, sensory organs, joints and all skeletal muscles. The skin is the largest sensory organ of the body and is home to the endings (both free and specialized) of primary afferent sensory neurons that transmit stimuli (mechanical, thermal, and chemical stimuli) from the environment to the CNS. Primary afferents provide the body with tactile, thermal and nociceptive (actual or potential tissue damage) information about the external world or the body's relationship to the external world (proprioception)<sup>8</sup>. Primary afferents are distinct from other types of neurons in the body because they are pseudo-unipolar. Pseudo-unipolar cell bodies are situated in between two axons capable of sending information bi-directionally. The axons of primary afferent neurons form terminals in the skin and transmit sensory information from a designated area called a receptive field<sup>8</sup>. Receptive fields of sensory neurons

can vary based on the type of neuron or location in the body. Primary afferent sensory neurons (including nociceptors) can be classified according to 1. structure and conduction velocity, 2. modality specificity, 3. threshold of activation and adaptability, 4. receptor expression and cell content.

### **1.1.1 Structure and Conduction Velocity of Primary Afferents**

The structure of primary afferent fibers determines function. There are four broad classes of primary afferents that have differing axon diameters and myelin thickness, which determine properties such as conduction velocity. These classes of fibers are A $\alpha$ -, A $\beta$ -, A $\delta$ - and C-fibers. A $\alpha$ -fibers are thickly myelinated and are the largest in diameter (12-20  $\mu\text{m}$ ). A $\alpha$ -primary afferent sensory neurons are proprioceptors that innervate skeletal muscles and provide information about limb and body position in space with conduction velocities of 70-170  $\text{m}\cdot\text{s}^{-1}$ . A $\beta$ -fibers are myelinated primary afferent sensory neurons that transmit mechanical information such as light touch. These have slightly smaller diameters of 6-12  $\mu\text{m}$  and relatively fast conduction velocities (35-75  $\text{m}\cdot\text{s}^{-1}$ ). A $\beta$ -fibers innervate specialized sensory organs with characteristic structures allowing detection of the quality (e.g. brief versus long in duration) of mechanical stimuli (Section 1.2.6). In addition to sensory neurons that convey information about mechanical stimuli, there are two broad classes of nociceptors that exist in the skin A $\delta$ - and C-fibers. A $\delta$ -fibers transmit acute or sharp pain, are thinly myelinated and have conduction velocities of 5-30  $\text{m}\cdot\text{s}^{-1}$ . C-fibers encoding dull, burning and diffuse pain are unmyelinated and have slow conduction velocities (0.5-2  $\text{m}\cdot\text{s}^{-1}$ )<sup>9</sup>. The above characteristics and categories of primary afferent neurons are not absolute and are an oversimplification of the true physiology. These characteristics in isolation cannot be used to identify whether a fiber is a nociceptor or



not without further evidence of encoding noxious stimuli <sup>10</sup>. For example, there is evidence that a small percentage of A $\alpha$ - and A $\beta$ -fibers are nociceptive <sup>11</sup>.

### **1.1.2 Modality Specificity of Primary Afferents**

The subset of primary afferent neurons responsible for the transmission and sensory phenomenon of pain are termed nociceptors. Nociceptors are broadly classified into polymodal, thermal, or mechanical categories <sup>12</sup>. Polymodal nociceptors respond to potentially harmful or harmful mechanical, thermal, and chemical stimuli and are the most ubiquitous type of nociceptor in the skin. Thermal nociceptors respond to temperatures associated with tissue damage (greater than 45 °C or less than 5 °C). Mechanical nociceptors respond to harmful or potentially harmful amounts of pressure applied to the skin <sup>8</sup>. It is believed that these nociceptors work in synergy to produce different qualities of pain <sup>12</sup>. For example, pain that is sharp in quality (“first” pain) and felt acutely is predominately carried by fast-conducting, myelinated A $\delta$ -fibers while dull, achy pain (“second” pain) is carried by slow-conducting unmyelinated C-fibers <sup>13</sup>. Mechanically-insensitive afferents (MIAs) have also been identified that respond to chemical, but not mechanical stimulation <sup>14</sup>. In primates, MIAs make up approximately 30% of C-fibers and 48% of A $\delta$ -fibers <sup>14</sup>. Other subsets of primary afferents have been characterized in the cat, rabbit, and rodent, and are sensitive to several modalities or selectively sensitive to different ranges of a certain modality such as Mechano-cold (C-MC) afferents and A $\delta$ -cold receptors <sup>15,16</sup>.

### **1.1.3 Threshold for Activation and Adaptation of Primary Afferents**

Activation thresholds and adaptation are two other characteristics of sensory neurons. The following characteristics mentioned commonly refer to cutaneous primary afferents that transmit mechanical stimuli (mechanoreceptors). Low-threshold

mechanoreceptors (LTM) respond to low grades of mechanical force (e.g. touch), whereas high-threshold mechanoreceptors respond to noxious, or potentially noxious mechanical forces<sup>17</sup>. Classically, nociceptors (A $\delta$ - and C-fibers) were thought to have a high activation threshold, responding only to strong, potentially-damaging stimuli, whereas A $\beta$ -fibers were thought to be LTM<sup>18</sup>. However, low threshold mechanonociceptors and “silent nociceptors” (nociceptors activated by sustained nociceptive input rather than immediately following tissue injury) have been identified<sup>19</sup>. Sensory neurons have also been categorized as slowly or rapidly adapting, based on the encoding of stimulus information. Sensory neurons are tuned to differentially provide information about the range of magnitude or frequency of the stimuli. Slowly adapting afferents generate trains of action potentials (APs) in response to long duration stimuli, while rapidly adapting afferents initially fire APs and then go silent (Figure 2). Therefore, slowly adapting afferents better encode a maintained stimulus, in contrast to rapidly adapting afferents, which encode a stimulus that is rapidly changing<sup>9</sup>. Types I and II can be used in conjunction with slowly- and rapidly-adapting to describe the receptive fields of primary afferents (Figure 2). Type I refers to a small area where activation thresholds are low, surrounded by an area where activation thresholds become very high. Type II refers to large receptive fields.

In addition to conduction velocity, structure, threshold for activation, and modality, the expression of transduction molecules and receptors is responsible for the properties of individual sensory neurons.

#### **1.1.4 Receptor Expression and Cell Content of Primary Afferents**

Primary afferent neurons have heterogeneous cell content and receptor expression, which contribute to their modality specificity. For example, the polymodal

nociceptive C-fibers can be divided into two classes: peptidergic (expressing peptides such as calcitonin gene-related peptide (CGRP) and substance P) and nonpeptidergic nociceptors. C-fibers can also be categorized on the basis of receptor expression. Peptidergic receptors express TrkA (the high affinity nerve growth factor receptor)<sup>20</sup>. Non-peptidergic nociceptors express the P2X3 purine receptor, receptors for glial-cell-derived growth factor and the IB4-lectin-binding site<sup>20</sup>. Alternatively, primary afferents can be classified by expression of ion channels. For instance, nociceptors express voltage-insensitive sodium channels (Na<sub>v</sub> 1.7 and Na<sub>v</sub> 1.8) and the non-selective cationic channel, transient vanilloid receptor 1 (TRPV1). Nociceptors often express multiple-channel types that vary from one afferent to the next and confer different properties<sup>10</sup>.

In summary, primary afferents, and specifically, nociceptors, are heterogeneous in their properties, which has made their classification, study and manipulation challenging.

### **1.1.5 Skin Morphology and Sensory Transduction**

Sensory transduction through primary afferent fibers begins first with a generator potential whereby a stimulus produces excitation of the membrane. Subsets of channels located on sensory neurons open in response to stimulation (e.g. mechanical, temperature, or chemical) producing graded generator potentials, which depolarize the membrane. If the magnitude of the stimulus reaches threshold, an action potential is generated proximal to the ending and propagates towards the CNS<sup>9</sup>. The original stimulus is thus converted into an electrical signal that is transmitted to the spinal cord and brain. Stimuli that are greater than the minimum intensity to produce an AP are encoded via frequency of action potentials<sup>18</sup>. In most neurons the

generation of an AP occurs at the junction between the axon and the cell body, called the axon hillock. However, in sensory neurons the generator potential occurs at the specialized ending, and when it reaches sufficient magnitude, it initiates an action potential just proximal to the sensory ending (Figure 1), which is distal to the cell body located in trigeminal ganglia or dorsal root ganglia (DRG).

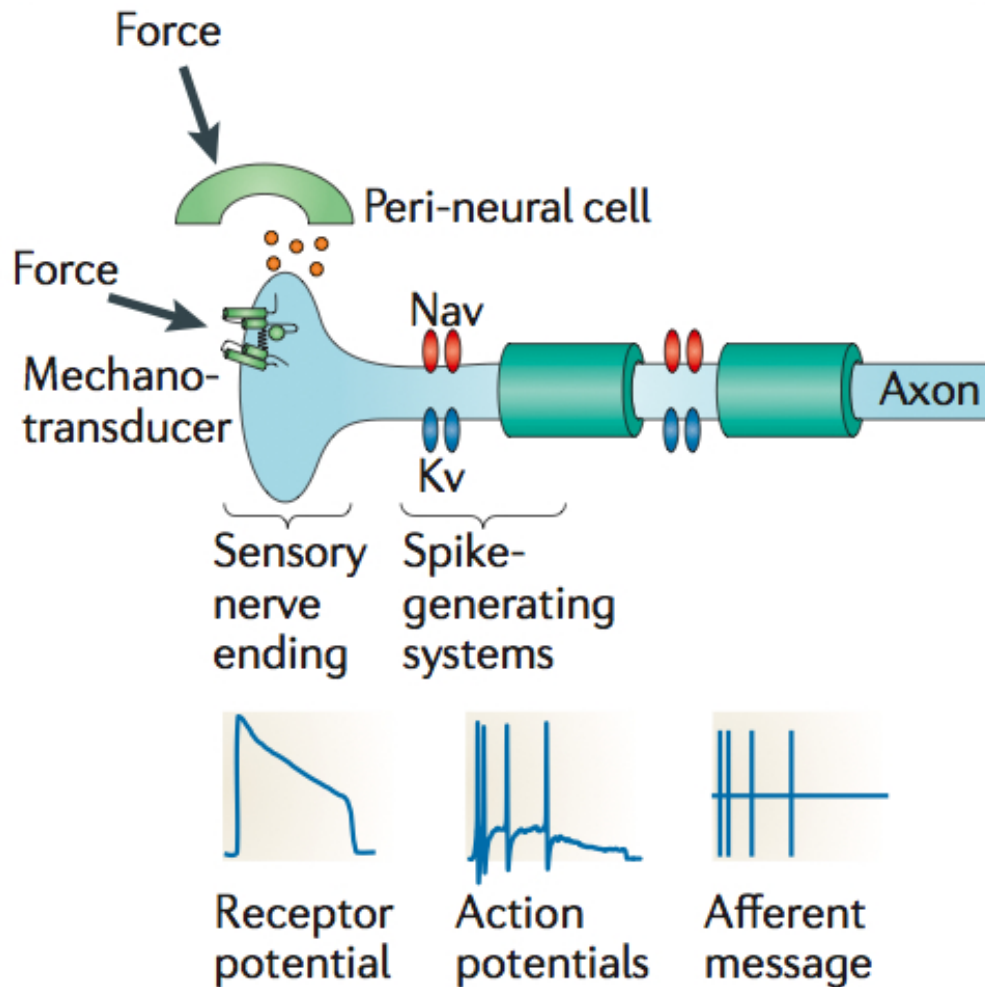


**Figure 1 Mechano-Transduction**

Ion channels open in response to mechanical stimulation, producing graded generator potentials (receptor potentials). If the magnitude of the stimulus reaches threshold, an action potential is generated proximal to the ending and propagates towards the central nervous system.

Reprinted from Nature Reviews Neuroscience 12, 139-153, Delmas P, Hao J, Rodat-Despoix L, Molecular mechanisms of mechanotransduction in mammalian sensory neurons. Copyright 2011, reprinted with permission from Nature Reviews Neuroscience.

Human skin is composed of epidermis (the most superficial outer layer), separated by a collagen basement membrane from the deeper-lying dermis. The dermis forms protrusions that are perpendicular to the skin's surface called dermal papillae. Human skin can be hairy or non-hairy (glabrous) <sup>21</sup>. Glabrous skin covers the palms and soles of the feet and has surface features known as epidermal ridges <sup>21</sup>. The epidermal ridges on the fingertip are colloquially referred to as fingerprints <sup>9</sup>. Epidermal ridges are structures that contribute to the pattern of organization of the skin <sup>22</sup>. Glabrous skin is affected during chemotherapy-induced neuropathy and is the subject of the following sections.

### **1.1.6 Mechanosensation**

Glabrous skin is innervated by encapsulated sensory organs (Merkel disks, Meissner's corpuscles, Pacinian corpuscles, and Ruffini endings) as well as free nerve endings. Merkel disks are oval structures 10-15  $\mu\text{m}$  in diameter located in the basal layer of the epidermis and are slowly adapting, indicating persistent firing in response to sustained indentation or pressure on the skin (Figure 2d) <sup>23,24</sup>. Merkel disks are low-threshold mechanoreceptors innervated by A $\beta$ -fibers in a variety of terminal branch patterns that is suggestive of the complex discharge rates of slowly adapting type I fibers <sup>9</sup>. The evidence suggests that Merkel disks act as mechanical transducers by releasing glutamate in response to stimulation and generating action potentials in axons <sup>24</sup>.

Ruffini corpuscles are slowly adapting mechanoreceptors identified in hairy mammalian skin (Figure 2e). Ruffini corpuscles contain a myelinated A $\beta$ -fiber that ends in a club-like structure. Individual fibers emanate from the club-like structure <sup>25</sup>. Despite their existence in the cat, several experiments suggest that Ruffini corpuscles

are absent in glabrous skin of raccoon, primates and humans, therefore, they will not be further discussed <sup>9</sup>.

Meissner's corpuscles (MCs) are another type of cutaneous mechanoreceptor with small receptive fields, located in the dermal papillae that line the epidermal ridges in skin (Figure 2b). They are composed of primary afferent terminals (multiple A $\beta$ - and at least two types of C-fibers) interdigitated between stacks of flattened epithelial (laminar) cells and rapidly adapt to 30 to 50 Hz low frequency, "flutter" stimuli <sup>9</sup>. A $\beta$ -afferents can innervate more than one MC. Additionally, each afferent can innervate different combinations of multiple MCs that are partially overlapping <sup>22</sup>. C-fiber innervation in MCs is both peptidergic and non-peptidergic. Based on optimal frequency for activation and location in the skin, it is thought that MCs provide information about an object moving over the skin or conversely, the skin moving over an object <sup>26</sup>.

Pacinian corpuscles are composed of an inner core (formed by specialized Schwann cells) and an outer core of lamellae layered like the skin of an onion around A $\beta$ -fibers (Figure 2c) <sup>27</sup>. This arrangement may allow for incompressible fluid between lamellae to press on A $\beta$ -fibers producing a generator potential, and if the stimulus is large enough, an action potential. Pacinian corpuscles are low-threshold, rapidly adapting structures that are located deeper than Merkel disks and Meissner's corpuscles in the dermis. They have relatively large receptive fields and respond optimally to high frequency stimuli such as vibration <sup>28</sup>.

A $\delta$ - and C-fibers terminate in the dermis and epidermis of the skin as free nerve endings where they contribute to nociception as well as the detection of mechanical, thermal, and chemical stimuli as previously mentioned (Figure 2g). A subset of C-

fibers are low-threshold mechanoreceptors that encode light and pleasant touch (Figure 2f) <sup>29</sup>. Although the presence of A $\delta$ - and C-fibers in the epidermis was initially elusive, these fibers can now be easily detected with an antibody against protein-gene product 9.5 (PGP 9.5), which is an enzyme located in the cytoplasm of nerves.

In summary, glabrous skin is populated with several structures, including sensory organs tuned to provide information about specific types of mechanical stimulation and free nerve endings conveying polymodal stimuli.



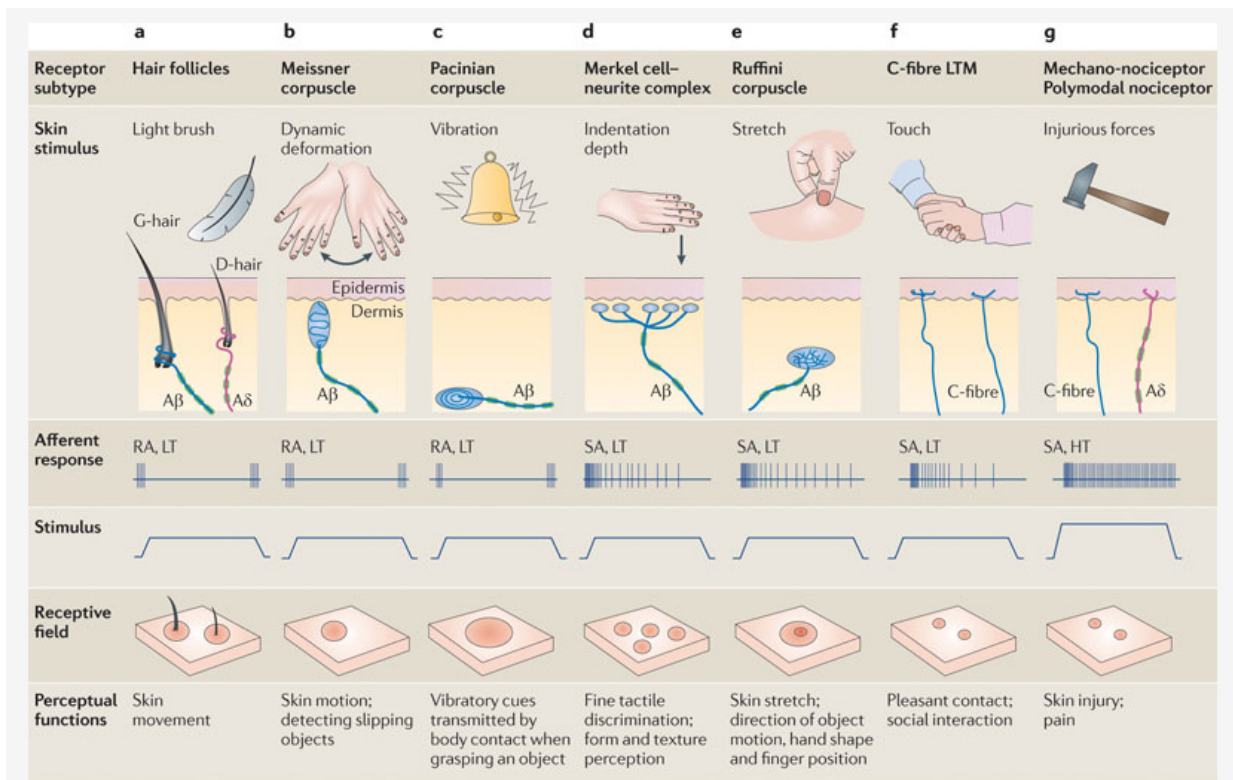


## Figure 2 Cutaneous Mechanoreceptors

Glabrous skin contains specialized endings of large myelinated  $A\beta$ -fibers (Meissner's corpuscles, Pacinian corpuscles, Merkel cell complexes, and Ruffini corpuscles) that encode different qualities of tactile information depending on whether they are rapidly adapting (RA) or slowly adapting (SA) and low-threshold (LT) or high-threshold (HT). Hairy skin contains guard hairs and down hairs innervated by  $A\beta$ - and  $A\delta$ -fibers, respectively. A subset of C-fibers convey light touch (C-fiber LTM). C-fibers and  $A\delta$ -fibers also serve as polymodal and mechano-nociceptors.

Reprinted from Nature Reviews Neuroscience 12, 139-153, Delmas P, Hao J, Rodat-Despoix L, Molecular mechanisms of mechanotransduction in mammalian sensory neurons. Copyright 2011, reprinted with permission from Nature Reviews Neuroscience.

### 1.1.7 Thermosensation

In addition to detecting mechanical stimuli, mammalian skin is also adept at sensing temperatures in the range of -10 °C to 60 °C<sup>30</sup>. Humans are able to qualitatively describe four types of thermal stimuli: painful heat, warmth, painful cold and cool<sup>8</sup>. Cultured sensory neurons retain sensitivity to temperature, which has allowed for electrophysiological investigation of mechanisms of thermosensation<sup>31</sup>. The non-selective cationic channel, TRPV1, is expressed on sensory neurons and allows depolarization in response to heat  $\geq 42$  °C or to the chili pepper derivative, capsaicin<sup>32</sup>. Although it is not the only channel involved in sensing heat, it is abundantly clear that TRPV1 plays a key role in the sensation of noxious heat. Knockout of TRPV1 in mice causes both a decrease in reaction to noxious heat as well as sensitivity to thermal stimulus after tissue injury<sup>33</sup>. Another TRPV family member channel, TRPV2, is activated by heat 52 °C and above and is expressed in A $\delta$ -nociceptors<sup>34</sup>. TRPV3 and TRPV4 are likely to contribute to the perception of warmth with activations at 27 to 34 °C and 32 to 39 °C, respectively<sup>30</sup>. There is also evidence that other TRP channels contribute to the detection of warmth and heat<sup>30</sup>.

Detection of cool stimuli is mediated through TRPM8, which is predominantly expressed in C-fibers and responds to slight decreases (30-32 °C) in skin temperature as well as to menthol<sup>35</sup>. Although controversial, it is thought that TRPA1 may contribute to the perception of extreme cold temperatures. TRPA1 expression may be responsible for the sensitivity of a population of in vitro sensory neurons to temperatures below 20 °C<sup>36</sup>.

## **1.2. Pain, Pain Processing, and Neuropathic Pain**

Pain is the disagreeable physical or emotional sensation experienced when the integrity of tissues and organs of an organism are threatened or damaged<sup>37</sup>. Pain is subjective, meaning that the same injury can cause different magnitudes of discomfort and be experienced for different lengths of time in different individuals. The difficulty in quantifying pain in both humans and animals due to a subjective emotional component of the sensation is one of many challenges to research in the field.

### **1.2.1 Pain Classifications and Definitions**

Nociceptors are specialized cells; a class of primary afferent sensory neurons capable of encoding and transmitting noxious or potentially noxious stimuli to the CNS<sup>38</sup>. They are composed of an axon located in the periphery, a cell body located in the dorsal root ganglion, and central terminals, which synapse on the dorsal horn of the spinal cord<sup>39</sup>. Nociceptors are located in skin, muscle, joints, and viscera and after they are activated by noxious stimuli, they become sensitized either by decreasing their threshold for activation, or increasing the magnitude of their response<sup>40</sup>. This increase in excitability is believed to underlie the hypersensitivity experienced after injury. For a brief review of central pain processing see Appendix A.

Nociceptive pain functions to protect tissue from further damage by compelling us to escape from the harmful stimulus. Three broad classifications of pain exist: nociceptive, inflammatory, and pathological pain<sup>41</sup>. Nociceptive pain is the high-intensity, acute pain felt when a noxious stimulus activates nociceptors. Inflammatory pain results from activation of the immune system following tissue damage or infection. Acute inflammatory pain is provoked by the recruitment of neutrophils, monocytes, and macrophages (mature monocytes) to the site of injury that eventually cause swelling,

redness, aching, and warmth associated with inflammation<sup>42</sup>. Prostaglandins and bradykinin are early mediators of inflammatory pain and increase excitability through modulation of ion channels on primary afferent sensory neurons. In persistent inflammatory states other molecules such as cytokines and growth factors induce upregulation of ion channels, receptors, and inflammatory molecules via gene transcription<sup>43</sup>. Inflammatory pain can be protective to the individual by causing sensitization of tissues so that further injury is avoided or maladaptive, such as in conditions such as rheumatoid arthritis.

Although pain is essential for survival, not all pain is protective. Pathological pain can be chronic or intermittent in nature and is due to dysfunction of the nervous system. This occurs when pain persists long after initial injury due to dissociation of the nociceptive stimulus from the pain-processing machinery. In these cases, pain may even spread distally or proximally from the initial site of injury. Dysfunctional pain and neuropathic pain are two types of pathological pain. Dysfunctional pain is pain that arises in the absence of tissue damage or inflammation. Neuropathic pain is defined as “pain arising as a direct consequence of a lesion or disease affecting the somatosensory system”<sup>44</sup>. Neuropathic pain is debilitating and refractory to conventional medications and treatments and consequently, is one of the major challenges clinicians face in treating their patients.

### **1.2.2 Neuropathic Pain**

Neuropathic pain is a type of maladaptive pain produced in response to a peripheral or CNS injury that persists long after the initial injury and is refractory to therapy. Many types of injuries and diseases provoke what is broadly termed neuropathic pain. Though neuropathic conditions are similar, underlying disease is

responsible for mechanistic differences and the manifestation of symptoms. For most patients, neuropathic pain is caused by focal or multifocal lesions of the PNS, generalized lesions of the PNS (polyneuropathies), lesions of the CNS, or complex neuropathic disorders<sup>45</sup>. Examples of focal or multifocal lesions of the PNS that cause neuropathic pain include postherpetic neuralgia, phantom limb pain and diabetic mononeuropathy. Generalized PNS lesions that cause neuropathic pain result from various conditions, including diabetes mellitus, amyloidosis, alcoholism, HIV-induced neuropathy, toxic neuropathy (e.g.: chemotherapy-induced), vitamin B deficiency and hereditary sensory neuropathies<sup>45</sup>. Lesions of the CNS that cause neuropathic pain are spinal cord injury, brain infarction (e.g. of the brainstem and thalamus), syringomyelia and neurodegenerative diseases such as multiple sclerosis. Complex neuropathic pain disorders that cause neuropathic pain refer to complex regional pain syndromes type I and II<sup>45</sup>. Therefore, both peripheral and central injury can lead to neuropathic pain.

### **1.2.3 Peripheral Mechanisms of Neuropathic Pain**

Peripheral nerve injury can lead to neuropathic pain through a change in the properties of primary afferents and how stimuli are encoded. For instance, primary afferents become hypersensitive and may fire spontaneously. An upregulation of  $Na_v$  1.7,  $Na_v$  1.8,  $Na_v$  1.9 and potentially,  $Na_v$  1.3 sodium channels may induce hyperexcitability of nociceptors after injury<sup>46</sup>.  $Na_v$  1.7 opens in response to small depolarizations near resting potential; thus modulation of  $Na_v$  1.7 expression can dictate the ease of firing an AP.  $Na_v$  1.8 is selectively expressed in DRG neurons and opens to allow depolarization in the absence of voltage change.  $Na_v$  1.3 is responsible for persistent sodium current and is capable of magnifying small depolarizations.

Na<sub>v</sub>1.9 opens at hyperpolarized voltages near resting potential and does not inactivate, thereby potentiating depolarization. Changes in receptor expression on nociceptors can hence change the firing properties of nociceptors by increasing excitability and neurally encoding hypersensitivity.

Due to their electrophysiological properties, sodium channels have been linked to pain in numerous studies. Clinically, mutations in the gene *SCN9A* that encodes Na<sub>v</sub> 1.7 have been linked to several of the following disorders: inherited erythromelalgia and paroxysmal extreme pain disorder patients, display abnormally high pain levels, as compared to patients who exhibit congenital insensitivity to pain and are unable to feel pain<sup>47-49</sup>. Na<sub>v</sub> 1.8 mutations are associated with small-fiber painful neuropathy<sup>50</sup>. Pre-clinical studies indicate that Na<sub>v</sub> 1.9 plays a role in diabetic neuropathic pain and inflammatory pain<sup>51</sup>. In addition to sodium channels, other channels, such as TRPV1, TRPV4 and TRPM8 are up-regulated in injured nociceptors and contribute to the development of neuropathic pain<sup>52-54</sup>. Other studies have suggested that molecular changes in undamaged primary afferents accompany injury and play as important a role in the experience of pain<sup>55</sup>.

#### **1.2.4 Central Mechanisms of Neuropathic Pain**

As mentioned in Appendix A, central sensitization plays a role in pain and particularly, in neuropathic pain. The literature implicates a wide array of neurons, ion channels, signaling pathways, molecules and non-neuronal cells in central sensitization<sup>56</sup>. (See Appendix A for further discussion about central pain processing.) Damage to peripheral nerves (particularly C-fibers) causes spontaneous activity, which in turn alters secondary order neurons in the spinal dorsal horn and results in hyperexcitability via diverse molecular changes. This is accomplished through release

of the excitatory neurotransmitter, glutamate, as well as peptide neurotransmitters from primary afferents and hence, an activation of NMDA receptors on second order neurons. Also, an upregulation of N-type calcium channels pre-synaptically and Na<sub>v</sub>1.3 channels post-synaptically is believed to underlie this excitability<sup>57,58</sup>. In addition to an up-regulation in the cellular machinery producing excitability, a decrease in inhibitory mechanisms has also been observed in neuropathic pain conditions<sup>59</sup>. This could be caused by a selective loss of an inhibitory class of neurons, γ-aminobutyric acid (GABA) neurons, or a loss of the potassium-chloride exporter (KCC2), which causes cells to become more excitable rather than inhibited in the presence of GABA<sup>59,60</sup>. Research also suggests that changes in descending inhibitory pain pathways may lead to the promotion rather than the repression of pain<sup>61</sup>. Central changes are not limited to the spinal cord and extend into the brain. Technologies such as functional magnetic resonance imaging (fMRI), positron emission tomography (PET) and magneto-encephalography (MEG) have facilitated detection of pain-related changes in the brain, which will not be further discussed here.

### **1.2.5 Inflammatory Mechanisms of Neuropathic Pain**

Recent evidence also points to an involvement of innate immune mechanisms in neuropathic pain syndromes, which include an upregulation of diverse inflammatory mediators<sup>62</sup>. Inflammatory substances may be capable of provoking long-lasting pain through inducing neuroplasticity<sup>62</sup>. This can be achieved by binding to respective receptors, thereby activating downstream signaling molecules capable of entering the nucleus and influencing gene transcription.

TNF-α is perhaps the most widely studied proinflammatory cytokine in neuropathic pain and evokes the release of other anti- and pro-inflammatory cytokines.

Animal models of neuropathic pain wherein the nerve is transected or crushed, produces demyelination, and degeneration of the distal axon, termed Wallerian degeneration<sup>63</sup>. In response to this type of nerve injury, Schwann cells, mast cells, endothelial cells, and fibroblasts release TNF- $\alpha$ , which in turn, provokes the release of other inflammatory mediators. Release of TNF- $\alpha$  is also thought to be responsible for activating immune mechanisms through the recruitment of phagocytic macrophages to the site of injury<sup>64</sup>. In Wallerian degeneration, non-resident macrophages localize to the nerve and degrade myelin, contributing to the pain phenotype<sup>65</sup>. In addition to TNF- $\alpha$ , there is strong evidence of the involvement of many other diverse inflammatory mediators and cytokines in pain. Interleukin-6 (IL-6) plays a complex role in pain. IL-6 is detected in injured primary afferent nerve fibers, DRG, and spinal cord and peripheral administration of IL-6 causes increased mechanical hypersensitivity<sup>66</sup>. However, IL-6 also plays a role in neuronal survival and regeneration in vitro and in vivo<sup>66</sup>. Interleukin-1 (IL-1)<sup>67</sup> and the chemokine receptors CXCR4, CCR5, CCR4, and CCR2 are upregulated following nerve injury and facilitate neuropathic pain conditions<sup>68</sup>. Upon binding to respective G-protein coupled receptors (GPCRs), chemokines potentiate inflammatory and pain states through downstream pathways such as the mitogen-activated protein kinase system (MAPK) signaling cascade<sup>68</sup>. In addition to central neuronal changes, non-neuronal changes also occur. For example, several types of glia, including microglia, astrocytes, and satellite glial cells of the DRG are activated in chronic pain states<sup>69</sup>. Thus, neuropathic pain can be initiated due to peripheral or central injury and potentiated by changes in cellular machinery and innate immune responses.



### **1.3. Multiple Myeloma Pathophysiology, Diagnosis and Staging**

Multiple myeloma patients and their sensory deficits prior to treatment as well as their development of neuropathic pain post-chemotherapy treatment are the subject of this thesis. The disease processes of multiple myeloma will be briefly reviewed here.

Multiple myeloma (MM) is a plasma cell neoplasm characterized by uncontrolled proliferation of plasma cells accompanied by hypercalcemia, renal dysfunction, anemia and bone lesions (called CRAB criteria)<sup>70</sup>. Plasma cells are terminally-differentiated B lymphocytes that secrete antibodies in response to antigens, thereby protecting the individual from infection<sup>71</sup>. Plasma cells are located in three areas of the body: spleen, lymph nodes, and bone marrow. These locations allow efficient interaction with antigens, stimulating release of antibodies, also known as immunoglobulins, into the bloodstream. B-cell maturation into plasma cells occurs in the bone marrow and is facilitated by contact with growth factors released from reticular stromal cells. Chemokines, a family of signaling molecules capable of inducing chemotaxis, are released from stromal cells and are critical for plasma cell survival<sup>72</sup>. When the transformation of B-cells into plasma cells becomes unregulated, plasma cells proliferate uncontrollably and overproduce immunoglobulins, which are not adaptive to fight infection, but rather, produce the co-morbid conditions present in MM patients.

Based on statistics from 2006 to 2010, the number of new cases (adjusted for age) of MM is projected to be 5.9 per 100,000 men and 3.4 per 100,000 women<sup>73</sup>.

Diagnostic criteria for MM are based on high numbers of monoclonal plasma cells, monoclonal immunoglobulin in serum and/or urine, and bone lesions (apparent in 80% of patients at diagnosis). Immunoglobulins (antibodies) are released from plasma cells and are Y-shaped. Immunoglobulins have two paratopes located on each arm of the

Y-shaped molecules that bind to epitopes on antigens. The Y-structure of an immunoglobulin is made up of four polypeptide chains: two identical smaller chains (light chains) linked by disulphide bridges to two identical larger polypeptides, called heavy chains<sup>74</sup>. There are five types of mammalian immunoglobulin heavy chains:  $\alpha$ ,  $\delta$ ,  $\epsilon$ ,  $\zeta$ ,  $\mu$ , which distinguish the immunoglobulin isotypes IgA, IgD, IgE, IgG, and IgM, respectively. In mammals, two light chains exist, termed  $\kappa$  and  $\lambda$ . Similar to MM, other disorders such as monoclonal gammopathy of undetermined significance (MGUS), smoldering multiple myeloma, macroglobulinemia, non-Hodgkin lymphoma, essential cryoglobulinemia, heavy chain disease, and idiopathic cold agglutinin disease, also present with paraproteinemia, but are all distinct conditions.

Paraproteinemia is the overproduction of paraprotein also known as an abnormal immunoglobulin light-chain. Patients with MGUS can be distinguished from MM patients because they have less than 5% monoclonal plasma cells, but no other CRAB symptoms; however, approximately 1% of MGUS cases will progress to MM<sup>75</sup>. Patients with MGUS or smoldering MM do not require treatment.

Individuals diagnosed with MM must exhibit monoclonal plasma cell proliferation by bone marrow aspiration and/or bone marrow biopsy. A bone marrow biopsy will allow the clinician to assess the immunophenotype of the plasma cells as well as the extent of bone marrow infiltration. A bone marrow aspiration is performed to further examine the monoclonal cell population with cytogenetics<sup>70</sup>. Patient serum and urine must also be checked for the presence of monoclonal proteins with serum or urine protein electrophoresis. Detection of IgG or IgA proteins is the most common, but detection of more than one monoclonal protein is also possible.

Two staging systems for MM are used to quantify severity of disease and predict survival: the Durie-Salmon Myeloma Staging System and the International Staging System. The Durie-Salmon System (Table 1) assesses tumor cell mass, whereas the International Staging System (Table 2) takes into account  $\beta^2$  Microglobulin ( $\beta 2M$ ), which is influenced both by tumor burden and renal function.  $\beta 2M$  is the light chain of the major histocompatibility complex of the cell membrane and high  $\beta 2M$  indicates high proliferation of tumor cells<sup>75</sup>. The presence and quantification of other factors have also been used as prognostic factors. For example, plasmablastic morphology and chromosome 13 deletions are associated with poor survival<sup>76,77</sup>.

STAGE	CRITERIA	MEASURED MYELOMA CELL MASS
STAGE 1 (low cell mass)	All of the following: <ul style="list-style-type: none"> <li>• Hemoglobin &gt; 10g/dL</li> <li>• Serum calcium value normal or &lt;10.5mg/dL</li> <li>• Bone X-ray: normal bone structure (scale 0), or solitary bone plasmacytoma only</li> <li>• Low M-component production rates IgG value &lt;5g/dL; IgA value &lt;3g/dL</li> <li>• Urine light chain M-component electrophoresis &lt;4g/24h</li> </ul>	600 billion/m <sup>2</sup>
STAGE II (intermediate cell mass)	Neither Stage I or Stage III	600 to 1200 billion in whole body
STAGE III	One or more of the following: <ul style="list-style-type: none"> <li>• Hemoglobin &lt;8.5g/dL</li> <li>• Advanced lytic bone lesions (scale 3)</li> <li>• High M-component production rates IgG value &gt;7g/dL, IgA value &gt;5g/dL</li> <li>• Bence Jones protein &gt;12g/24h</li> </ul>	>1200 billion
Subclassification (either A or B)	A: relatively normal renal function (serum creatinine value) <2.0 mg/dL  B: abnormal renal function (serum creatinine value) >2.0 mg/dL	

**Table 1 Durie-Salmon Staging for Multiple Myeloma** <sup>78</sup>

STAGE	CRITERIA
STAGE I	<ul style="list-style-type: none"> <li>• Serum <math>\beta^2</math> microglobulin &lt;3.5 mg/L</li> <li>• Serum albumin <math>\geq</math>3.5g/dl</li> </ul>
STAGE II	Neither Stage I or Stage III
STAGE III	<ul style="list-style-type: none"> <li>• Serum <math>\beta^2</math> microglobulin &gt;5.5 mg/L</li> </ul>

**Table 2 International Staging System for Multiple Myeloma <sup>79</sup>**

## **1.4. Treatment of Multiple Myeloma**

### **1.4.1 Bortezomib: Clinical Overview**

Bortezomib (Millenium Pharmaceuticals Inc. VELCADE<sup>®</sup>) is a proteasome inhibitor first approved in 2003 for the treatment of MM in patients after the failure of three previous therapies<sup>80</sup>. It was approved following a successful phase 2 open-label, nonrandomized trial that showed a 35% complete, partial, or minimal response in MM patients that had not improved with other agents<sup>81</sup>.

Proteasomes breakdown and remove damaged proteins in cells by selectively catalyzing the degradation of peptides that have been tagged with a small protein, ubiquitin. Bortezomib reversibly inhibits mammalian proteasome 26S, which disrupts its ability to cleave and degrade ubiquitin-tagged proteins. The tolerability and efficacy of bortezomib are due in part to an increased sensitivity of cancerous plasma cells to the drug as opposed to normal cells to the drug. Though bortezomib was designed as a proteasome inhibitor, its mechanism for eliminating cancer cells is not fully understood<sup>82</sup>. One possible mechanism of action of bortezomib is that inhibition of proteasomes causes an accumulation of damaged proteins in the cell that interfere with cellular function and induce apoptosis<sup>82</sup>. Another potential mechanism of the anti-cancer effects of bortezomib is that through proteasome inhibition it modulates key cellular pathways, such as the nuclear factor  $\kappa$ B (NF- $\kappa$ B) pathway. NF- $\kappa$ B is a family of transcription factors that modulates immune and inflammatory responses. It also plays a role in tumorigenesis by inducing growth and proliferation, suppressing apoptosis, and enhancing tumor cell invasiveness and metastasis. Inhibitor of nuclear factor  $\kappa$ B (I $\kappa$ B) is a protein that binds NF- $\kappa$ B in the cytoplasm and inhibits it from travelling to the nucleus and initiating transcription of growth factors<sup>82</sup>. Normally, proteasome 26S

cleaves I $\kappa$ B, however, administration of bortezomib blocks proteasomal degradation of I $\kappa$ B. I $\kappa$ B is then able to bind and inhibit NF- $\kappa$ B, thereby blocking cell survival activities in tumor cells<sup>82</sup>. Bortezomib may also induce apoptosis in tumor cells by promoting mitochondrial Ca<sup>2+</sup> dysregulation, thereby activating pro-apoptotic mediators: caspase 3, 8, 9 and 12<sup>83</sup>. Although bortezomib affects several key cellular pathways, interference with these pathways likely has numerous downstream effects, which remain to be characterized. Regardless of mechanism, bortezomib shows impressive partial and complete response rates when administered as a single agent<sup>81</sup>.

Bortezomib is typically administered at a dose of 1.3 mg/m<sup>2</sup> or 1.0 mg/m<sup>2</sup> by intravenous bolus or subcutaneously on days 1, 4, 8, and 11 of a 21-day cycle. Patients receive multiple cycles depending on individual response rate. The most common adverse events associated with bortezomib are fatigue, thrombocytopenia, gastrointestinal issues, and sensory neuropathy<sup>81,84-86</sup>. In an initial study, 34% of patients reported new or worsening symptoms of neuropathy with bortezomib<sup>81</sup>. Subsequent trials using bortezomib as a single-agent induction therapy for multiple myeloma reported treatment-emergent sensory neuropathy in 64% of patients<sup>85</sup>. In an analysis of two bortezomib phase II studies with 256 enrolled patients, 90 patients experienced treatment-emergent neuropathy, 5% of patients discontinued treatment due to neuropathic symptoms, and 12% of patients received a dose reduction due to peripheral neuropathy<sup>85</sup>. Bortezomib-induced neuropathy (BIPN) is typically sensory, although motor neuropathy has also been reported<sup>87</sup>. The incidence of peripheral neuropathy varies depending on the trial, grading scales, and detection methods of neuropathy. To increase the efficacy of bortezomib, polymodal therapy has been implemented; bortezomib has been combined with several other agents including

dexamethasone alone, dexamethasone and thalidomide, prednisone alone, melphalan and prednisone and lenalidomide. Richardson et al. reported that multiple therapies do not increase the incidence of reported neuropathy<sup>86</sup>.

Neuropathy is the most clinically relevant side-effect of bortezomib. Due to the prevalence of neuropathy, BIPN provokes dose reduction and/or discontinuation of therapy. The incidence of neuropathy typically increases as patients receive more cycles of chemotherapy and cumulative dose of the drug increases<sup>87</sup>. Furthermore, the most significant risk factor for the development of neuropathy is a previous history of neuropathy<sup>88</sup>. Fortunately, BIPN may be reversible: 60% of cases return to baseline levels of neuropathy within a median of 5.7 months. However, other studies still observe neuropathy at a year following treatment<sup>88,89</sup>. The etiology and mechanisms underlying BIPN are poorly understood. BIPN is debilitating and treatment-limiting and requires further investigation in animal models.

#### **1.4.2 Bortezomib-Induced Neuropathy: Pre-Clinical Studies**

Animal studies have attempted to characterize the pathophysiology of BIPN. Rats treated with bortezomib at a clinically-equivalent dose display neurophysiological and histopathological differences compared to control animals. Sensory nerve conduction velocity is significantly reduced and the sciatic nerve in these rats exhibits damaged Schwann cells and degeneration of myelin, though recovery was observed after 4 weeks. The dorsal root ganglions (DRGs) of these animals showed increased recruitment of satellite cells<sup>90</sup>. Bortezomib-treated animals also have an abundance of ubiquitin-tagged proteins in DRG neurons and signs of abnormal transcription and translation, which likely contributes to sensory neuron dysfunction<sup>91</sup>. Taken together, these data show that bortezomib damages peripheral nerves and their cell bodies, yet



the underlying pathways leading to this destruction are unclear. Despite carefully conducted animal studies, the mechanism by which bortezomib induces neuropathy remains elusive.

### **1.4.3 Other Therapies**

Thalidomide is another chemotherapeutic agent used to treat MM. Thalidomide modulates the immune system to increase natural killer cells and T-cells, inhibiting cytokine production and angiogenesis and inducing apoptosis. Potential mechanisms of thalidomide-induced neuropathy include the down regulation of tumor necrosis factor- $\alpha$  (TNF- $\alpha$ ), which induces demyelination and Wallerian degeneration or direct damage of the DRG<sup>92</sup>. Symptoms include dose-dependent abnormalities in the form of distal paresthesias or dysesthesias and possible weakness. Aside from chemotherapy, autologous stem-cell therapy is usually considered as an option for the treatment of MM and may prolong life if a complete response is attained<sup>93</sup>. The severity of neuropathy induced by chemotherapeutic agents in individual patients dictates the future dose that can be administered. In order to quantify neuropathy, several grading scales have been implemented.

### **1.4.4 Overview CIPN Symptoms and Grading Scales**

Primary afferent neurons and their cell bodies located in the DRG are particularly vulnerable to the toxic effects of chemotherapy because they do not have a protective blood-brain barrier like the CNS. Without the blood-brain barrier, substances in the blood can freely exchange across the walls of DRG and affect primary afferents<sup>92</sup>. In cancer patients this produces an array of sensory disturbances (e.g. numbness, tingling, burning, or dysesthesias) broadly known as chemotherapy-induced peripheral neuropathy (CIPN) that affect the hands and feet in a glove and stocking distribution

<sup>94</sup>. Patients typically present with symptoms consistent with CIPN weeks or months after beginning chemotherapy treatment. Several chemotherapies are notorious for causing CIPN, however the presentation and onset of symptoms varies depending on the drug, perhaps due to mechanistic differences. CIPN is generally thought to improve after chemotherapy treatment has ended; however, the platin family of compounds (e.g. oxaliplatin, carboplatin and cisplatin) is known to cause worsening of symptoms after treatment has been stopped (a phenomenon known as “coasting”) <sup>92</sup>. Bortezomib-treated patients most commonly describe their sensory symptoms as tingling (paresthesia), hypersensitivity (hyperesthesia), numbness (hypoesthesia), abnormal sense of touch (dysesthesia), burning, or pain and their motor symptoms as weakness <sup>95</sup>. Although much less common, some chemotherapies such as bortezomib, may also affect the autonomic nervous system causing orthostatic hypotension, sex organ dysfunction and constipation. For a complete discussion of different chemotherapeutics, the potential mechanisms by which they induce neuropathy, and the quality of neuropathic symptoms induced, see review articles <sup>92,96,97</sup>.

CIPN is challenging to quantify because of the subjectivity of patient and provider reports. Hence several grading systems have been developed in an effort to increase objectivity. Historically, three different grading scales of peripheral neuropathy have been implemented that categorize neuropathy numerically from Grade 0 to Grade 4. These include the World Health Organization (WHO) Common Toxicity Criteria for Peripheral Neuropathy, National Cancer Institute (NCI) Common Toxicity Criteria, and the Eastern Cooperative Oncology Group (ECOG) Grading Scale for CIPN <sup>98</sup>. According to the WHO rating scale, a Grade 0 corresponds to no symptoms of

neuropathy, Grade 1 corresponds to paresthesias (a tingling, tickling or prickling sensation) and/or decreased tendon reflexes, Grade 2 corresponds to severe paresthesias and/or mild weakness, Grade 3 corresponds to intolerable paresthesias and/or marked motor loss and Grade 4 corresponds to paralysis. NCI and ECOG ratings make slight modifications to the WHO rating system. The Total Neuropathy Score (TNS) is slightly different in that it rates patients with a cumulative score ranging from 0 to 32 based on deep tendon reflexes, pin sensation, vibration sense, nerve conduction, and subjective self-report of symptoms from the patient <sup>99</sup>.

Another sensitive, yet non-invasive method of assessing the extent of neuropathy is quantitative sensory testing (QST). QST is a battery of testing administered to patients that measures sensory function in several different modalities and assesses the function of discrete fiber types. Touch detection thresholds measure A $\beta$ -function, temperature thresholds measure function of different populations of A $\delta$ - and C-fibers, and sharp detection thresholds measure A $\delta$ -fiber function. A 2010 study using QST on 1236 neuropathic pain patients in a multi-center study found both loss and gain of sensory function in patients as compared to healthy controls as well as a high degree of heterogeneity between patients in the modalities tested <sup>100</sup>. This emphasizes the complex array of sensory phenotypes attributable to neuropathic pain syndromes that can be differentiated by testing discrete fiber types using QST.

### **1.5. Hypothesis and Specific Aims**

Peripheral neuropathy as a consequence of chemotherapy is a common cause of dose reduction or discontinuation of therapy in cancer patients, thereby limiting treatment and negatively impacting survival. In both human and animal models, treatment with chemotherapeutics is associated with the development of sensory neuropathy and a distal loss of peripheral nerve fibers in glabrous skin <sup>6</sup>. However, it is unclear whether pre-existing subclinical deficits predispose patients to developing chemotherapy-induced peripheral neuropathy and whether pre-clinical therapies utilized in clinical trials will successfully treat CIPN. These studies address the following hypotheses:

**Hypothesis 1:** Multiple myeloma patients exhibit decreases in peripheral innervation and sensory changes that can be quantified prior to chemotherapy treatment.

**Specific Aim 1.1:** Use QST to compare sensory thresholds of multiple myeloma patients to age-and-sex matched healthy volunteers.

**Rationale:** Colorectal cancer patients prior to induction therapy display sensory deficits <sup>153</sup>. Ten percent of MM patients present with overt clinical neuropathy prior to chemotherapy treatment. Sensory thresholds of MM patients that are different from those of healthy volunteers may indicate deficits in the fiber types mediating those modalities. Sub-types of fibers with subclinical deficits may be particularly vulnerable to the effects of bortezomib. A recently published study suggests that pre-existing sensory deficits in MM patients are associated with patient reports of pain and numbness during treatment <sup>107</sup>. In addition, research

suggests that pre-existing neuropathy puts patients at risk for developing treatment-emergent neuropathy.

**Specific Aim 1.2:** Determine if MM patients exhibit decreases in peripheral innervation. Correlate densities of touch receptors (Meissner's corpuscles) to performance on fine tactile discrimination tasks in MM patients and volunteers using non-invasive confocal microscopy .

**Rationale:** Pre-clinical studies in animals and biopsies in patients indicate that sensory neuropathy is and neuropathic-like symptoms are associated with a dearth of nerve fibers in distal glabrous skin.

In addition to subclinical deficits likely caused by disease-related processes, studies demonstrate that chemotherapy administration induces or exacerbates sensory deficits. The development and application of preventative treatments would be useful to avoid this detrimental and dose-limiting side effect. Minocycline is a tetracycline antibiotic with neuroprotective properties that reduces hypersensitivity and spares primary afferent fibers in rodent models of CIPN.

**Hypothesis 2:** Oral minocycline administered with the chemotherapeutic agent, bortezomib, will prevent sensory neuropathy induced by bortezomib and decrease patient-reported outcomes of neuropathy.

**Specific Aim 2.1:** Assess the efficacy of 200 mg/day oral minocycline HCL in preventing bortezomib-induced neuropathic pain in multiple myeloma patients by measuring sensory thresholds using QST and assessing patient reports of

tingling and numbness in a randomized, double-blind placebo-controlled, clinical trial.

**Rationale:** Minocycline has neuroprotective properties in preclinical studies investigating both spinal cord injury-induced and chemotherapy-induced neuropathic pain.

## **2. Subclinical peripheral neuropathy in multiple myeloma patients prior to chemotherapy is correlated with decreased fingertip innervation density**

*Chapter 2 is adapted from the publication Kosturakis et al., Subclinical peripheral neuropathy in multiple myeloma patients prior to chemotherapy is correlated with decreased fingertip innervation density, Journal of Clinical Oncology (Accepted).*

### **2.1. Introduction**

The goal of this study was to quantify sensory deficits MM patients exhibit prior to receiving chemotherapy to address Hypothesis 1 of this thesis.

MM patients typically seek care with signs of renal insufficiency, anemia and bone lesions<sup>101</sup>. Bone lesions occur due to bone resorption and include lytic abnormalities or diffuse osteopenia, both of which lead to increased calcium in extracellular fluid and may cause hypercalcemia. Renal failure can occur due to non-paraprotein-related causes (e.g., hypercalcemia, nephrotoxic drugs, dehydration, hyperviscosity, and myeloma cell infiltration) or paraprotein-related causes (e.g., cast nephropathy, amyloidosis, light chain deposit disease or Fanconi syndrome). Anemia in MM patients is usually caused by treatment with chemotherapeutics, deficient production of erythropoietin, and tumor infiltration of the bone marrow.

Overt neurological complications may also occur from tumor invasion into the vertebral space that compresses the spinal cord, cranial nerves or nerve roots, intracranial invasion of tumor and metabolic derangements<sup>102,103</sup>. Clinically significant peripheral neuropathy without clear etiology prior to treatment is reported in 5 to 20% of patients<sup>89,102,104,105</sup>. The incidence of CIPN affects approximately 70% of patients,

depending on the therapeutic agent<sup>104,105</sup>. In fact, the development of treatment-emergent peripheral neuropathy is the most common cause of dose reduction or discontinuation of chemotherapy, potentially impacting survival<sup>86,106</sup>. The proteasome inhibitor bortezomib (Velcade<sup>®</sup>) is a common treatment for MM and is associated with high rates of peripheral neuropathy that may become chronic and refractory to treatment<sup>89,105</sup>.

Given the potential profound impact of neurological complications on disease treatment and quality of life, interest has centered on identifying means to avoid the occurrence of treatment-related neuropathy in MM patients. QST are a series of non-invasive measures capable of detecting deficiencies in sensory nerve fiber function. In one recently published study, the presence of subclinical sensory deficits in MM patients was suggested as predictive of the development of CIPN<sup>107</sup>. While patients with pre-treatment impairments in sharpness detection (a test assessing A $\delta$ -fiber function) were at decreased risk for developing CIPN, baseline impairments in warmth detection (a test assessing C-fiber function), were associated with more severe pain and numbness after chemotherapy treatment<sup>107</sup>.

Biopsies collected from glabrous skin sites in patients treated with chemotherapy show decreases in peripheral innervation, including loss of both intraepidermal nerve fibers and Meissner's corpuscles (MCs)<sup>89</sup>. MCs are rapidly adapting cutaneous receptors that detect tactile stimuli moving at frequencies of 30 to 50 Hz<sup>9</sup>. This sensation can be described as "flutter." Non-invasive in vivo confocal microscopy is a novel imaging technique for visualizing the epidermis and superficial dermis that allows clear identification of MCs within dermal papillae. MC density assessed by in vivo confocal microscopy is well correlated to MC density assessed by



skin biopsy<sup>108</sup>. The goals of this study were to quantify the sensory changes in MM patients prior to chemotherapy treatment, thereby determining the prevalence of subclinical peripheral neuropathy and to correlate impairments in touch thresholds with decreased peripheral innervation density assessed with in vivo laser reflectance confocal microscopy.

## **2.2. Subjects and Methods**

### **2.2.1 Patients and Volunteers**

Twenty-seven patients with no previous symptoms, complaints of peripheral neuropathy or clear risk factors for neuropathy were recruited into this study through the Multiple Myeloma Clinic at The University of Texas MD Anderson Cancer Center. A group of 30 age- and sex-matched healthy volunteers recruited from the institution staff provided comparative data. All subjects provided informed consent to participate in the research protocols that had been reviewed and approved by the Institutional Review Board of the MD Anderson Cancer Center.

### **2.2.2 Quantitative Sensory Analysis**

Quantitative sensory analysis was performed as previously described<sup>89,108,109</sup>. Based on the distribution of sensory disturbances that have been documented in CIPN<sup>89,109</sup>, three areas, the fingertip, thenar eminence (palm) and volar surface of the forearm (forearm), were selected for sensory testing. The dermatomes that correspond to the fingertip, thenar eminence and volar forearm are C6, C6, and either C6 or C8, respectively<sup>110</sup>.

### **2.2.3 Touch Detection Thresholds and Grooved Pegboard Test**

Touch detection thresholds were determined using von Frey monofilaments (Semmes-Weinstein) (Figure 3) in an up/down manner<sup>89,109</sup>. Starting with a bending force of 0.02 grams, each filament was applied to the skin for approximately 1 second in each of the three test sites mentioned above. During this test, subjects were instructed to close their eyes or look away so that they did not see the application of the filament. If the subject failed to detect the stimulus, the next higher force was applied to the same location. When the subject detected the presence of the stimulus, the next lower force was administered. This procedure continued until the same filament was detected for three applications, and the associated force was considered the touch detection threshold.

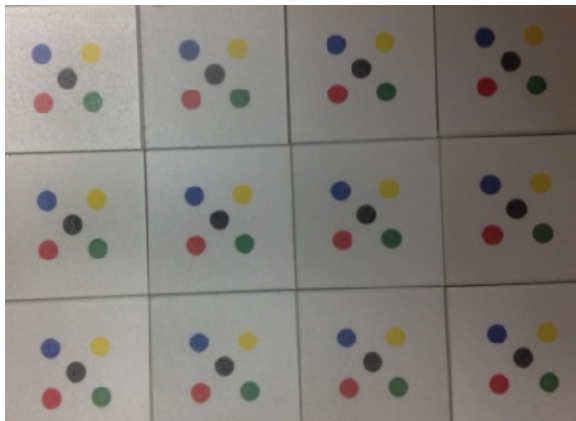
To assess fine touch discrimination, a second method based on the detection of minute elevations (bumps detection) on a smooth surface was employed<sup>89,111</sup>. The bumps device consists of three etched glass plates (11.5 cm x 15 cm), each of which contains twelve 1.5 x 1.5 inch squares (Figure 4). Within each square are 5 flat circles, each of a different color. Located over one of the circles within each square is a bump that is 550  $\mu\text{m}$  in diameter. Bumps on plate 1 vary from 2.5 to 8.0  $\mu\text{m}$  in height, bumps on plate 2 vary from 8.5 to 14.0  $\mu\text{m}$  in height, and bumps on plate 3 range from 14.5 to 26  $\mu\text{m}$  in height. Participants began each session using bumps that ranged from 8.5 to 14  $\mu\text{m}$ . Subjects were instructed to use the index finger of the dominant hand to explore the five circles within each square. Patients were unable to see the location of the bump and reported to the examiner which color they perceived the bump to be located on. If participants could correctly identify the location of bumps on plate 2, they progressed to plate 1 (2.5 to 8  $\mu\text{m}$ ). Patients unable to detect the location of bumps on

plate 2 were presented with plate 3 (14.5 to 26um). The Bumps detection threshold was determined to be the smallest bump correctly identified in sequence to the next two higher bumps <sup>111</sup>.



**Figure 3 Touch Detection Assessed With Von Frey Monofilaments**

Monofilaments based on the Semmes-Weinstein monofilament set. When pressed against the skin in sequence (from smallest to largest), these filaments apply an approximately logarithmic scale of actual force and a linear scale of perceived intensity.



**Figure 4 Fine Tactile Discrimination Assessed With the Bumps Detection Plate**

A bump of known size ranging from 2.5 to 26  $\mu\text{m}$  was present in one of the five colored circles in each square. Subjects reported the color that corresponded to the location of the bump.

Manual dexterity was assessed with the grooved pegboard test (Figure 5) <sup>112</sup>. Patients were instructed to fill a 5 × 5 slotted pegboard in an ordered fashion, either across rows or down columns. The time a subject took to complete the board was measured for both dominant and non-dominant hands. A faster time indicated greater dexterity <sup>112</sup>.

#### **2.2.4 Sharpness Detection Threshold**

The ability to detect sharpness was determined using weighted needle devices of 8, 10, 16, 20, 30, 32, 64, and 128g (Figure 6) <sup>113</sup>. Each stimulus was applied for 1 second in ascending order using a modified Marstock method <sup>114</sup>. The subjects were instructed to state whether the sensation produced by each stimulus was that of touch, pressure, sharpness, or pain. The sharpness detection threshold was the weight corresponding to the sensation of “sharp” or “painful.” Sharpness was measured in three separate trials separated by an average interval of 30 to 90 seconds. The average of three trials was the recorded sharpness detection threshold.



**Figure 5 Manual Dexterity Assessed with Grooved Pegboard Test**  
A grooved pegboard with irregularly shaped slots oriented at different angles and pegs.

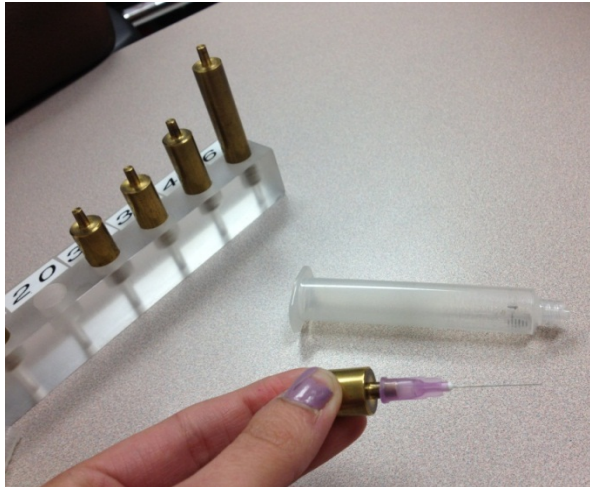


**Figure 6 Weighted, Blunted Needle Assessed Sharpness Detection**

A blunted needle and attached weight were inserted into a plastic tube. The needle was applied to the test site and freely moved in the barrel of the plastic tube so that the associated weight was applied. Patients were instructed to report whether they perceived touch, pressure, sharp or pain. End points for sharpness detection were reports of pain or sharp.

### **2.2.5 Heat and Cold Detection Thresholds**

Warmth detection and heat pain threshold were determined by applying heat stimuli to the testing site with a 3.6 by 3.6-cm Peltier probe (Figure 7)<sup>89,109</sup>. The baseline temperature of the probe was set at 32°C and the temperature increased at a rate of 0.30°C/second. Subjects signaled when the probe was first perceived as warm and then, painful. The trial was subsequently terminated and the probe returned to baseline temperature. The final warmth detection and heat pain threshold for each site was defined as the mean of three trials that were separated by an average of 30 to 90 seconds. If a subject failed to perceive warmth or heat pain, the cutoff temperature of 52°C was recorded as the default.

The threshold to detect cooling of the skin (cool threshold) and then cold pain (cold threshold) was determined as described above, except that the temperature decreased at a rate of 0.50°C per second. If a subject failed to perceive cold pain, the cutoff of 3°C was recorded as the default value.

### **2.2.6 Skin Temperature**

Skin temperature was measured using a radiometer placed gently against the skin for approximately 2 seconds (Figure 8).



**Figure 7 Peltier Thermode Probe Assessed Temperature Thresholds**

A thermode was applied to the testing site and increased or decreased in temperature to assess warm detection, heat pain, cool detection, and cold pain.

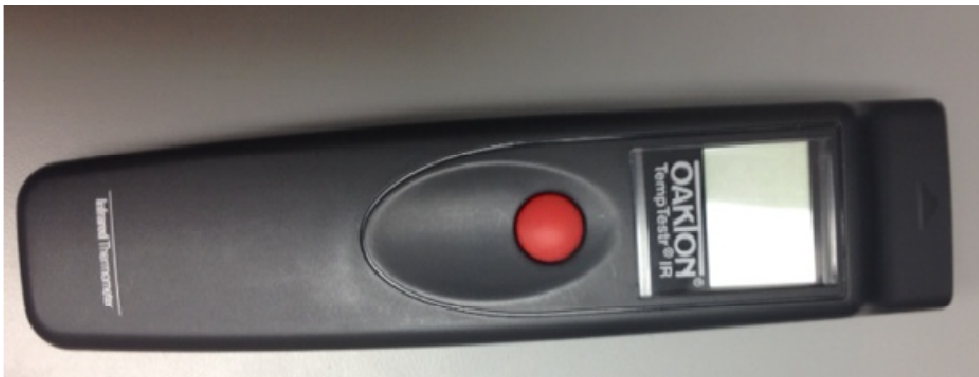


**Figure 8 Skin Temperature Radiometer**

Skin temperature at the testing sites was assessed using a radiometer



### **2.2.7 Imaging and Meissner's Corpuscle Quantification**

In vivo confocal imaging was performed on the skin of 12 patients and 10 healthy controls using Lucid Vivascope 1500 as previously described (Figure 9) <sup>108</sup>. The microscope was centered on the tip of the fifth digit over a plastic ring and produced an image with a 2.0 mm by 2.0 mm field of view. Skin architecture was assessed using a stack of four images with a vertical resolution of 3 to 5  $\mu\text{m}$  at different depths (z plane = 20  $\mu\text{m}$ ). MCs were quantified at the depth that was most easily visualized by a research assistant blinded to the study group. Images that were 4.0 mm<sup>2</sup> were divided into four quadrants and MCs were quantified on one randomly chosen quadrant. Meissner's corpuscles were identified as round light-colored structures 40 to 60  $\mu\text{m}$  in diameter located in dermal papillae as previously described <sup>108</sup>.



**Figure 9 Lucid Vivascope 1500 Non-Invasive Confocal Scanner**

The lens was attached to the site of interest and the non-invasive confocal scanner obtained a series of images of different layers of skin. The scanner produced a stack of four 2.0 mm x 2.0 mm images taken at depths that varied by 20  $\mu\text{m}$ . The density of the touch receptors, Meissner's corpuscles, were visualized as round, light colored structures and quantified on one of the images.

### **2.2.8 Statistical Analysis**

Comparisons of sensory and sensorimotor thresholds were performed between volunteers and patients by first, evaluating for normality using the Shapiro-Wilk test and then, using the non-parametric Wilcoxon signed-rank test. Results are reported as mean  $\pm$  standard error of the mean. Correlations were performed with the non-parametric Spearman's Rank-Order correlation. For every comparison,  $P < 0.05$  was considered significant.

## **2.3. Results**

### **2.3.1 Study group**

Patient characteristics are presented in Table 3. None of the patients had a history of chemotherapy treatment, AIDS, diabetes or irradiation exposure that might have contributed to the development of neuropathy. All QSTs on patients were collected before chemotherapy had been initiated. Healthy volunteers had no exposure to equipment or testing procedures prior to undergoing QST. QST and scans were collected by a study coordinator who did not participate in the data analysis.

Patient demographics (n=27)		
Characteristic	<i>n</i>	%
Age-years, mean (SD)	60.4 (9.7)	
Gender		
Male	13	48.1
Female	14	51.9
Race		
White	20	74.1
Black	5	18.5
Hispanic	2	7.4
International Staging System		
Stage I	11	40.7
Stage II	10	37.0
Stage III	6	22.3
Amyloidosis		
Yes	3	11.1
No	24	88.9

SD= Standard Deviation

**Table 3 Patient Demographics**

### 2.3.2 Touch Detection Thresholds and Grooved Pegboard Times

Touch detection thresholds, a gauge of A $\beta$ -fiber function<sup>115-117</sup> were obtained using von Frey monofilaments. Touch detection was higher (implying impairment) at the thenar eminence and the volar forearm, but not the fingertip, in the MM patients as compared to healthy volunteers (Figure 10A). Specifically, the touch detection thresholds in the palm and the forearm were  $0.26\pm 0.03\text{g}$  and  $0.32\pm 0.04\text{g}$  in the volunteers, whereas the respective values for MM patients at these sites were  $0.52\pm 0.07\text{g}$  ( $P<0.01$ ) and  $0.56\pm 0.10\text{g}$  ( $P<0.05$ ). Importantly, patients exhibited significant impairment in Bumps detection (Figure 10B). The mean Bumps detection threshold for MM patients was  $6.30\pm 0.86\ \mu\text{m}$  but only  $3.37\pm 0.38\ \mu\text{m}$  for the volunteers ( $P<0.01$ ). Thus, the Bumps test was more sensitive than von Frey monofilament in detecting impaired touch sensation at the fingertip.

Patients also showed a pronounced impairment in the sensorimotor slotted pegboard task (Figure 10C). The completion times for the dominant hand were  $69.36\pm 2.56$  seconds for volunteers and  $90.63\pm 6.60$  seconds for patients; ( $P<0.01$ ). The respective values for the non-dominant hand were  $74.30\pm 3.08$  seconds and  $86.33\pm 3.20$  seconds; ( $P<0.01$ ). Combined, these findings indicate that MM patients with no outward signs or symptoms of neuropathy have impaired A $\beta$ -fiber function and dexterity prior to chemotherapy.

### 2.3.3 Sharpness Detection Thresholds

The results of the sharpness detection task are shown in Figure 10D. Sharpness detection is a measure of A $\delta$ -fiber function. No significant deficits in sharpness detection were observed between the patient and the volunteer groups, suggesting that MM does not alter this subset of A $\delta$ -fibers.

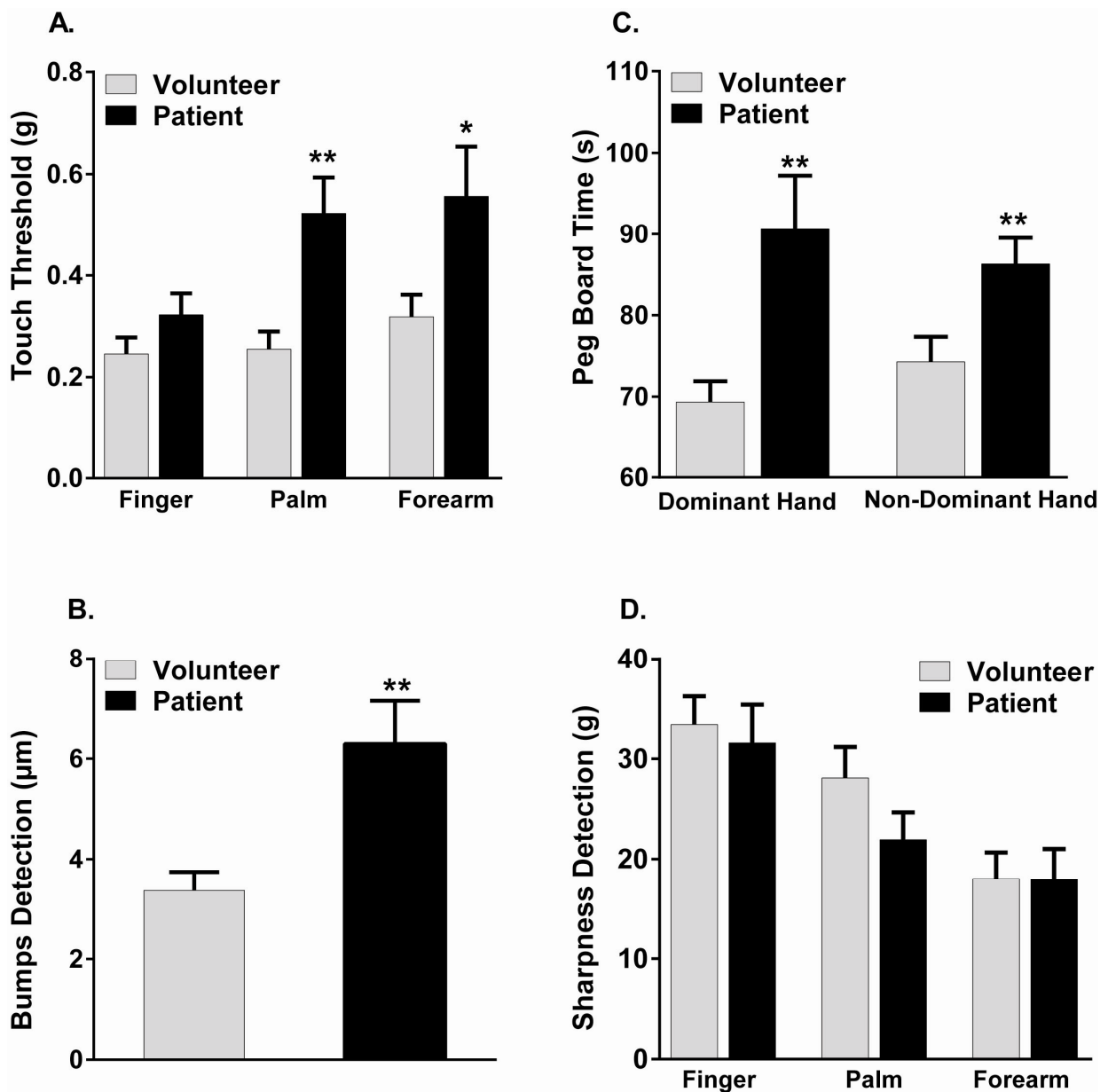


**Figure 10 MM Patients Show Differences in Touch Detection and Peg Board Performance, But Not Sharpness Detection**

To assess mechanosensation, touch and bumps detection tests were employed (A&B). Subjects completed the grooved pegboard as an assessment of sensorimotor performance (C). Weighted-blunted needles assessed the ability to detect sharp (D). The bar graphs show the mean values (and standard errors) of sensory tests for multiple myeloma patients (black bars) and healthy volunteers (gray bars). (A) Touch detection (g) determined with von Frey monofilaments measured Aβ-fiber function. (B) Dominant and non-dominant hands in completing the slotted pegboard task (s) measured sensorimotor function. (C) Bumps detection (µm) was performed using the index finger of the dominant hand and measured fine tactile discrimination. (D) Sharpness detection threshold (g) measured Aδ-fiber function.

\*=  $P < 0.05$ , \*\*=  $P < 0.01$

### 2.3.4 Skin Temperature and Thermal Detection Thresholds

Baseline skin temperature was significantly higher at the thenar eminence, but not at the other test sites (patients  $34.56 \pm 0.24$  °C vs.  $33.66 \pm 0.35$  °C) ( $P < 0.05$ ) (Figure 11A). Figure 11 also shows differences between the groups in detection thresholds for heat and cold. The MM patient group showed significantly higher ( $P < 0.05$ ) thresholds for warmth detection across all three test sites (patients—fingertip:  $39.45 \pm 0.38$  °C ( $P < 0.01$ ), thenar eminence:  $37.83 \pm 0.29$  °C ( $P < 0.01$ ), volar forearm:  $37.78 \pm 0.34$  °C ( $P < 0.05$ ) vs. volunteers—fingertip:  $37.90 \pm 0.45$  °C, thenar eminence:  $36.72 \pm 0.26$  °C, volar forearm:  $36.54 \pm 0.40$  °C) (Figure 11B). Heat pain threshold was similar between groups at all sites. Heat threshold at the fingertip occurred at the expected range of 45 to 47°C. Heat thresholds were slightly lower at the thenar eminence and volar forearm of both MM patients and healthy volunteers due to inherent differences in the sensitivity at the testing site (Figure 11B). The threshold to detect innocuous cool sensation was comparable between the patients and volunteers (Figure 11C). However, cold pain thresholds were significantly elevated at the thenar eminence and volar forearm of MM patients. Mean cold pain thresholds for patients vs. volunteers were  $14.67 \pm 1.55$  °C vs.  $7.33 \pm 1.10$  °C at the thenar eminence ( $P < 0.001$ ), and  $13.31 \pm 1.62$  °C vs.  $7.46 \pm 1.04$  °C at the volar forearm ( $P < 0.01$ ) (Figure 11C).

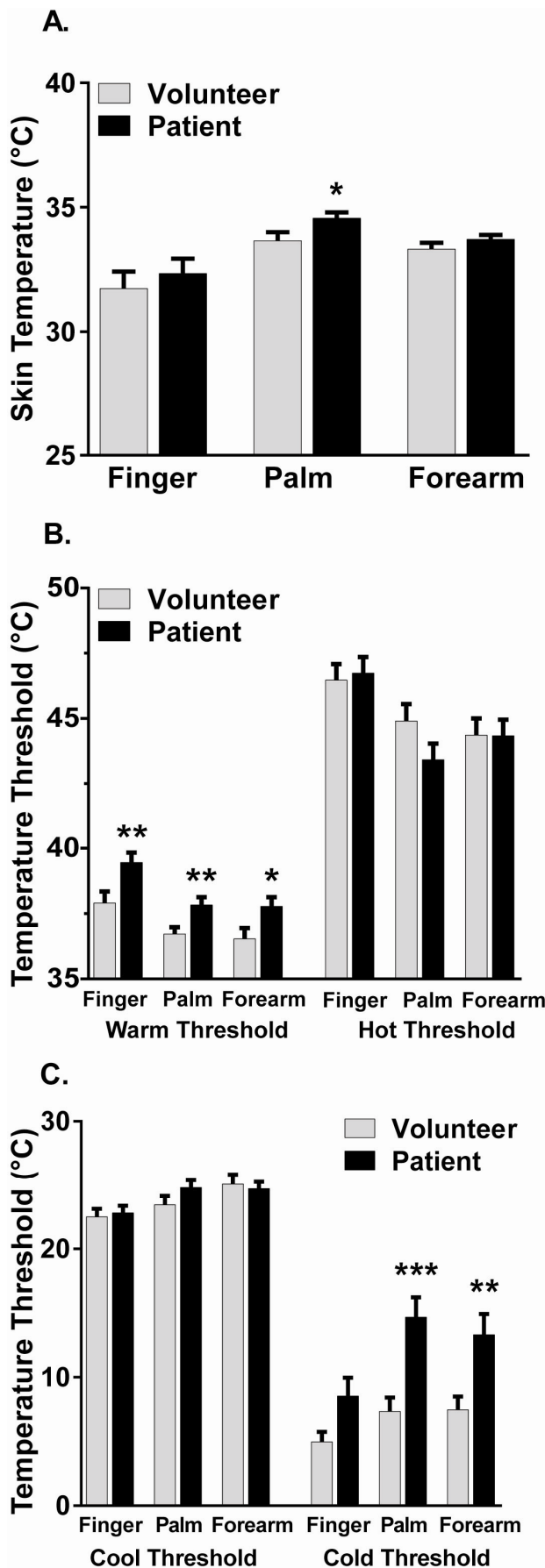


**Figure 11 MM Patients Show Differences in Skin Temperature and Thermal Detection Thresholds**

The bar graphs show the mean (and standard error) (A) baseline skin temperature and (B&C) thermal detection thresholds (°C) for MM patient (black bars) and volunteer (gray bars) groups. (B) Warm detection (left hand bar group) and heat pain threshold (right hand bar group). (C) Cool detection (left hand bar group) and cold pain threshold (right hand bar group).

\*=  $P < 0.05$ , \*\*=  $P < 0.01$ , \*\*\* =  $P < 0.001$



### **2.3.5 General Neuropathy Score**

An overall neuropathy score was generated for each patient and volunteer by summing the number of observations for each subject where any of the measures listed above were greater than 2 standard deviations from the mean of the volunteer dataset. In total, 22 of 27 (81.5%) patients vs. 10 of 30 (33.3%) of healthy volunteers had at least one out-of-range measure (Figure 12). Patients had a mean of  $2.48 \pm 0.34$  observations of out of range measures. In contrast, volunteers had a mean  $0.60 \pm 0.19$  out-of-range observations ( $P < 0.0001$ ) (Figure 12).

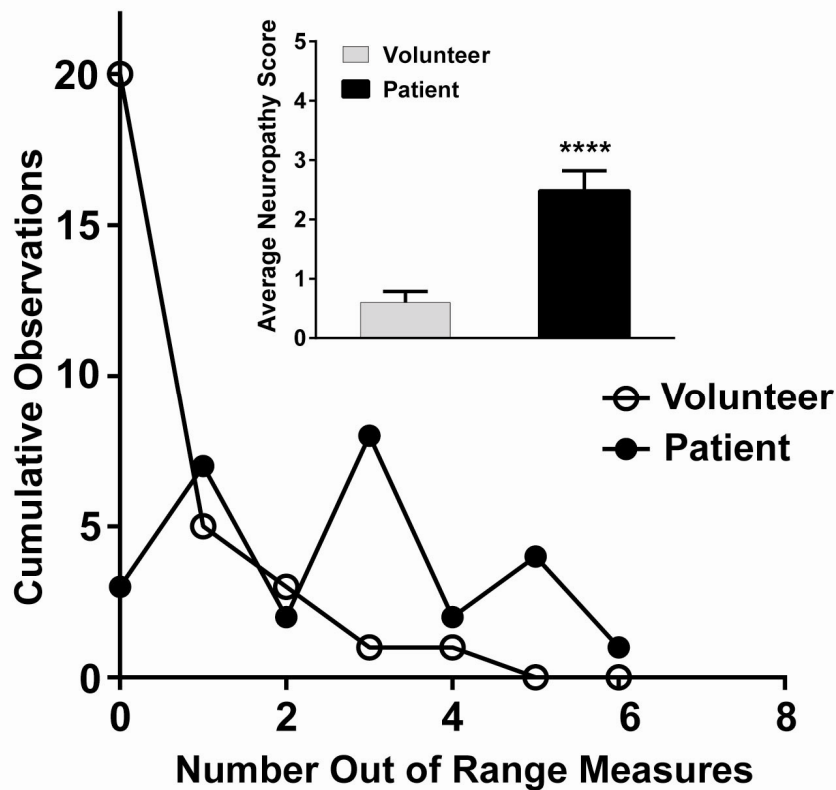


**Figure 12 Greater Numbers of MM Patients Displayed Out-of-Range Measures Compared to Volunteers**

The scatter and line plot shows the number of out-of-range measures (measures more than 2SD outside the mean) present in individual subjects (cumulative observations). (open symbols: healthy volunteers; solid symbols: patients). The inset bar graph shows the mean out-of-range QST observations for volunteers (gray bar) and MM patients (black bar).

\*\*\*\* =  $P < 0.0001$

### 2.3.6 Quantification of Meissner's Corpuscles

A subset of thirteen MM patients and ten healthy volunteers underwent non-invasive confocal imaging of the fingertip of the fifth digit (Figure 13A). Two MM patients underwent one repeat scan three months after the first scan, for a total of 15 patient images that were quantified. To correlate Bumps score with MC density, Bumps detection was performed in this patient subset. Patients had a significantly higher mean Bumps score than healthy controls ( $5.73 \pm 0.78 \mu\text{m}$  and  $3.50 \pm 0.53 \mu\text{m}$  respectively,  $P < 0.05$ ). Confocal images showed that patients had a decreased mean density of MCs as compared to controls ( $2.63 \pm 0.28 \text{ MCs}/\text{mm}^2$  vs.  $4.88 \pm 0.62 \text{ MCs}/\text{mm}^2$ ,  $P < 0.01$ ) (Figure 13B). The Spearman's Rank-Order correlation was used to assess the linear relationship between MC density and Bumps detection threshold. As Bumps detection threshold increased, MC density decreased ( $\rho = -0.69$ ,  $P < 0.001$ ) (Figure 13C).

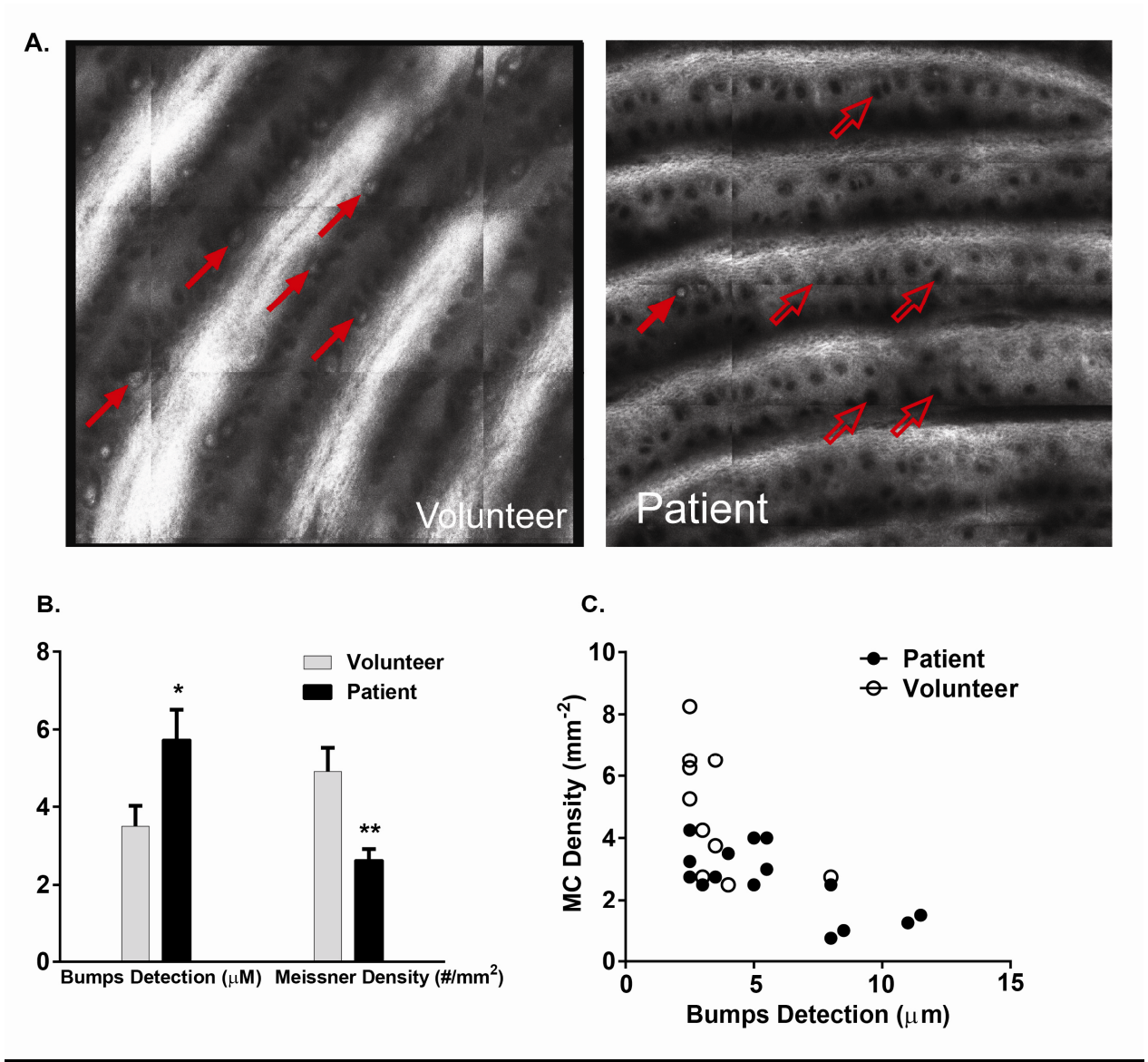


### Figure 13 Inverse Correlation Between Meissner's Corpuscle Density and Touch Detection

(A) Representative healthy volunteer and patient images of 1.0 X 1.0 mm in vivo laser reflectance confocal micrograph. In the volunteer image, numerous Meissner's corpuscles (MCs) can be seen as white orb shaped structures sitting in the base of the dermal papillae (dark circles). Several MCs are indicated by red arrows. Unfilled arrows demarcate several of many dermal papillae missing MCs. One MC is visible in the patient image. Light color bands are the elevated fingertip ridges. (B) Mean (and standard error) Bumps detection score and MC density for a subset of MM patients (black bar) and healthy volunteers (gray bar). (C) The inverse correlation between Bumps detection threshold and MC density in patients and volunteers is illustrated in the scatter plot. As Bumps detection threshold increases, MC density decreases (overall,  $\rho=0.69$ ,  $P < 0.001$ ).

\*=  $P < 0.05$ , \*\*= $P < 0.01$

## **2.4. Discussion**

The results shown here indicate that subclinical sensory dysfunction consistent with early onset neuropathy is highly prevalent in patients with MM prior to chemotherapy treatment. Impairments were observed in low-threshold mechanosensation, sensorimotor tasks and in thermal detection, consistent with dysfunction in A $\beta$ -, A $\delta$ - and C-primary afferent fibers<sup>118-121</sup>. MC density on confocal scans was similar to MC density quantified in skin biopsies, which suggests that in vivo confocal microscopy is a non-invasive, quantitative method to assess MC density<sup>108</sup>. Patients showed decreased densities of MCs by confocal imaging that were negatively correlated with their ability to detect small bumps in the Bumps detection test. These data suggests that a decrease in tactile sensitivity is well correlated with MC density as visualized by in vivo confocal imaging and is consistent with studies comparing Bumps threshold to MC density quantified in skin biopsy<sup>118</sup>. Taken together, this suggests that nervous system complications are more prevalent in chemotherapy-naïve MM patients than previously appreciated.

Neurological complications in MM are multifaceted. The most common neurologic involvement is radicular pain due to spinal cord or nerve root compression following lytic bone lesions<sup>121</sup>. Consistent with the findings reported here, electrophysiological assessments prior to therapy reveal that roughly one third of newly diagnosed MM patients have evidence of peripheral nerve involvement<sup>121,122</sup>. The increased incidence of patients identified with subclinical neuropathy here is simply due to the higher sensitivity for quantitative sensory tests to reveal nerve fiber dysfunction than electrophysiological methods. The important implication in this work is that pre-treatment sensory deficits likely predispose patients to develop drug-

induced neuropathy because CIPN occurs more frequently and manifests more severely in patients with existing neuropathy<sup>106,107,123</sup>.

Neuropathy prior to treatment in MM patients implicates mechanisms based on individual and disease-related factors. In part, the patient cohort affected by MM is largely an elderly patient population diagnosed at a median age of 66<sup>124</sup>. Advanced age is associated with a decline in innervation density (e.g. density of MCs)<sup>125,126</sup>. This factor was accounted for with an age-match of the non-patient volunteers, indicating that a disease-related process is linked with a decrease in MCs in MM patients. Despite having a similar age, healthy volunteers had significantly more distal fingertip innervation than patient counterparts evidenced by higher MC density. MC density visualized on confocal scans was correlated with fine tactile discrimination. Of note, healthy volunteers with varying numbers of MCs were able to discern the smallest bump during the Bumps test. Thus, individuals with the highest density of MCs may have been able to detect bumps smaller than 2.5  $\mu\text{m}$  (the smallest bump used in the QST) creating a floor effect in the data and a dampened correlation between MCs and tactile discrimination. Despite the presence of a floor effect, individuals who performed worse on the tactile discrimination test had lower densities of MCs and more sensory abnormalities consistent with sensory neuropathy. These data suggests that in vivo confocal imaging may be a novel and sensitive method for early detection of sensory deficits consistent with neuropathy. Although this technology is a potentially useful tool to quantify peripheral innervation, several limitations of this technology warrant mention. MC innervation is composed of at least two types of C-fibers and both unbranched and branched A $\beta$ -fibers. It is not clear how long the structure of MCs can persist in the absence of innervation by myelinated and unmyelinated sensory fibers,

or whether MC structure depends on both or one type of innervation. While the density of MCs is easily quantifiable with in vivo confocal microscopy, innervation of the structures cannot be assessed in these images.

Contributions of the disease process to the generation of neuropathy are well documented as overt clinical signs secondary to the plasma cell dyscrasia (particularly in POEMS syndrome), or the result of compression of the nerve roots, cryoglobulinemia or light chain deposits from amyloidosis<sup>102,127</sup>. Amyloidosis refers to precipitation of normally soluble protein due to abnormal folding. The most common type of amyloidosis is light-chain amyloidosis (AL) and is associated with multiple myeloma. In AL, light chains become unstable and self-aggregate forming amyloid fibrils in tissues. This can lead to painful, bilateral sensory neuropathy with progressive motor involvement<sup>128</sup>. POEMS is an acronym that stands for polyneuropathy, organomegaly, endocrinopathy, M-protein, and skin abnormalities and refers to a rare monoclonal plasmaproliferative disorder associated with osteosclerotic myeloma<sup>129</sup>. Similar to MM, POEMS patients have monoclonal light chains or immunoglobulins in their serum, urine, or bone marrow, and typically suffer from a symmetrical neuropathy due to demyelination and axonal loss of primary afferents<sup>130</sup>. The development of neuropathy in POEMS patients may be due to the secretion of cytokines (e.g. vascular endothelial growth factor (VEGF), IL-6, and TNF- $\alpha$ ) from abnormal plasma cells and plasmacytomas<sup>131</sup>. A similar mechanism may be driving the neuropathy in multiple myeloma patients. In support of this perspective, MM typically show elevated plasma cytokines including elevations in TNF- $\alpha$  and IL-6<sup>132,133</sup>.

Systemic or perineural administration of TNF- $\alpha$  or IL-6, induces mechanical allodynia and thermal hyperalgesia<sup>134-137</sup> and an increase in the expression of these

pro-inflammatory cytokines following nerve injury is observed in and around peripheral nerves and in the DRG<sup>138-140</sup>. Peripheral blockade of pro-inflammatory cytokines prevents the development of both inflammatory and neuropathic pain. Several mechanisms by which pro-inflammatory cytokines influence the function of primary afferent neurons have been described<sup>137,141-145</sup>. TNF- $\alpha$  has a rapid, sensitizing effect on primary afferent neurons resulting in heat-induced CGRP release from nociceptor terminals in skin and a lowered activation threshold in A $\beta$ - and C-fibers<sup>146-148</sup>; mediated at least in part by sensitization of the TRPV1 and TTX-resistant sodium channels<sup>149</sup>. IL-6 has similarly sensitizing effects on primary afferent fibers through both its own receptor mediated signaling as well as by potentially inducing TNF- $\alpha$ <sup>150</sup>

Kelly *et al.* suggested that neuropathy associated with disease in myeloma is a heterogeneous entity resembling carcinomatous neuropathy and that treatment of myeloma does not affect the course of neuropathy<sup>151</sup>. Others have noted that a number of common disorders of the peripheral nervous system, termed paraproteinemic neuropathies, are closely connected with the presence of excessive amounts of an abnormal immunoglobulin in the blood<sup>152</sup>. In at least some patients, these antibodies are directed at components of myelin or the axolemma, resulting in complement mediated damage to Schwann cells and axons<sup>152</sup>. Yet, baseline testing of colorectal cancer patients with no clinical evidence or reported symptoms of neuropathy prior to chemotherapy revealed subclinical peripheral neuropathy is a surprisingly common occurrence (an incidence of 46 of 52 subjects) in this type of cancer as well<sup>153</sup>. This suggests that cancers in general engage biological responses that impair nerve function. Given the strong connection between pre-existing



neuropathy and its exacerbation by disease treatment, these findings underscore the need for careful screening and individualized treatment plans for patients at risk.

### **3. Preliminary analysis of a phase I study of minocycline vs. placebo to prevent treatment-induced neuropathy in multiple myeloma**

#### **3.1. Introduction**

To address Hypothesis 2 of this thesis, the goal of this section was to investigate whether the antibiotic, minocycline, administered orally during the course of bortezomib treatment, would prevent sensory neuropathy induced by bortezomib and decrease patient-reported symptoms of neuropathy. Below is an overview of minocycline and its potential utility in preventing or treating neuropathic pain and neurodegenerative disorders.

Neuropathic pain is a catch-all description for a spectrum of abnormal sensory symptoms that arise due to peripheral or central nervous system damage and can affect diverse areas of the body depending on the underlying root cause <sup>45</sup>. As discussed in Chapter 1, CIPN is a side-effect of chemotherapy that interferes with quality of life for patients and compels providers to scale back chemotherapeutic dose. Neuropathic pain conditions, including CIPN, are often chronic and debilitating medical conditions that are either incompletely managed by, or refractory to opioids and medications purposed to treat neuropathic pain (e.g. gabapentin and pregabalin) <sup>154</sup>. Chemotherapy is a scheduled, non-emergency treatment. The most efficient treatments for CIPN will be preventative measures, rather than reactive medications to treat already established symptoms of neuropathy. The search for more efficacious treatments with improved side effect profiles is warranted.

Minocycline is an FDA-approved tetracycline-derived antibiotic predominately used in the treatment of acne vulgaris. Minocycline is part of a larger class of tetracyclines, considered broad-spectrum antibiotics effective in eradicating both gram-

positive and gram-negative bacteria. Tetracyclines interfere with bacterial protein production by binding to the bacterial 30S ribosome subunit and inhibiting translation of mRNA into polypeptide chains <sup>155</sup>. Minocycline is a second-generation tetracycline, chemically engineered to have increased absorption and bioavailability due its lipophilic properties and effectively crosses the blood-brain barrier <sup>156</sup>. In addition to well-documented efficacy as an antibiotic, there is a large body of literature that indicates that minocycline can be used to treat an array of diseases and conditions through its diverse properties. In the past twenty years, minocycline has been shown to have anti-inflammatory, immunomodulatory, and neuroprotective effects in both clinical and pre-clinical studies that suggest a potential therapeutic effect in the treatment of rheumatoid arthritis, ischemia, aortic aneurysms, cancer metastasis, traumatic brain injury, spinal cord injury, Parkinson's disease, Huntington's disease, multiple sclerosis and neuropathic pain, among others.<sup>155</sup>. The neuroprotective properties of minocycline have been attributed to cellular actions, including the ability to inhibit microglial activation, microglia-induced release of pro-inflammatory cytokines, apoptosis, as well as its anti-oxidant properties <sup>157</sup>. In rodent models of CIPN, pre-treatment with minocycline attenuates hypersensitivity, prevents the loss of intraepidural nerve fibers, the activation of astrocytes and the downregulation of astroglial glutamate transporters, GLAST and GLT-1. Furthermore, the use of minocycline as a neuroprotective agent has yielded favorable results in several clinical studies with minimal adverse events <sup>158,159</sup>. Spinal cord injury patients treated with minocycline showed improvement in motor performance in a phase II placebo-controlled randomized trial, though statistical significance was not achieved <sup>160</sup>. Pre-clinical literature indicates that minocycline can prevent the onset of neuropathic pain,

but cannot reverse pre-established neuropathic pain, making its application ideal as a preventative treatment <sup>161</sup>. These findings, combined with its success in preventing the development of CIPN in rodents <sup>162,163</sup> suggests that minocycline may be an attractive candidate for use in the clinical treatment of CIPN.

As previously discussed in section 1.4, treatment of multiple myeloma with the frontline-chemotherapeutic agent, bortezomib, causes dose-dependent sensory neuropathy as a side-effect <sup>86</sup>. Bortezomib-induced neuropathy (BIPN) causes discomfort and more importantly, frequent dose reductions, which limit its anti-cancer efficacy. Bortezomib-treated patients show impairments in A $\beta$ -, A $\delta$ -, and C-primary afferent subtypes by QST <sup>109</sup>. These clinical findings complement the changes seen in the primary afferent neurons, DRG and spinal cord of bortezomib-treated rodents <sup>90</sup>. Changes in sensory ganglia neurons due to bortezomib include nucleolar hypertrophy, upregulation of rRNA synthesis, damage of mitochondria and recruitment of satellite glial cells <sup>90,164</sup>. The literature presents mixed findings about the duration and reversibility of clinical BIPN. Some studies report median times to improvement of neuropathy grade to be 3 to 4 months for grade 1 or 2 neuropathy and 8 months for grade 3 or 4 neuropathy <sup>165</sup>. Other quantitative studies report BIPN-induced sensory deficits that are detectable as far as one year following treatment <sup>89</sup>. To investigate the hypothesis that oral minocycline administered with the chemotherapeutic agent, bortezomib, would prevent sensory neuropathy induced by bortezomib and decrease patient-reported outcomes of neuropathy, quantitative sensory thresholds and patient-reported outcomes were compared to patients randomized to placebo in a double-blind clinical trial.

### **3.2. Subjects and Methods**

#### **3.2.1 Study Site**

This study was conducted at the University of Texas MD Anderson Cancer Center, Houston, TX from March 2011 to October 2013. All enrolled subjects provided written and oral informed consent and were explained the risks and benefits of participating in this Phase I protocol as reviewed and approved by the Institutional Review Board of UT MD Anderson Cancer Center. All subjects signed a written informed consent before they were enrolled in the study and data was collected.

#### **3.2.2 Study Design**

This was a double blind, Phase I, randomized placebo-controlled clinical study to assess the efficacy of minocycline in preventing bortezomib-induced neuropathy. MM patients underwent QST (including quantitative and qualitative measures) after myeloma diagnosis, but prior to beginning chemotherapy as previously described in Chapter 2. Subjects were then randomized to receive either minocycline 200 mg, or placebo orally for the first dose, and then 100 mg twice a day for the next ten weeks. Patients were counseled on accountability and willingness to comply with taking the study drug as prescribed. The study drug was mailed to study participants with instructions to begin the first dose on the first day of the first cycle of chemotherapy treatment. A follow-up quantitative sensory testing was performed on patients during the course of chemotherapy and minocycline/placebo treatment. The primary endpoint of this study was fingertip touch detection threshold.

#### **3.2.3 Randomization and Blinding**

Study participants were registered in the institutional database Clinical Oncology Research system (CORe) and randomized to receive placebo or minocycline. This

information was provided to the institutional pharmacy for disbursement to study participants. Pharmacy personnel did not interact with personnel collecting the data or with healthcare providers and were separated by space and department. The pharmacy maintained records of the randomization list. After seventy-two patients were enrolled, the randomization list was provided to the institutional statistical department for analysis.

### **3.2.4 Inclusion and Exclusion Criteria**

Study inclusion criteria were men and women greater than 18 years of age newly diagnosed with symptomatic MM, having previously received no chemotherapeutic treatment, but scheduled to receive bortezomib as part of induction therapy for their disease. Additionally, included patients exhibited no symptoms of neuropathy at baseline as per physician's clinical assessment, and pre-menopausal female patients were willing to use adequate birth control for the duration of the study. Patients were also required to read and speak English. Patients with a documented allergy to tetracycline, history of poorly controlled or advanced diabetes mellitus (lab value HA1c  $\geq$  8%), signs and symptoms of progressive or uncontrolled renal, hepatic, gastrointestinal, endocrine, pulmonary, cardiac, neurologic, or cerebral disease documented, peripheral neuropathy of  $\geq$  grade 2 by CTCAE Version 4.0 as per treating physician, history of malignancy other than MM or a history in the last 5 years, and significant drug or alcohol use as per social history clinic notes were not approached for consent.

### **3.2.5 Protocol Deviations**

Deviations from the protocol include individuals who consented to the study, but had already begun induction therapy and therefore did not provide a baseline test.

Furthermore, these same individuals were administered the first dose of minocycline or placebo after induction of chemotherapy.

### **3.2.6 Clinical Outcome Measures and Methods**

Sensory function was assessed by QST on three skin sites: fingertip, thenar eminence and volar forearm. The primary study endpoint was the touch threshold of the fingertip. All QST data was collected by research coordinators blind to study group and experimental design. Sensory testing assessing skin temperature, touch detection (von Frey and Bumps test), temperature threshold (detection of warm, cool, noxious heat, and noxious cold), and sharp detection were performed on three skin sites: fingertip, palm and forearm and a sensorimotor pegboard task was administered as described in Chapter 2. Patient-reported outcomes were also assessed.

### **3.2.7 Safety and Tolerability**

Previous studies evaluating the safety of 200 mg/day oral minocycline reported no major concerns and an adverse event profile similar to the placebo group<sup>166</sup>. Adverse events were monitored continuously throughout the study and several patients discontinued the study drug.

### **3.2.8 Statistics**

All analyses were performed using GraphPad Software, Inc. (La Jolla, CA). Fisher's exact test was performed to compare frequency distribution for categorical variables. Continuous variables (QST measures) were compared between placebo and minocycline groups with the Kruskal Wallis test (the non-parametric equivalent of the one-way ANOVA). To compare patients' initial with follow-up QST, the paired non-parametric Wilcoxon-rank sum test was used. No adjustment was made for performing multiple tests, as this was an exploratory study. Due to the complexity of the data set

the UT MD Anderson Department of Biostatistics was consulted to perform additional analyses. These included a backward stepwise regression approach to select variables to include in a multivariable analysis. The results of the multivariable analysis can be found in Chapter 5, Appendix B.

### **3.2.9 Ethics**

This study was approved by the Internal Review Board of UT MD Anderson Cancer Center and conducted in accordance with the principles of the Declaration of Helsinki and the Guidelines of Good Clinical Practice.

## **3.3. Results**

### **3.3.1 Patient Population Analyzed**

A total of 72 patients met the inclusion criteria of the study, signed the necessary informed consent documents and completed at least one QST. Follow-up tests (tests conducted after baseline) were administered after chemotherapy treatment was initiated, when patients returned to the hospital for their necessary clinic appointments. Although this testing schedule was the most convenient option for patient schedules, patients had different cumulative doses of bortezomib at the time of testing. Bortezomib was typically administered to patients on days 1, 4, 7, and 11 of a 21-day cycle at a dose of 1.3 mg/m<sup>2</sup>, but some patients received a modified version of the standard dosing due to advanced age, the development of neuropathy, or the use of adjunctive agents. Bortezomib-induced neuropathy literature suggests that the development of neuropathy in patients is most likely dose-dependent in nature, with symptoms worsening as cumulative dose increases<sup>86</sup>. Therefore, the cumulative dose of bortezomib (in total milligrams) at each test for each patient was calculated to standardize the analysis. Over the course of the study, patients were tested at



cumulative bortezomib doses ranging from 0 mg to 53.8 mg. Due to the variability in cumulative dose and number of days between the start of bortezomib and the study drug (minocycline or placebo), the approach taken in this analysis was to first analyze a subset of the patients that met all of the initial inclusion criteria for the study (including a baseline test) and subsequently, to expand the analysis to include a greater number of patients. Preliminary analysis of primary endpoints did not reach statistical significance and the study was then closed to future patient entry.

Patient inclusion is depicted in Figure 14. Of the 72 patients initially enrolled in the study, three patients were removed upon patient request. Two patients were removed prior to completion due to adverse events. Of these, the first patient was disenrolled after 24 days of taking the study drug due to high liver function enzymes; at the conclusion of the study, the patient was found to be in the placebo group, indicating that high liver function enzymes was unrelated to the study drug. The other patient was disenrolled after two weeks of taking the study drug due to the development of a rash. This patient was also in the placebo group. Two additional placebo patients discontinued the medication for four days or less during the study due to a presumed allergic reaction. Only one of these patients was included in the final analysis.

Nineteen patients received a baseline test prior to the start of bortezomib and a follow-up test during bortezomib treatment. These patients were used for the initial analysis. A second analysis was performed by grouping 32 patients with a low dose of chemotherapy with the 19 patients who had received a baseline test for a total of 51 patients. The patients excluded from this analysis lacked an initial test at <13 mg bortezomib or a follow-up test at >13 mg bortezomib.

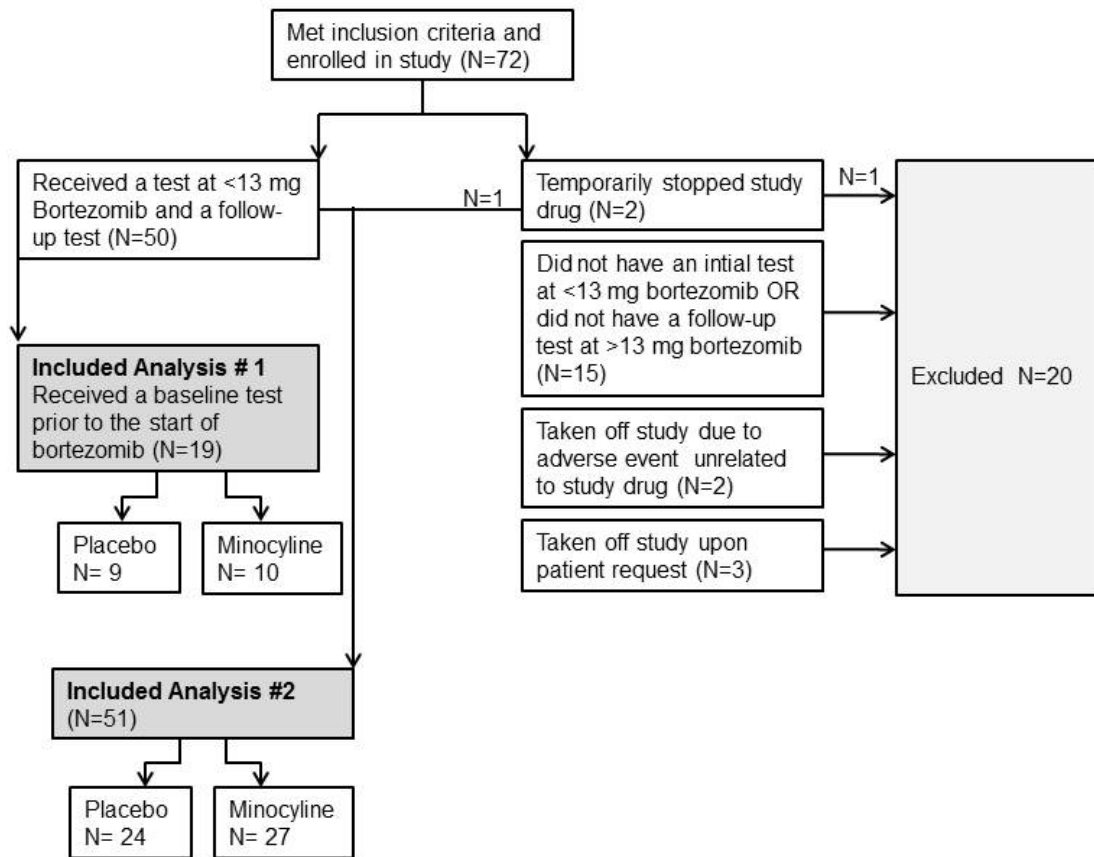


**Figure 14 Study Design**

Flow-chart of patients excluded or included in the analysis.

### 3.3.2 Analysis #1

#### 3.3.2.1 Patient Demographics

The first group of patients analyzed (N=19; Placebo: n= 9, Minocycline: n=10) all received a “true” baseline test (prior to the start of chemotherapy), began taking the study drug (placebo or minocycline) no later than a week after induction chemotherapy, and received a follow-up test at cumulative doses in the range of 14.0

mg to 52.8 mg. A cumulative dose of 14.0 mg roughly corresponds to greater than 1.5 cycles of bortezomib. Due to the already limited sample size, 14.0 was arbitrarily chosen as the smallest cumulative dose bortezomib at follow-up test to maximize inclusion of patients. Differences in demographic variables were assessed with the non-parametric Mann Whitney test for continuous variables or Fisher's exact test for discrete variables. Age, sex, and cumulative dose at follow-up test were not significantly different between the two groups. The minocycline group had significantly more patients who had undergone radiation treatment prior to their baseline test. Radiation treatment has the potential of damaging peripheral nerves, although symptoms of damage often surface years after treatment<sup>167</sup>. Because these patients had received radiation therapy just prior to the baseline test and because baseline QST did not significantly differ between the two groups, it was considered reasonable to proceed with the analysis.

		Placebo (n=9)		Minocycline (n=10)		P value
		Median	n(%)	Median	n(%)	
Age		57		57.5		P = 0.65
Sex	Female		3 (33.3%)		2 (20%)	P=0.63
	Male		6(66.7%)		8 (80%)	
Previous Radiation Treatment	Yes		0 (0%)		5 (50%)	<b>P=0.03*</b>
	No		9 (100%)		5 (50%)	
Cumulative Dose Bortezomib at Follow-Up test		23.2		22.8		P = 0.65

#### **Table 4 Patient Demographics: Analysis #1**

Median patient age and cumulative dose were similar between placebo (n=9) and minocycline (n=10) groups. The numbers of females and males did not differ between minocycline and placebo groups, however, significantly more patients in the minocycline group had received prior radiation treatment.

\*=P<0.05

Each of the groups (placebo and minocycline) received a baseline test and a follow-up test during concurrent study drug administration and bortezomib treatment ( $\geq 13$  mg). The analysis consisted of four groups: (placebo at baseline (placebo-baseline), placebo-post-chemotherapy (placebo-post-chemo), minocycline at baseline (minocycline-baseline), and minocycline-post-chemotherapy (minocycline-post chemo). Intragroup comparisons (between placebo-baseline and placebo-post-chemo; minocycline-baseline and minocycline-post-chemo) were performed with the paired non-parametric Wilcoxon-rank sum test. Intergroup comparisons (between placebo-post-chemo and minocycline-post-chemo) were performed with the non-parametric

Kruskal-Wallis test. The minocycline-post-chemo and placebo-post-chemo groups were denoted with the word “max” in all graphs in this analysis.

### **3.3.2.2 Touch Detection**

To assess A $\beta$ -fiber function, mechanical sensitivity of patients was tested. Touch detection measured with von Frey monofilaments at the volar forearm was significantly higher in the placebo group post-chemo treatment ( $0.33\pm 0.10\text{g}$  at baseline versus  $0.73\pm 0.21\text{g}$  post-chemo,  $P=0.03$ ) (Figure 15A), indicating a reduction in tactile perception at this site. No significant differences were observed at the fingertip or thenar eminence, or between the other groups. The Bumps detection test measures fine tactile discrimination of the fingertip. No significant differences were observed in Bumps detection thresholds of placebo and minocycline groups at either baseline or post-chemo (Figure 15B). A comparison of baseline versus post-chemo for both von Frey touch detection and Bumps detection tests suggests that bortezomib does not alter fine tactile discrimination in placebo-treated MM patients.

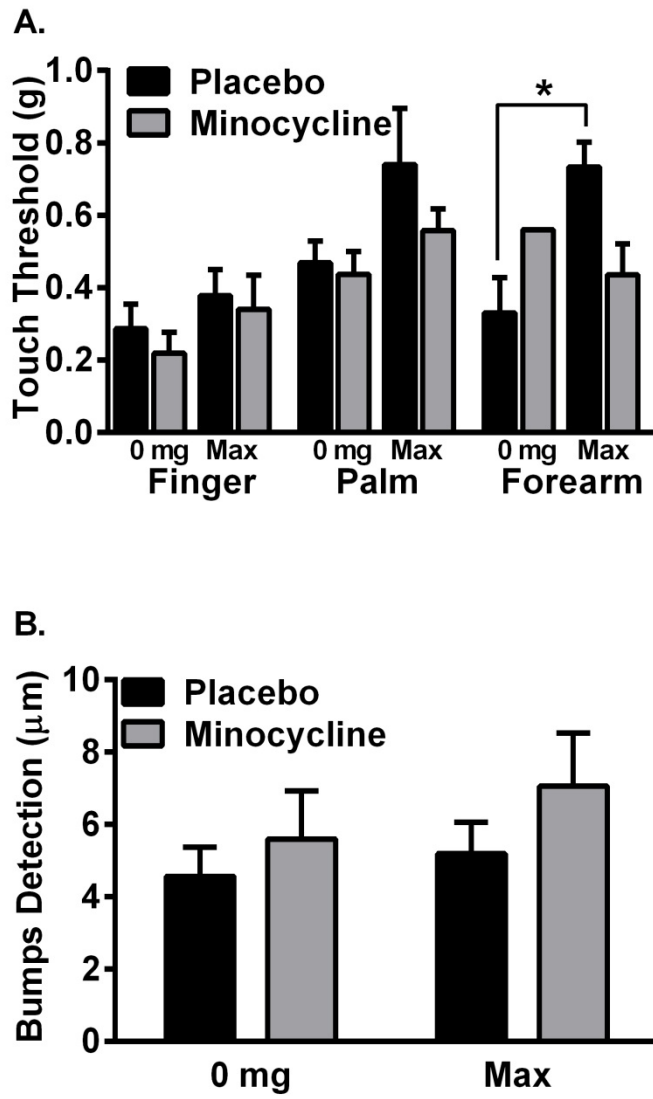


**Figure 15 Touch and Bumps Detection Thresholds Showed Few Differences Between Minocycline and Placebo Groups**

(A) Touch threshold measured with von Frey monofilaments at the fingertip, thenar eminence and volar forearm for the placebo group (black bars) and the minocycline group (gray bars) at baseline (0 mg) and post-chemotherapy treatment (Max). Touch threshold in the placebo group significantly increased at the volar forearm after chemotherapy, but did not differ between any other groups at any other sites. (B) Fine tactile discrimination of the fingertip assessed with the Bumps detection test. No significant differences were observed.

\*=  $P < 0.05$

### **3.3.2.3 Peg Board Completion, Sharpness Detection and Skin Temperature**

The peg board completion task assessed dexterity by measuring the latency for subjects to fit odd-shaped pegs into corresponding holes in a board. The minocycline group exhibited significantly faster completion of the pegboard with the dominant hand after bortezomib treatment ( $75.5\pm 4.9$  s) compared with their baseline test ( $84.6\pm 4.5$  s) ( $P=0.01$ ) (Figure 16A). However, completion times did not differ significantly between the minocycline group post-chemo and the placebo group post-chemo. Completion times for the non-dominant hand did not differ within or between groups.

No significant differences were observed in the sharpness detection test or in skin temperature (Figure 16B&C).

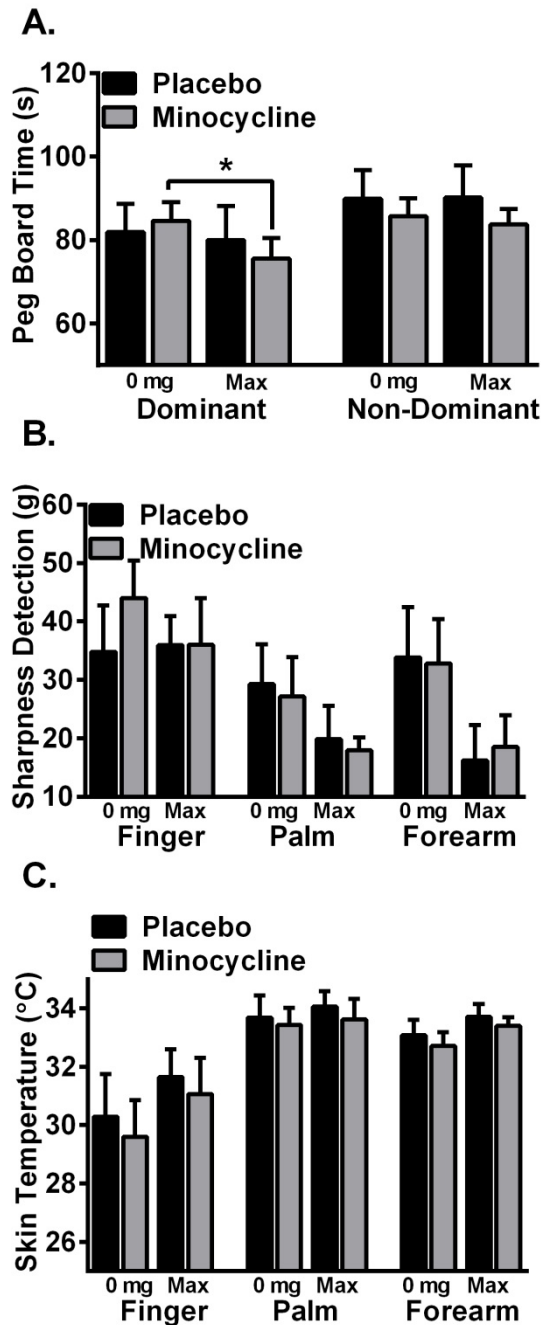


**Figure 16 Minocycline Group Showed Faster Dominant Hand Peg Board Completion, but No Differences in Sharpness Detection and Skin Temperature**  
 (A) The time to fit pegs in a pegboard for placebo (black bars) and minocycline (gray bars) groups. The minocycline group had significantly faster completion times after bortezomib ( $P=0.01$ ), but there was no significant difference between the minocycline and placebo groups post-chemotherapy treatment (Max). (B) Sharpness detection was assessed (C) Skin temperature was measured. No significant differences were observed in sharpness detection or skin temperature.  
 \*= $P<0.05$



### 3.3.2.4 Temperature Detection

For temperature detection, patients reported the first detection of a change in the temperature of a probe (“cool” or “warm”) and then, when the temperature became painfully cold or hot as a measure of both C- and A $\delta$ -fiber function. The temperature at which subjects first reported feeling “cool” significantly increased for both placebo ( $24.54\pm 2.40$  °C) and minocycline ( $24.55\pm 0.83$  °C) groups post-chemotherapy as compared to respective baseline tests ( $22.04\pm 0.78$  °C and  $22.99\pm 0.84$  °C,  $P= 0.03$  and  $P=0.04$ ) at the fingertip (Figure 17A). However, there was no difference in the cool fingertip threshold of placebo-post-chemo and minocycline-post-chemo. This suggests that an increased ability to detect cool is not impacted by treatment with minocycline. The inverse was seen at the thenar eminence and volar forearm. At both the thenar eminence and volar forearm, ability to detect cool decreased in the placebo-post-chemo group. The threshold at the thenar eminence in the placebo-post-chemo group was  $15.18\pm 1.60$  °C, which was significantly lower than  $26.08\pm 0.81$  °C in the placebo group at baseline ( $P=0.004$ ) and  $24.49\pm 1.25$  °C in the minocycline-post-chemo group ( $P<0.01$ ). The threshold at the volar forearm for the placebo-post-chemo group was  $14.24\pm 2.22$  °C, which was significantly lower than the placebo group at baseline ( $25.12\pm 0.77$  °C,  $P=0.004$ ) and the minocycline-post-chemo ( $23.10\pm 1.50$  °C,  $P<0.01$ ). These data suggest the placebo group was less able to detect cool temperatures after chemotherapy treatment at the volar forearm and that minocycline may preserve cool detection at these sites.

Cold pain threshold increased significantly at the fingertip and thenar eminence in the minocycline-post-chemo group as compared with the minocycline-baseline group,  $9.77\pm 2.46$  vs.  $6.54\pm 1.76$  ( $P=0.002$ ), respectively, at the fingertip and  $14.98\pm 2.57$  vs.

13±2.57 ( $P=0.048$ ), respectively, at the thenar eminence) (Figure 17B). No other significant differences were observed in cold pain thresholds. The patterns in cool detection would have been expected if the minocycline had a neuroprotective effect. However, the minocycline-post chemo group showed increases in cold pain that do not support a neuroprotective role of minocycline in nociceptive cold fibers.

Bortezomib-induced peripheral neuropathy is thought to affect C-fibers controlling warm and heat pain<sup>89,109</sup> therefore, these modalities were assessed with a Peltier thermode (Chapter 2, Figure 7). No significant differences were observed within or between any groups in warmth detection and heat pain thresholds (Figure 18A&B).

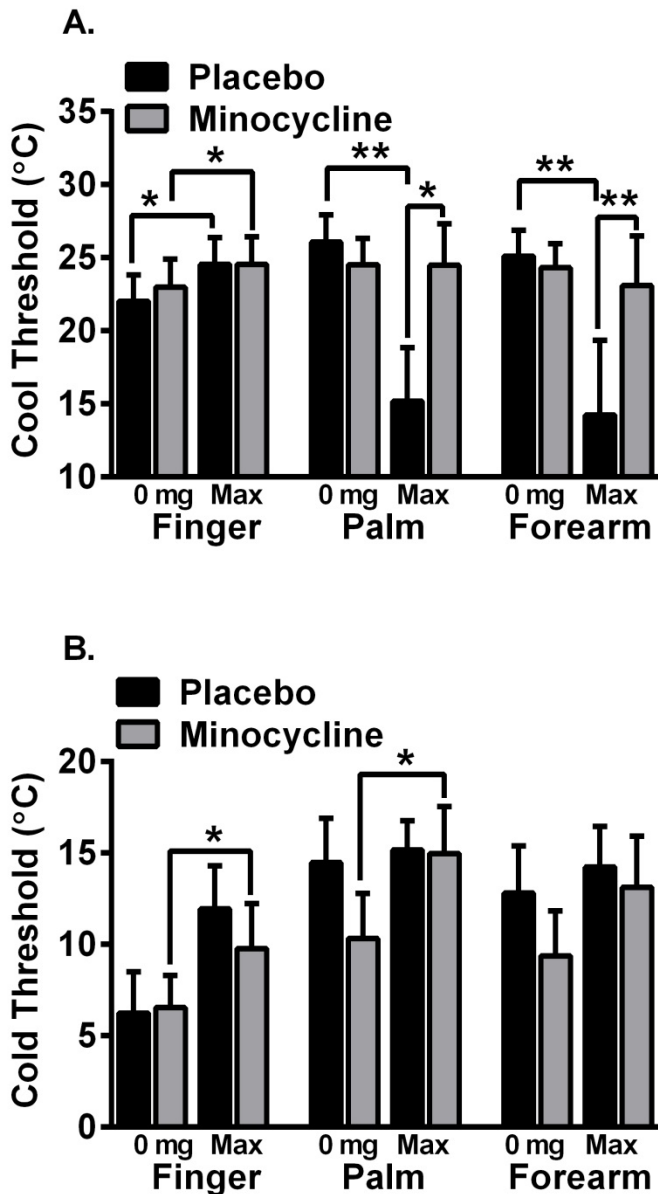


**Figure 17 Minocycline and Placebo Groups Exhibit Differences in Cool Detection, and Minocycline Does not Attenuate Increases in Cold Pain Thresholds**

(A) Cool detection threshold measured at the fingertip, thenar eminence and volar forearm for the placebo group (black bars) and the minocycline group (gray bars). Cool detection threshold in the placebo and minocycline groups significantly increased at the fingertip after chemotherapy, but did not differ between any other groups. At the palm and forearm, the cool threshold was significantly lower in the placebo group after chemotherapy indicating less ability to discriminate cold. (B) Cold pain threshold increased at the fingertip and palm in the minocycline group after chemotherapy. No differences in cold pain at the volar forearm were noted.

\*=  $P < 0.05$ , \*\*= $P < 0.01$

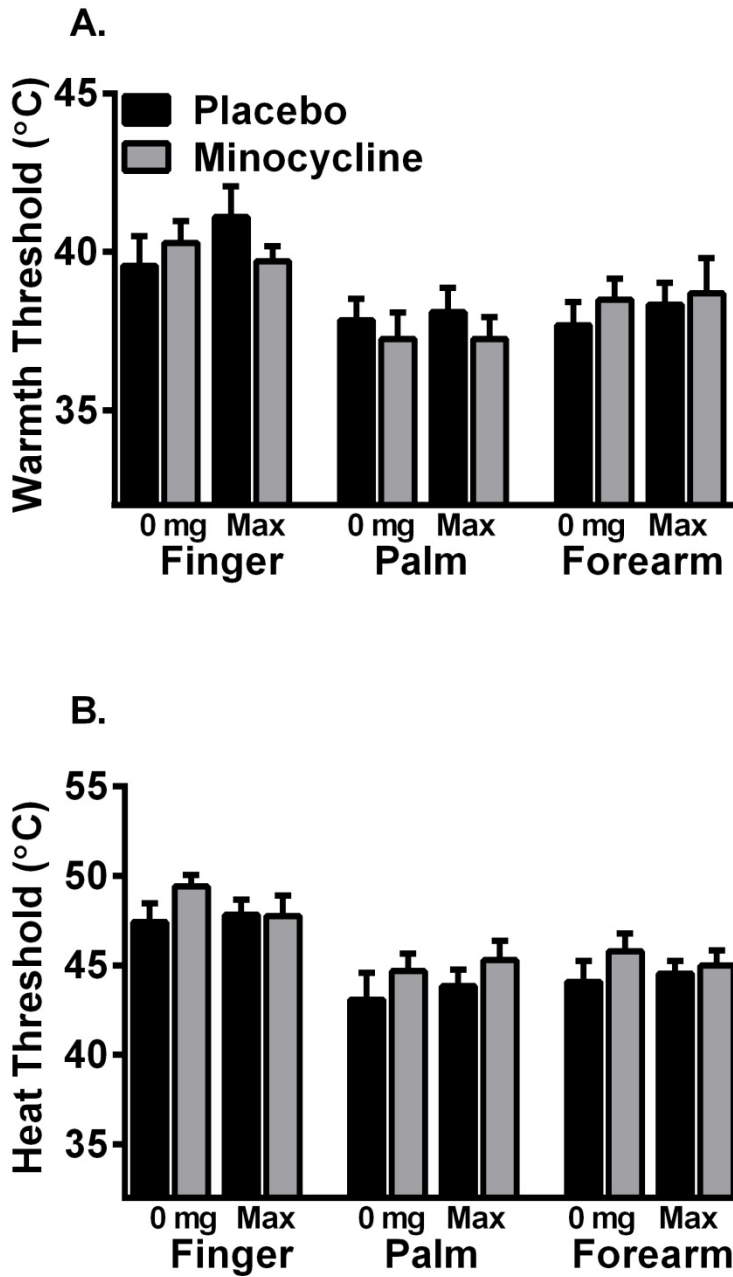


**Figure 18 Warmth and Heat Pain Thresholds Were Not Different Between Minocycline and Placebo Groups**

(A) Warmth detection threshold measured at the fingertip, thenar eminence and volar forearm for the placebo group (black bars) and the minocycline group (gray bars). (B) Heat pain thresholds were measured at the same sites. No significant differences were found in warmth detection or heat pain thresholds.

### 3.3.2.5 Rationale for Performing Analysis #2

The pilot study was not suggestive of any conclusive trend regarding the impact of bortezomib on QST with or without minocycline. Due to the small sample size, it was decided to utilize less stringent inclusion criteria to expand the number of patients analyzed. Thirty-two of 72 patients did not have a baseline test prior to beginning chemotherapy treatment, but did have a test performed at a low dose of bortezomib (less than 13 mg of bortezomib) and a follow-up test performed during course of treatment with bortezomib. These patients were added to the previously analyzed group for a total of 24 patients randomized to receive placebo and 27 to receive minocycline. First, it was important to determine whether it was appropriate to combine the QSTs of patients at a true baseline with QSTs of patients at a low initial dose of bortezomib. To assess this, QSTs of patients randomized to placebo with a true baseline were compared to those at a low dose of chemotherapy for all tests (e.g.: Bumps, touch, and temperature detection, etc.) at all sites (e.g.: fingertip, palm, forearm) using the non-parametric Mann-Whitney test. Although none of the comparisons were statistically significant, the Bumps test approached statistical significance with a mean Bumps detection threshold of  $4.5 \pm 0.71 \mu\text{m}$  in the placebo-baseline group versus  $7.28 \pm 0.94 \mu\text{m}$  in the placebo group with a low initial cumulative dose bortezomib ( $P=0.07$ , Figure 19A). The increase in Bumps detection threshold in the placebo group with a low dose of bortezomib could not solely be explained by the infusion of chemotherapy because the age of the two groups also approached a statistically significant difference (placebo:  $56 \pm 2.39$  years, low-dose:  $62.13 \pm 1.96$  years,  $P=0.07$ , Figure 19B). Fine tactile discrimination decreases with age<sup>126,168</sup>; therefore, these differences could have been age-related rather than due to bortezomib infusion .

In addition, no difference in Bumps detection was observed in the previous analysis in the placebo group before and after chemotherapy (Figure 15B). Therefore, it was deemed appropriate to group together the patients with a low dose of chemotherapy and the patients with a baseline to compare initial and follow-up QSTs. QST tests were compared as described above using the nonparametric Wilcoxon matched-pairs test within groups (e.g.: placebo-initial versus placebo-follow-up ) and the non-parametric Kruskal-Wallis test between groups (e.g.: placebo-follow-up versus minocycline-follow-up).

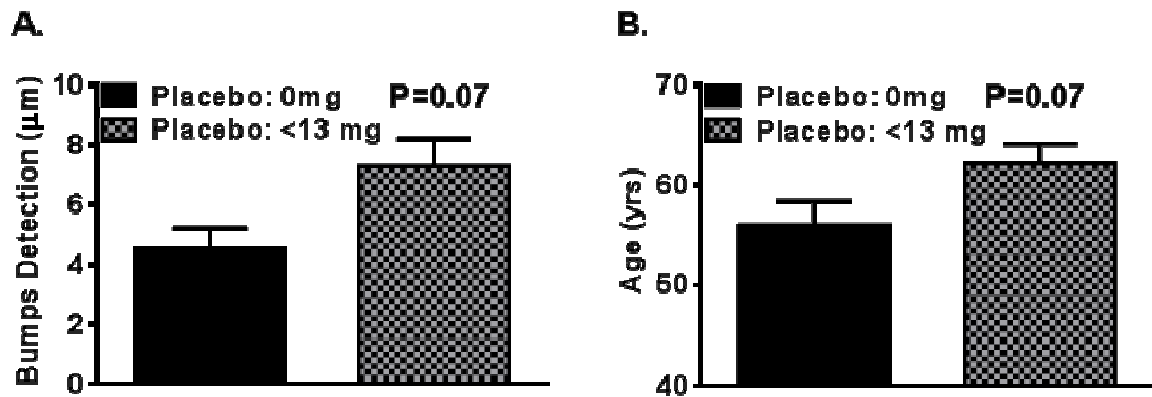


**Figure 19 Bumps Detection and Age of Placebo Groups Approach, But Do Not Reach Statistical Significance Between Placebo 0mg Versus Low-Dose Bortezomib**

(A) Bumps detection and (B) Age of the placebo group prior to chemotherapy (black bars) versus placebo low dose bortezomib group (dotted bars) both approached ( $P=0.07$ ), but did not reach statistical significance.

### 3.3.3 Analysis # 2

#### 3.3.3.1 Patient Demographics

A total of 51 patients were analyzed in the subsequent analysis expanded to include patients with an initial test performed at a low initial dose of bortezomib, and a follow-up test at a higher cumulative dose bortezomib. The median age of the placebo group (n=24) and minocycline (n=27) group was 61.5 and 58 years old, respectively (P=0.79). Sex, previous radiation treatment and cumulative dose of bortezomib at follow-up test were not different between the two (Table 3.2).

**Table 2** Patient demographics (N=51)

	Placebo (n=24)		Minocycline (n=27)		P value
	Median	n(%)	Median	n(%)	
Age	61.5		58		P = 0.79
Sex	Female	10(41.7%)	9	33.3%	P = 0.57
	Male	14(58.3%)	18	66.7%	
Previous Radiation	Yes	2(8.3%)	6	22.2%	P=0.26
	No	22(91.7%)	21	77.8%	
Cumulative Dose Bortezomib at Follow-Up Test	26.79		25.2		P = 0.37

**Table 5 Patient Demographics: Analysis #2**

Median patient age and cumulative dose were similar between placebo (n=24) and minocycline (n=27) groups. The numbers of females vs. males and the number of patients who had received prior radiation were also similar between minocycline and placebo groups.



### 3.3.3.2 Touch Detection

No significant differences were observed in fingertip and thenar eminence touch detection using von Frey filaments (Figure 20A). Touch detection threshold at the volar forearm was significantly lower in the minocycline group at follow-up as compared with their initial test ( $0.44\pm 0.05$  g vs.  $0.52\pm 0.02$  g,  $P=0.01$ ). Lower thresholds indicate better touch detection. Interestingly, the touch threshold at this site was not significantly different between the two follow-up groups (minocycline and placebo). Similarly, Bumps detection threshold was significantly higher in the minocycline-follow-up group as compared to their initial test (minocycline-follow-up:  $7.14\pm 0.84$  vs. minocycline-initial:  $5.80\pm 0.74$ ,  $P=0.03$ ) (Figure 20B), indicating worsening fine tactile discrimination. Bumps detection for minocycline-follow-up group was not significantly different from the placebo-follow-up group.

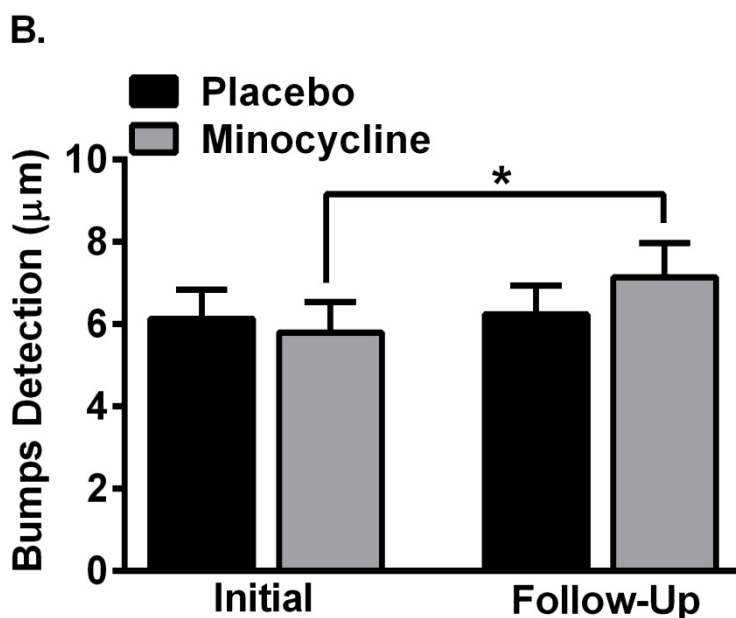
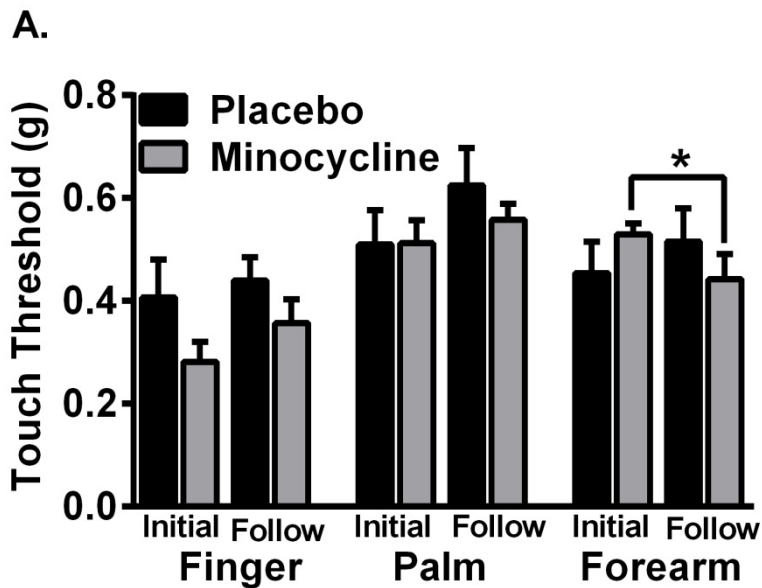


**Figure 20 Touch Detection at Volar Forearm Improved and Bumps Detection at the Fingertip Worsened in the Minocycline-Follow-Up Group**

(A) Touch threshold was measured with von Frey monofilaments at the fingertip, thenar eminence and volar forearm for the placebo group (black bars) and the minocycline group (gray bars). Touch threshold in the minocycline group significantly decreased at the volar forearm after chemotherapy, but did not differ between any other groups at any other sites. (B) Bumps detection threshold. Fine tactile discrimination of the fingertip significantly increased in the minocycline follow-up group.

\* =  $P < 0.05$

### **3.3.3.3 Peg Board Completion, Sharpness Detection and Skin Temperature**

The completion time for peg board was significantly shorter in the minocycline-follow-up group as compared to their initial test (follow-up:  $78.71 \pm 3.57$  s vs. initial:  $83.45 \pm 3.52$  s) (Figure 21A). There were no differences in sharpness detection and skin temperature between any of the groups (Figure 21B&C).

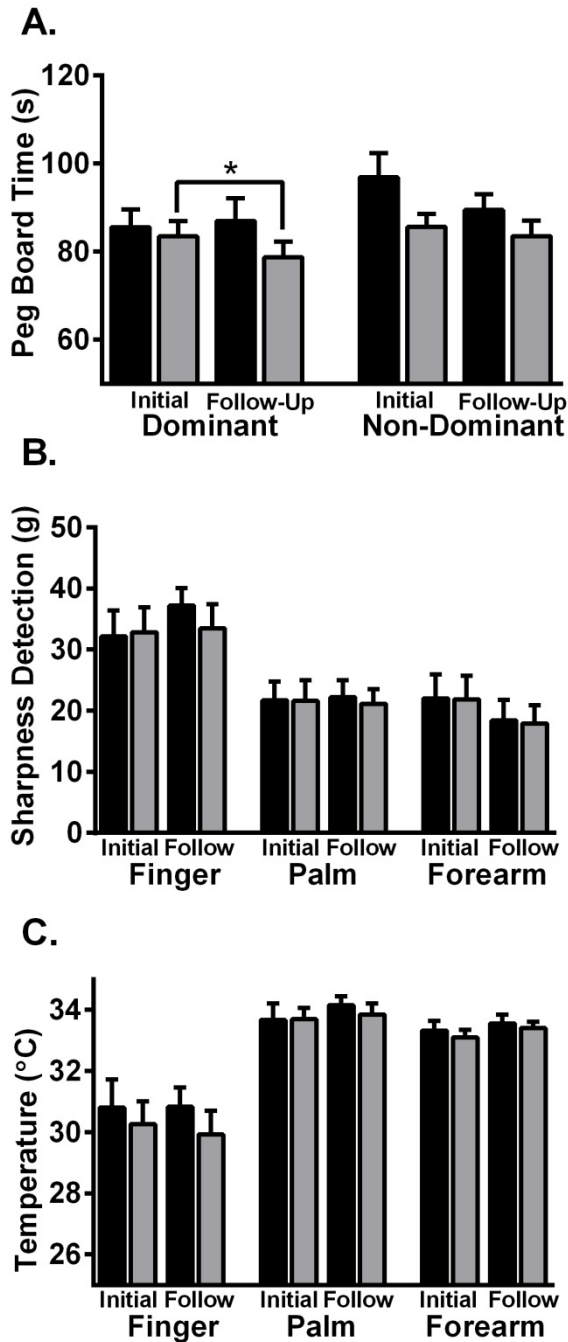


**Figure 21 Peg Board Completion, Sharpness Detection, and Skin Temperature**

(A) The latency to fit pegs in a pegboard was compared between placebo (black bars) and minocycline (gray bars) groups. The minocycline-follow-up group had significantly faster completion times compared to minocycline-baseline ( $P < 0.05$ ), but there was no significant difference between minocycline-follow-up and placebo-follow-up groups. (B) Sharpness detection was assessed. (C) Skin temperature was measured. No significant differences were observed in sharpness detection or skin temperature.

\*= $P < 0.05$

### 3.3.3.4 Temperature Detection

The temperature for detecting “cool” was not significantly different between the placebo and minocycline groups at follow-up test, however, both groups had cool detection thresholds that were significantly higher in temperature when compared to respective initial tests (placebo-follow-up:  $24.02 \pm 0.63$  °C, placebo-initial:  $21.89 \pm 0.56$  °C,  $P=0.007$ ) and (minocycline-follow-up:  $24.21 \pm 0.46$  °C, minocycline-initial:  $22.69 \pm 0.50$  °C,  $P=0.003$ ) (Figure 22A). Cool threshold at the volar forearm was significantly higher in the placebo-follow-up group compared to the initial test (placebo-follow-up:  $25.81 \pm 0.31$  °C vs. placebo-initial:  $24.43 \pm 0.56$  °C,  $P=0.03$ ) (Figure 22A). There were no significant differences in the cool threshold at the thenar eminence.

Cold pain thresholds were parallel to cool thresholds. The cold pain fingertip thresholds in both minocycline and placebo groups at follow-up were significantly higher than respective initial tests (placebo-follow-up:  $12.57 \pm 1.57$  °C vs. placebo-initial:  $7.39 \pm 1.27$  °C,  $P=0.005$  and minocycline-follow-up:  $9.77 \pm 1.23$  °C vs.  $7.18 \pm 1.05$  °C minocycline-initial,  $P=0.003$ ) (Figure 22B). There were no significant differences in cold pain at the thenar eminence and volar forearm (Figure 22B).

There were no significant differences in warm detection thresholds at any site (Figure 23A).

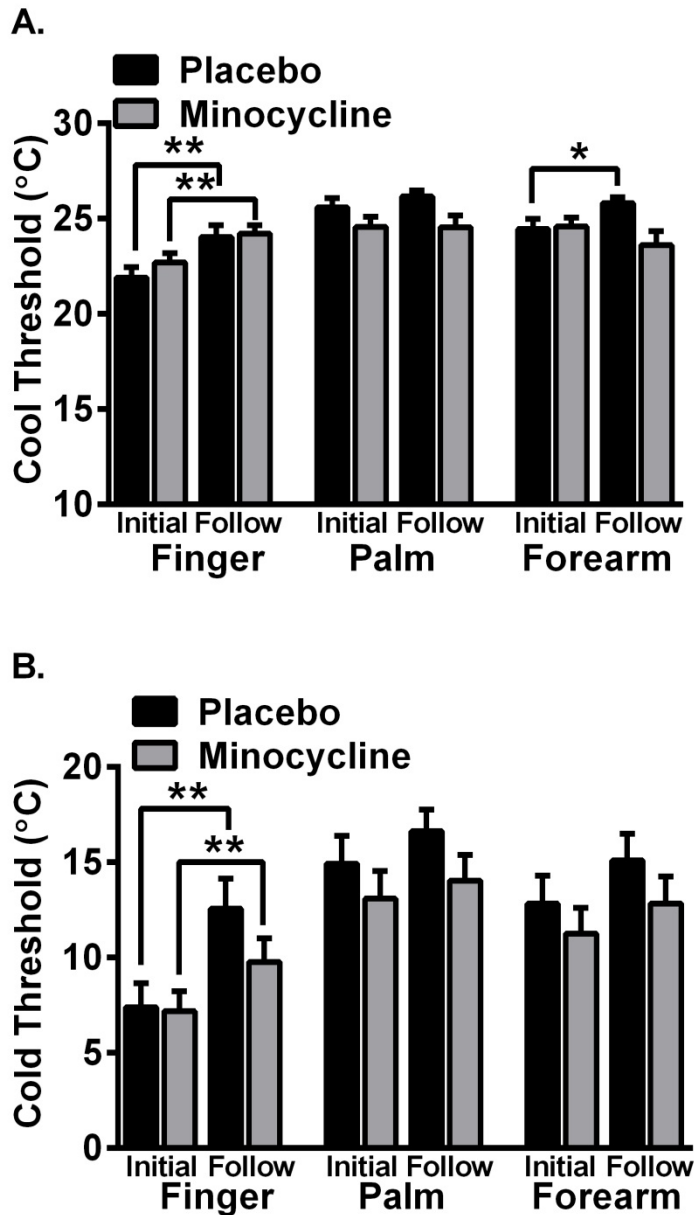


**Figure 22 Fingertip Cool and Cold Pain Thresholds**

(A) Cool detection threshold measured at the fingertip, thenar eminence and volar forearm for the placebo group (black bars) and the minocycline group (gray bars). Cool detection threshold in the placebo-follow-up and minocycline-follow-up groups significantly increased at the fingertip compared to their respective initial tests. At the forearm, the cool threshold was significantly higher in the placebo-follow-up group. No differences in cool detection were seen at the palm. (B) Cold pain threshold increased at the fingertip in both placebo and minocycline-follow-up group.

\*=  $P < 0.05$ , \*\*= $P < 0.01$

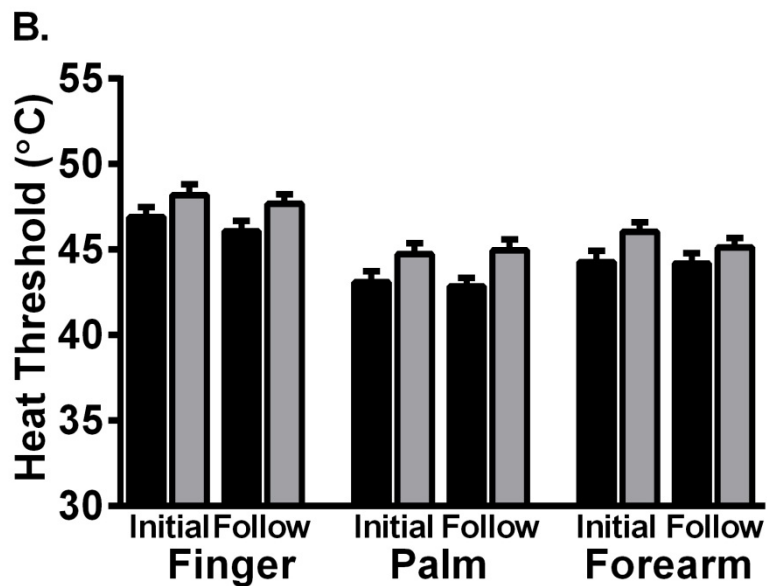
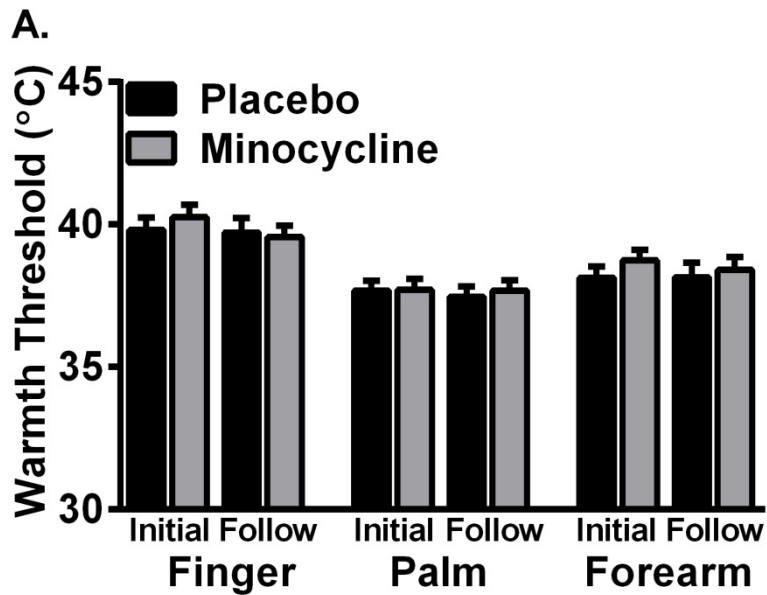


**Figure 23 Warm and Heat Pain Thresholds**

(A) Warmth detection threshold measured at the fingertip, thenar eminence and volar forearm for the placebo group (black bars) and the minocycline group (gray bars). No significant differences were found in warmth threshold. (B) Heat pain thresholds measured at the same sites. Heat pain in the placebo-follow-up group occurred at significantly lower temperatures than the minocycline-initial group.

\*=P<0.05

### 3.3.3.5 Patient Reported Symptom Descriptors

Rates in patient-reported tingling and numbness were analyzed. As expected, initial rates of tingling and/or numbness were not different between minocycline and placebo groups. At follow-up test, 10 of 27 patients reported tingling and 10 of 27 reported numbness in the minocycline group (Figure 24B&D). In the placebo group 11 of 24 patients reported numbness and 14 of 24 reported tingling (Figure 24A&C). Rates of tingling were lower in the minocycline-follow-up group compared to placebo-follow-up group, but statistical significance was not achieved ( $P=0.11$ ). Patient-reported numbness was not statistically significant between minocycline-follow-up and placebo-follow-up groups by the Fischer's exact test. However, placebo group reports of numbness significantly increased at follow-up with 4 patients reporting tingling at the initial test compared to 14 at the follow-up test ( $P=0.007$ ) (Figure 24A). Placebo group reports of numbness approached a statistically significant increase after bortezomib treatment (at follow-up) ( $P=0.06$ ) (Figure 24C). No significant differences were observed between minocycline-patient reported tingling and numbness at the follow-up test (Figure 24B&D).



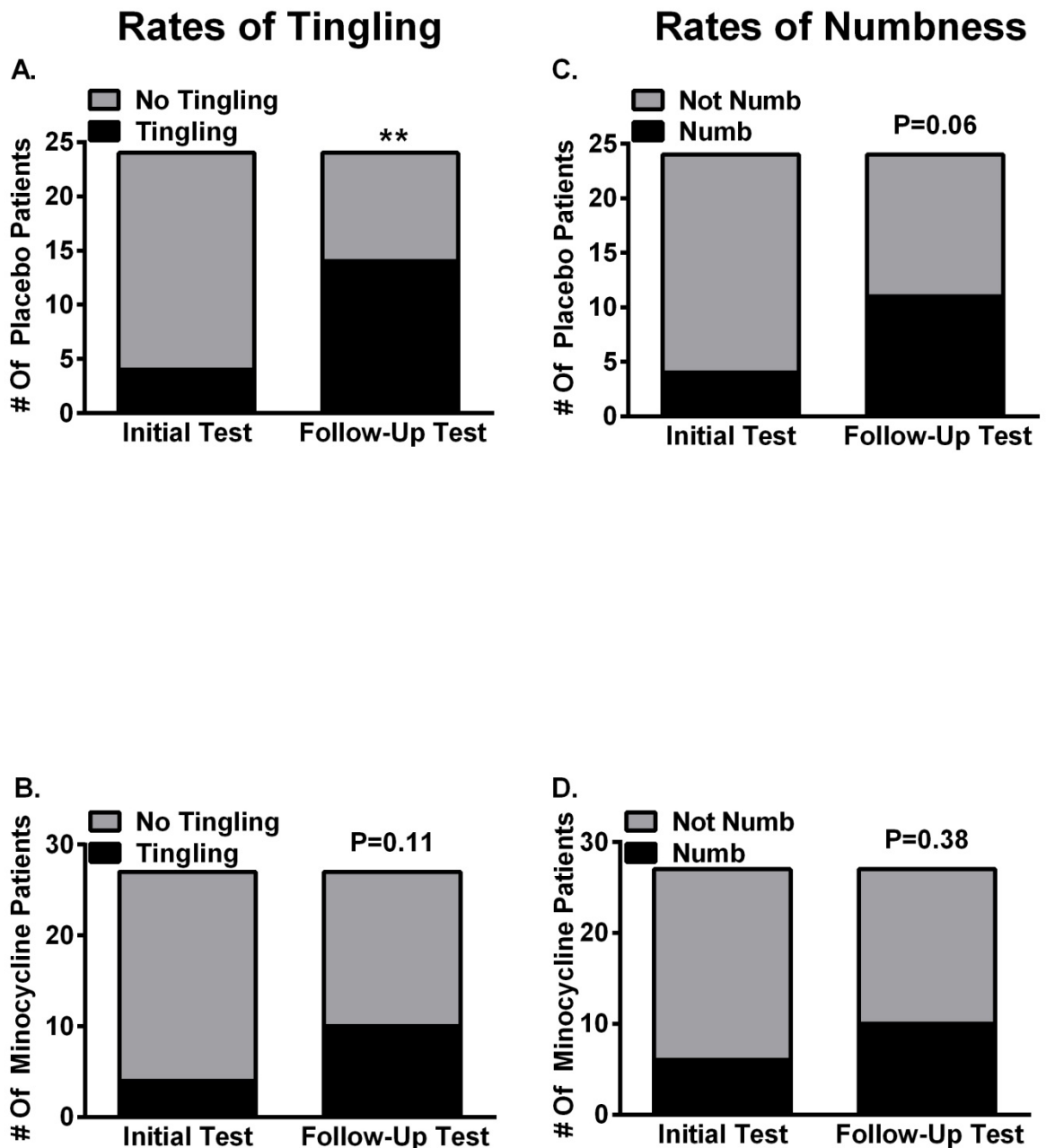


**Figure 24 Patient Descriptors**

(A&B) The number of patients in placebo and minocycline groups who reported numbness (black bars) or did not report numbness (gray bars) during initial and follow-up tests, respectively. (C&D) Rates of tingling in both groups. Significantly more placebo patients reported numbness after bortezomib as compared to at the initial test. No other significant differences were observed.

\*\*=P<0.01

### **3.4. Discussion**

The present study describes the sensory function of multiple myeloma patients treated with chemotherapy, including, but not limited to bortezomib, and randomized to receive minocycline (200 mg/day for ten weeks) or placebo. The first analysis was performed on patients, who had received baseline testing before chemotherapy. The second analysis included additional patients, who received initial testing immediately following induction therapy with a low cumulative dose of bortezomib. All patients received a follow-up test during the course of their chemotherapy treatment for comparison. The hypothesis that co-administration of minocycline with bortezomib would prevent changes in sensory thresholds induced by bortezomib was not supported. Although patients randomized to receive oral minocycline with bortezomib treatment displayed few differences in sensory thresholds as measured with QST, placebo-treated patients did not develop quantifiable sensory deficits after bortezomib treatment. The hypothesis that administration of minocycline during chemotherapy treatment would improve patient-reported outcomes was moderately supported by a reduction in the rates of tingling and numbness in patients randomized to minocycline, although statistical significance was not achieved.

Surprisingly, the placebo group in this study showed no overall detectable decline in sensory function after chemotherapy treatment. The cool detection thresholds of the palm and forearm in Analysis #1 were the only tests in which the placebo group displayed a significant decline in sensory perception after chemotherapy treatment (Figure 17). All other tests either showed no significant differences or improvement of sensory perception after chemotherapy (Figures 16 and 18-23). Despite the lack of decline in sensory function by QST, patient reports of tingling in the placebo group

significantly increased from 16.7% at the initial test to 58.3% at the follow-up test. Patient-reported rates of numbness approached, but did not reach a statistically significant difference in the placebo group ( $P=0.06$ ) (Figure 24B). Patients treated with placebo throughout the course of bortezomib treatment reported increased tingling and numbness at the follow-up test, suggesting that they had developed neuropathy. Despite an increase in patient-reported symptoms consistent with neuropathy, no differences in sensory thresholds were measured with QST after chemotherapy treatment. The seeming incongruence between patient-reported and QST data may be because patients reported symptoms that were present in their distal extremities, which included hands and feet, but sensory thresholds were only measured in the hands. Clinicians note that bortezomib-induced neuropathy presents sooner, more frequently, and more severely in the feet as opposed to the hands (*unpublished observation*). Given the short ten-week interval between initial and follow-up testing it is possible that sensory thresholds in the hands were not yet affected by the bortezomib treatment. It is also a possible that patient-reported symptoms of neuropathy precede measurable changes in sensory threshold measured with QST.

There are several other possible explanations for the lack of change in sensory thresholds in MM patients treated with bortezomib and placebo. First, Analysis #1 was conducted in a very small set of patients ( $n=9$  in the placebo group) making it difficult to see reliable changes. Analysis #2 was conducted in larger number of patients, but the majority of these patients underwent initial testing after a small cumulative dose of chemotherapy. Treatment-emergent peripheral neuropathy can occur in 21% and 37% patients given a single dose of 1.0 mg/m<sup>2</sup> and 1.3 mg/m<sup>2</sup>, respectively<sup>85</sup>. Therefore, sensory changes could have already occurred in some patients prior to receiving the

initial test, making it difficult to detect significant changes at the follow-up test. In fact, when the baseline test of placebo patients with no prior chemotherapy was compared to placebo patients with a small cumulative dose of chemotherapy, the Bumps detection test showed a reduced fine tactile discrimination that approached significance ( $P=0.07$ ) (Figure 19A). However, this near-significant difference could not solely be attributed to chemotherapy treatment because the mean age of the latter patient group was higher ( $P=0.07$ ). There is an age-related decline in tactile perception<sup>168</sup>, therefore, it remains unclear as to whether this difference in tactile perception was due to aging of the somatosensory system or to chemotherapeutic treatment.

In addition, literature reports the peak of BIPN symptoms to occur at approximately the fifth cycle of chemotherapy. The follow-up test conducted on this group of patients occurred less than 10 weeks after starting treatment, meaning that most patients were tested prior to the fourth cycle of bortezomib. Previous studies report that patients tested during, and at a year post-bortezomib show similar magnitudes of QST deficits<sup>89</sup>. The stability and lack of worsening in initial versus follow-up sensory testing of placebo patients in the present study, together with a lack of improvement at one year post-treatment may be indicative of “coasting.” Although typically associated with the platin therapies (e.g. cisplatin and oxaliplatin), coasting refers to symptoms that develop late, but persist or worsen after the end of therapy.

Another possible explanation for the lack of treatment-emergent differences in the QSTs of placebo patients is the presence of a disease-related neuropathy. Several studies acknowledge the existence of these subclinical deficits most likely related to primary cancer<sup>169</sup>. Previous psychophysical studies perhaps fail to report subclinical sensory deficits in treatment-naïve MM patients due to small sample size<sup>109</sup>. Future

QST studies should focus on distinguishing treatment-related from cancer-related sensory deficits and should investigate whether sub-clinical deficits are associated with an increased susceptibility for developing CIPN.

In the spinal nerve ligation (SNL) model of neuropathic pain, minocycline attenuates mechanical hypersensitivity when administered at post-operative day 1 and 3, but cannot reverse established hypersensitivity when administered at later time points <sup>161</sup>. In the SNL rodent model of neuropathic pain, the activation of microglia is thought to contribute to the development of mechanical hypersensitivity through the release of inflammatory cytokines <sup>149</sup>. The attenuation of neuropathic pain by minocycline is hypothesized to be due to its suppressive effects on the activation of microglia <sup>170</sup>. This proposed mechanism of action, however, does not account for minocycline's efficacy in preventing neuropathic pain caused by chemotherapy, as rodents treated with chemotherapy do not show microgliosis <sup>171</sup>. In CIPN rodent models the ability of minocycline to block hypersensitivity is likely related to prevention of astrocyte proliferation and prevention of a chemotherapy-induced downregulation of glutamate transporters <sup>171</sup>. Other supporting evidence for the use of minocycline as a neuroprotective agent comes from its antioxidant properties, suppression of chemokines and their receptors, inhibition of T-cell migration into the CNS, protection of mitochondria, and promotion of anti-apoptotic and suppression of pro-apoptotic pathways <sup>157</sup>. In the present study, the group treated with minocycline showed no evidence of improvement in sensory function at the follow-up test conducted during the course of chemotherapy treatment. Some measures such as pegboard completion time by the dominant hand suggest significant improvement in patients co-treated with minocycline and bortezomib compared to their initial tests, however this difference was

not significantly different from the bortezomib-treated patients and most likely represents a training effect. Thus, we failed to see reliable differences following minocycline that would suggest neuroprotective effects. Even if improvement had been observed, no conclusion could be made due to the lack of effect seen in the placebo group.

Given the clinical importance of this study in evaluating the potential application of minocycline in bortezomib-induced neuropathic pain, it was decided to consult the University of Texas MD Anderson Department of Biostatistics for a more formal analysis capable of adjusting for the complexities present in the dataset. For a description of the methods and findings of this analysis see Appendix B.

Limitations to this study were primarily related to the complexities of collecting prospective clinical data. The most significant limitation was the inability to obtain a baseline test on the vast majority of patients, which required that two separate analyses be performed. The first analysis had more restricted inclusion criteria, thereby limiting the sample size, while the second analysis included more patients, the majority of whom had already received chemotherapy at the initial test. Chemotherapy treatment prior to the initial test not only added a confounding factor, it also potentially diluted the effect of the chemotherapy on sensory function that could be observed at the follow-up test. Additionally, this subset of patients did not take minocycline at the start of chemotherapy. Pre-clinical studies indicate that the therapeutic time window for minocycline is limited to the initiation stage of neuropathic pain development<sup>161</sup>. This could be a contributing factor for the lack of effect seen with minocycline. In addition, the majority of patients in this study received polymodal chemotherapy: bortezomib, in combination with lenalidomide, thalidomide, cyclophosphamide, and/or

dexamethasone. Administration of polymodal therapy likely impacts the development of neuropathy, and research suggests that bortezomib in combination with thalidomide or the related analog, lenalidomide, produces lower rates of neuropathy, perhaps due to anti-inflammatory effects of these drugs<sup>172</sup>. Patients also received their follow-up testing at a large range of doses, which introduced additional variability.

Furthermore, the primary end point of the study was touch detection at the fingertip site. For this test, von Frey filaments of different forces were applied in an up/down fashion and the subject indicated when the stimulus was perceived. The recorded threshold was the force that the subject was able to detect three separate times. The filaments increase in force logarithmically (instead of linearly), which dramatically increases the probability that the subject detects the next heaviest filament and may underestimate potential differences. A lack of significance of the primary endpoint provoked the early closure of this study, which also limited the sample size.

Given the limitations inherent in the study, future clinical trials investigating the efficacy of minocycline in preventing bortezomib-induced neuropathy should ensure that all patients received a baseline test and begin the study medication prior to induction of chemotherapy. Patients should also be stratified based on the presence of baseline sensory deficits to ensure that treatment and control groups are balanced and display similar sensory thresholds at baseline. Quantitative sensory testing should be performed on the feet in addition to the hands, given that symptoms of bortezomib-induced neuropathy predominate in the lower distal extremities. As mentioned, follow-up testing in this study was performed approximately ten weeks after the initial testing, meaning that the majority of patients had not yet completed their fourth cycle of bortezomib. Given that sensory neuropathy increases with cumulative dose of

chemotherapy, quantitative testing in future studies should be performed at higher cumulative doses chemotherapy, which would allow testing of sensory thresholds at the peak of patient complaints of neuropathy. Lastly, given the potentially promising effect of minocycline in preventing bortezomib-induced patient reports of tingling and numbness, future studies should focus on patient-reported outcomes. Symptom quality as well as distribution on the body would be important aspects to consider.

In summary, this was a preliminary analysis performed on quantitative sensory data from a double-blinded randomized placebo/controlled study to evaluate the efficacy of minocycline in the prevention of bortezomib-induced neuropathy. Co-administration of minocycline with bortezomib decreased patient reports of tingling and numbness, although statistical significance was not achieved. However, patients co-treated with bortezomib and placebo did not experience sensory deficits as measured by QST compared to initial tests. In addition, co-administration of minocycline and bortezomib, did not produce measurable improvements as compared to placebo in sensory thresholds. Thus, the hypothesis that oral minocycline co-administered with the chemotherapeutic agent, bortezomib, would prevent sensory neuropathy induced by bortezomib and decrease patient-reported outcomes of neuropathy was only partially supported with a non-significant decrease of tingling and numbness in minocycline-treated MM patients after bortezomib. The dearth of patients with a baseline, inconsistencies in the time course that the study drug was administered, the use of different regimens of polymodal chemotherapy and variations in the dose at which the follow-up test was conducted are all inherent flaws with the dataset. The previous success of minocycline as a neuroprotective agent in clinical and pre-clinical studies as well as its potential to decrease patient reports of neuropathy in the above



study indicates that this drug may indeed have an effect in CIPN. The effect of minocycline on CIPN warrants further investigation in a more carefully controlled prospective trial.

#### **4. Overall Discussion and Future Directions**

Along with surgery and radiation, chemotherapy is the treatment of choice for cancer. According to the Center for Disease Control, the number of patients in the United States receiving chemotherapy is 650,000 annually. During and after their treatment, many of these patients will develop CIPN, a serious side effect that affects proper sensory function interfering with daily living and treatment administration. The studies that are the subject of this thesis focus on the subset of cancer patients diagnosed with MM prior to and following treatment with the proteasome inhibitor, bortezomib. The goals of these studies were to quantify changes in sensory thresholds induced by underlying disease processes of cancer as well as to assess the efficacy of minocycline in preventing sensory neuropathy.

Given that approximately 10% of MM patients present with overt clinical neuropathy prior to receiving chemotherapy, it was hypothesized that greater numbers of MM patients exhibit quantifiable changes in sensory thresholds prior to receiving chemotherapy. To investigate this hypothesis MM patients underwent QST prior to having received any chemotherapy treatment and were compared to healthy volunteers. This is the first study conducted on treatment-naïve MM patients to quantitatively describe changes in sensory thresholds that are suggestive of impairments in A $\beta$ -, A $\delta$ -, and C-fiber function. In addition, failure to detect small-sized bumps in a fine tactile discrimination task was correlated with a decreased density of touch receptors, MCs, in the skin of MM patients. Thus, prior to treatment with chemotherapy, MM patients already exhibit impairments in mechanosensation, thermal sensation, and sensorimotor tasks and decreased densities of touch receptors. These findings are most likely indicative of the direct or indirect effects of

the MM disease, which have been reviewed in the literature <sup>173,174</sup>. It has been suggested that the presence of subclinical sensory deficits in patients predisposes them to develop treatment-emergent peripheral neuropathy. If this is the case, those patients with disease-related neuropathy may require smaller initial doses of bortezomib or increased monitoring throughout treatment. Future studies should aim to establish whether there is a connection between subclinical sensory deficits and treatment-emergent neuropathy. Specifically, it would be interesting to evaluate whether those patients with subclinical deficits develop treatment-emergent neuropathy sooner and whether the manifestation is more severe than those who do not have subclinical deficits. If a clear link is established, this will be a patient population who may benefit from the application of preventative therapies.

The second hypothesis explored was that MM patients treated with bortezomib show chemotherapy-induced deficits in sensory function that can be detected by QST and reversed with the administration of the preventive therapy, tetracycline antibiotic, minocycline. Killing cancer by reversibly inhibiting proteasomes and facilitating cell death by allowing the build-up of toxic levels of proteins seemed like an unlikely cancer therapy until it proved efficacious and was approved for use in multiple myeloma patients under the trade name Velcade<sup>®</sup> (bortezomib) <sup>82</sup>. While quite effective at treating MM, bortezomib does not only selectively destroy cancer cells, but also preys on non-cancer cells. The somatosensory system is particularly vulnerable to the effects of bortezomib via its ability induce changes in the DRG, which is unprotected by the blood-brain barrier. Injury of the somatosensory system by bortezomib is a toxicity causing neuropathic pain to develop in a glove-and-stocking distribution on patients and frequently results in dose-reduction or cessation of treatment. The utility

of bortezomib as a treatment for multiple myeloma is restricted by its damage to the peripheral nervous system (PNS). Optimization of bortezomib treatment will include reducing or eliminating the damage to the PNS, thereby eliminating the symptoms of neuropathic pain in patients.

In the second study, we explored the presence of bortezomib-induced deficits and described the first double blind, placebo-controlled study investigating minocycline as preventative agent for bortezomib-induced neuropathy. A preliminary analysis of QST data from MM patients co-administered placebo and bortezomib showed no detectable decline in sensory function of the placebo group. However, bortezomib did increase patient reports of tingling and numbness consistent with neuropathy in the placebo group. Although statistical significance was not achieved, it appeared that minocycline may have prevented increases in patient-reported tingling. Difficulties inherent in the collection of prospective clinical data that resulted in the presence of confounding factors may have disguised any positive effect of minocycline, making it difficult to discount the potential therapeutic value of this drug. Therefore, the neuroprotective effects of minocycline observed in pre-clinical and clinical studies warrant further investigation in a more thoroughly conducted study.

Despite much investigation, chemotherapy-induced peripheral neuropathy is still a problem pervasive in cancer patients treated with chemotherapy, few novel agents have proved effective in pre-clinical studies and of these, no single agent has proved effective in clinical trials. The failure to develop effective therapies stems from our lack of understanding of mechanisms underlying bortezomib-induced peripheral neuropathy and more broadly, CIPN. Understanding the changes chemotherapy induces in receptor and protein expression in neurons associated with symptoms of

neuropathy will inform the development of drugs aimed to protect these targets. It is this gap of knowledge that will most adequately be addressed with animal studies. Several correlate animal studies will be described in Appendix C as a supplement to the clinical data previously discussed.

## 5. Appendices

### 5.1. Appendix A: Central Processing of Pain

The spinal cord and brain comprise the CNS. Primary afferent sensory neurons of the peripheral nervous system project axons to synapse in the spinal cord (Figure 25). The spinal cord is composed of central gray matter (containing cell bodies of central neurons) surrounded by white matter (containing afferent and efferent axons). The dorsal portion of the gray matter receives sensory afferent input from the periphery, and the ventral gray sends efferent motor information to the periphery. The central gray matter is divided into eight distinct areas called laminae I- VIII (Figure 25). Nociceptive primary afferents (A $\delta$ - and C-fibers) project to secondary neurons located in laminae I and II of the spinal dorsal horn, which project to the brain in the spinothalamic tract. In addition, to these nociceptive-specific neurons, wide-dynamic-range neurons (WDRs) are also present in lamina I and receive information about mechanical stimuli (both nociceptive and non-nociceptive)<sup>13</sup>. WDRs are also located in lamina V and project to the brainstem and thalamus. WDRs in lamina V have dendrites that extend into laminae I and II and make direct contacts with C-fibers. They also receive indirect information from C-fibers via interneurons and monosynaptic input from A $\beta$ - and A $\delta$ -fibers<sup>13</sup>. Nociceptive visceral afferents also terminate in lamina V. Non-nociceptive A $\beta$ -fibers predominately terminate in laminae III and IV and have topographically organized receptive fields. Finally, some neurons in laminae VII and VIII may receive ipsilateral and contralateral polysynaptic nociceptive input and contribute to the sensation of diffuse pain.

When stimulated, primary afferent nociceptors release excitatory (glutamate) and peptide neurotransmitters that bind to their respective receptors on central neurons.

Glutamate release from A $\delta$ - and C-fibers produces fast depolarization and action potentials in dorsal horn neurons <sup>12,175</sup>. Peptide neurotransmitters, such as substance P, are also released by peptidergic C-fibers and produce a slower depolarization than glutamate in spinal dorsal horn neurons <sup>13</sup>. Peptidergic and non-peptidergic transmitters have different properties and may contribute to different aspects of synaptic transmission. Non-peptidergic transmitters (e.g.: glutamate) have a more limited range of action than peptide transmitters due to their reuptake by nerve terminals or glial cells <sup>13</sup>. The lack of a reuptake mechanism for peptide transmitters means that they will stay longer in the synaptic cleft and activate a larger area of secondary neurons in the spinal cord. Peptidergic transmitters also work synergistically with non-peptidergic transmitters by perpetuating their effects.

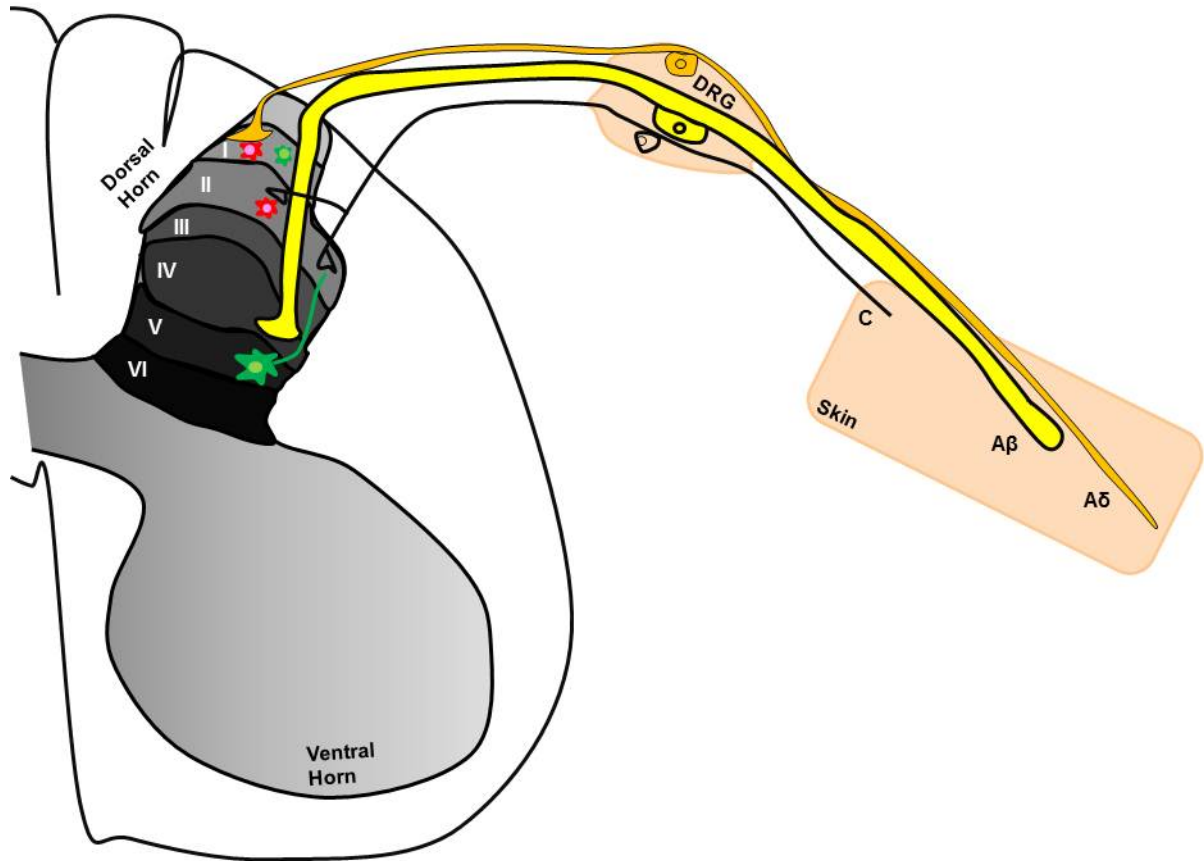


**Figure 25 Primary Afferent Neuron Synapses in Dorsal Spinal Cord**

Illustration of a hemisected spinal cord with gray matter surrounded by white matter. Primary afferent fibers in the skin have cell bodies located in the dorsal root ganglion (DRG) and synapse in an organized fashion on different laminae in the spinal cord. Unmyelinated C-fibers (black) synapse in laminae II of the spinal dorsal horn on secondary order nociceptors (red) and wide dynamic range neurons (green). Thinly myelinated Aδ-fibers (orange) project to lamina I on nociceptive secondary neurons. Large myelinated Aβ-fibers synapse predominantly on WDR neurons in lamina V of the spinal dorsal horn.



When an individual sustains a localized tissue injury, that area becomes and remains tender long after the initial damage. Subsequent stimulation of that area induces pain even if the magnitude is much lower than the initial damaging stimulus. This is called hyperalgesia and is caused by the sensitization of nociceptors. Nociceptors are sensitized when the threshold for activation is lowered; damaged cells and tissues release substances such as prostaglandin, substance P, acetylcholine, bradykinin, serotonin and leukotriene, which sensitize nociceptors<sup>43</sup>. Although primary afferents receive sensory information, they are also capable of releasing substances (e.g., substance P and cGRP) synthesized in the cell body in response to injury<sup>176</sup>. These chemical mediators cause vasodilation and lead to inflammation and the release of other substances that sensitize nearby primary afferents, in a process termed axon reflex<sup>176,177</sup>. Activation of N-methyl-D-aspartate (NMDA) channels by glutamate underlies “wind-up” and is one of the mechanisms that produces central sensitization<sup>56</sup>. Wind-up occurs due to the persistent firing of C-fibers after serious injury. Central sensitization occurs when input from primary afferents provokes spinal dorsal horn neurons to change expression of certain genes, thereby causing an intrinsic change in firing patterns and hyperexcitability<sup>56</sup>. This can lead to the perception of pain in the absence of stimulation.

Spinal dorsal horn neurons relay pain information to the brain in five ascending pathways: spinothalamic, spinoreticular, spinomesencephalic, cervicothalamic, and spinohypothalamic<sup>13</sup>. The spinothalamic pathway is the major pain pathway, which carries axons of contralateral spinal dorsal horn neurons from laminae I, V, VI, and VII in the anterolateral white matter to the thalamus for further processing. Descending

inhibitory pathways modulate transmission of pain by inhibiting spinal dorsal horn neurons and thereby evoking analgesia <sup>178</sup>.

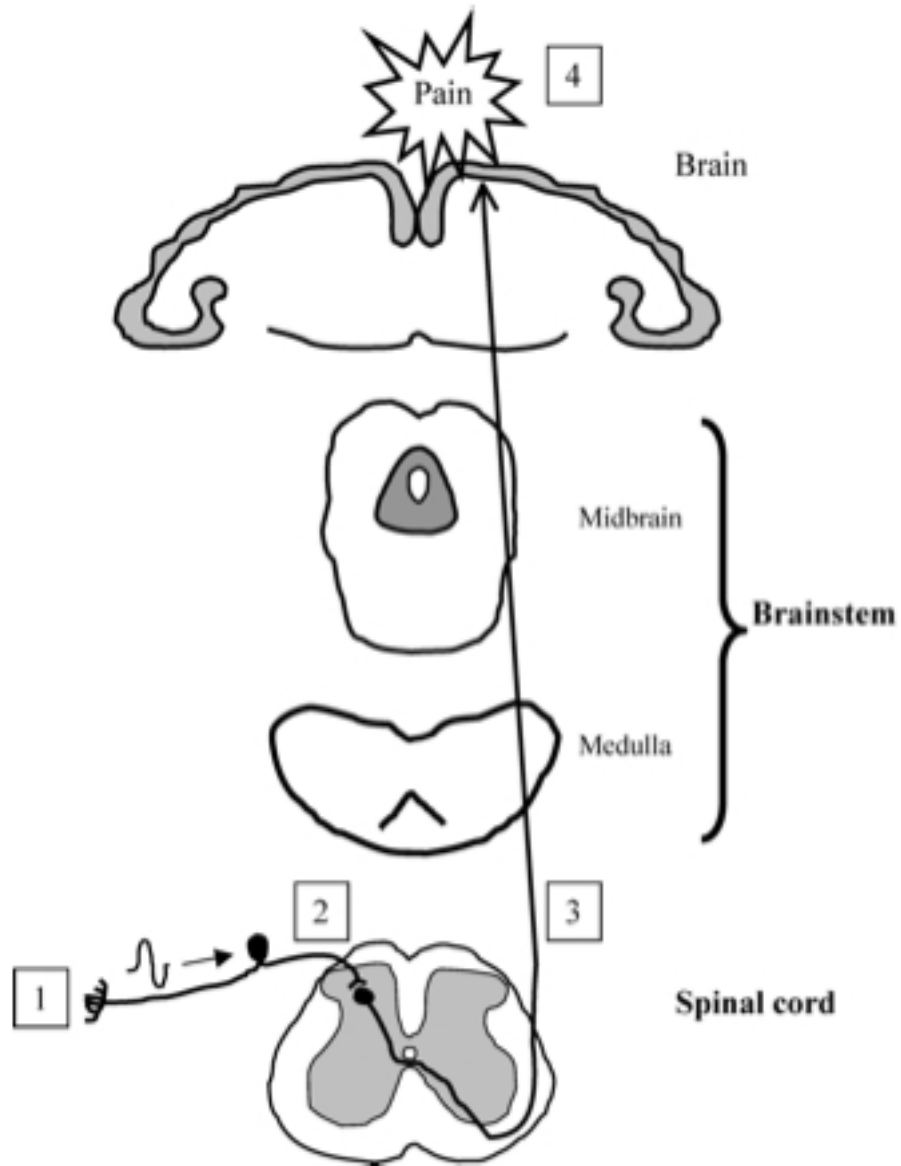


**Figure 26 Central Pain Processing**

Nociceptive primary afferent neurons (1) relay the sensation of pain to the central nervous system by synapsing on second order spinal dorsal horn neurons (2). Spinal dorsal horn neurons decussate and ascend in the spinothalamic tract located in the contralateral anteriorlateral funiculus (3) to the brain (4).

Reprinted from American Association of Critical Care Nurses (ACCN), Renn C and Dorsey S. Physiology and Processing of Pain: A Review. Copyright 2005, reprinted with permission from Wolters Kluwer Health.

## **5.2. Appendix B: Additional Statistical Analysis for Chapter 3**

Chapter 3 describes a preliminary analysis of the quantitative sensory data from a phase II study of minocycline vs. placebo to prevent treatment-induced neuropathy in multiple myeloma patients. Given the limitations of the analysis performed, the Department of Biostatistics was consulted and asked to perform a separate analysis in order to account for the effect of multiple independent variables on the dependent variable (quantitative sensory measure).

The study design was explained at length, and the statistician was provided with a spreadsheet populated with de-identified patient data. Sixty of 72 patients received at least two tests and were included in the analysis. Patients with only one QST were excluded. The following analysis included more patients than Analysis #2 in Chapter 3 because all patients with two tests were included regardless of whether the initial test was performed at less than 13 mg of chemotherapy. The same measures as above were analyzed for the fingertip, thenar eminence and forearm. The dependent variable in this analysis was either analyzed using the value at the follow-up QST at the maximum cumulative dose of bortezomib or converted into a difference score by subtracting the value recorded at the lowest cumulative dose of bortezomib (the initial test) from the value at the highest cumulative dose of bortezomib (the follow-up test). Backward stepwise regression approach was used for variable selection of multivariable analyses. The outcome variable (the dependent variable) was either the follow-up QST value at the highest cumulative dose or the difference score. The input variables (independent variables) were study drug (minocycline or placebo), whether study drug was administered prior to bortezomib treatment (yes or no), myeloma stage (I, II, or III) and cumulative dose in milligrams. P-values less than 0.05 were

considered statistically significant and all tests were two-sided. Due to the exploratory nature of this study, no adjustment of multiple tests was performed. All analyses were performed using SAS 9.3 (SAS Institute Inc., Cary NC).

Adjusting for cumulative dose, whether the study drug was administered prior to bortezomib, and multiple myeloma stage, minocycline treatment was significantly associated with a higher temperature of heat pain detection at the fingertip ( $P=0.04$ ) and thenar eminence ( $P=0.01$ ), and lower temperatures of cool detection at the fingertip ( $P=0.04$ ), thenar eminence ( $P=0.03$ ), and volar forearm ( $P=0.04$ ). Using the difference score for QST measurements and adjusting for whether the study drug was administered prior to chemotherapy and the stage, minocycline was only associated with a decrease in the temperature of cool detection at the forearm ( $P=0.02$ ).

Limitations of this analysis include the fact that adjustments for cumulative dose and whether the study drug was administered prior to chemotherapy were performed for the total group of patients ( $N=60$ ) analyzed. However, these adjustments should have been made separately for the minocycline versus placebo group because it would be expected that the administration of treatment prior to bortezomib would only be important for the minocycline group if there were a time-dependent effect of the drug, but not for placebo. Adjustments for cumulative dose should also have been adjusted for separately in minocycline vs. placebo groups because if minocycline impacts QST then it may change a dose-dependent effect of bortezomib on sensory function.

### **5.3. Appendix C: Related Preclinical Studies**

To complement the clinical studies presented in this thesis, several pre-clinical studies in animal studies were performed in animal models of chemotherapy-induced neuropathy. Two additional frontline chemotherapeutic agents that commonly cause neuropathy were investigated in the following studies.

Prior to investigating peripheral innervation in patients using in vivo confocal microscopy as explained in Chapter 2, biopsies were collected at skin sites that depicted symptoms of neuropathy. Skin biopsies from patients treated with chemotherapy showed reduced numbers of nerve fibers compared to biopsies of healthy controls. Similar quantifications were performed in rodents treated with chemotherapy.

A $\delta$ - and C-fibers are subtypes of nerve fibers that originate in the dermis layer of skin and usually cross the dermal-epidermal junction to terminate in the epidermis as free nerve endings, called intraepidermal nerve fibers (IENFs) (Figure 27). A hallmark of many small fiber peripheral neuropathies is a decrease in the density of IENFs <sup>179</sup>. Decreases in IENF density are present in patients with symptomatic bortezomib-induced peripheral neuropathy <sup>89</sup> and in rodent models of paclitaxel- and oxaliplatin-induced neuropathic pain <sup>162,163</sup>. Loss of IENFs seems to approximately correlate with symptoms of neuropathy, but it is unclear whether or not their loss is responsible for the hypersensitivity, pain, dysesthesias or paresthesias felt by patients. If the loss of IENFs underlies symptoms, the question becomes how missing fibers are able to produce the uncomfortable symptoms of pain and tingling and why they instead do not produce numbness. The release of cytokines from injured fibers may be driving symptoms of neuropathy. Since the loss of IENFs may contribute to symptoms of

neuropathy, treatments that are able to block development of neuropathy might also be expected to spare nerve fibers. Based on a recently-published study, monocyte chemoattractant protein-1 (MCP-1) and its chemokine receptor 2 (CCR2) are involved in the induction and maintenance of paclitaxel-induced neuropathic pain. Knockdown of CCR2 with intrathecal siRNA attenuates behavioral sensitivity of rodents after paclitaxel treatment and has IENF densities similar to vehicle-treated animals (Figure 28)<sup>179</sup>.

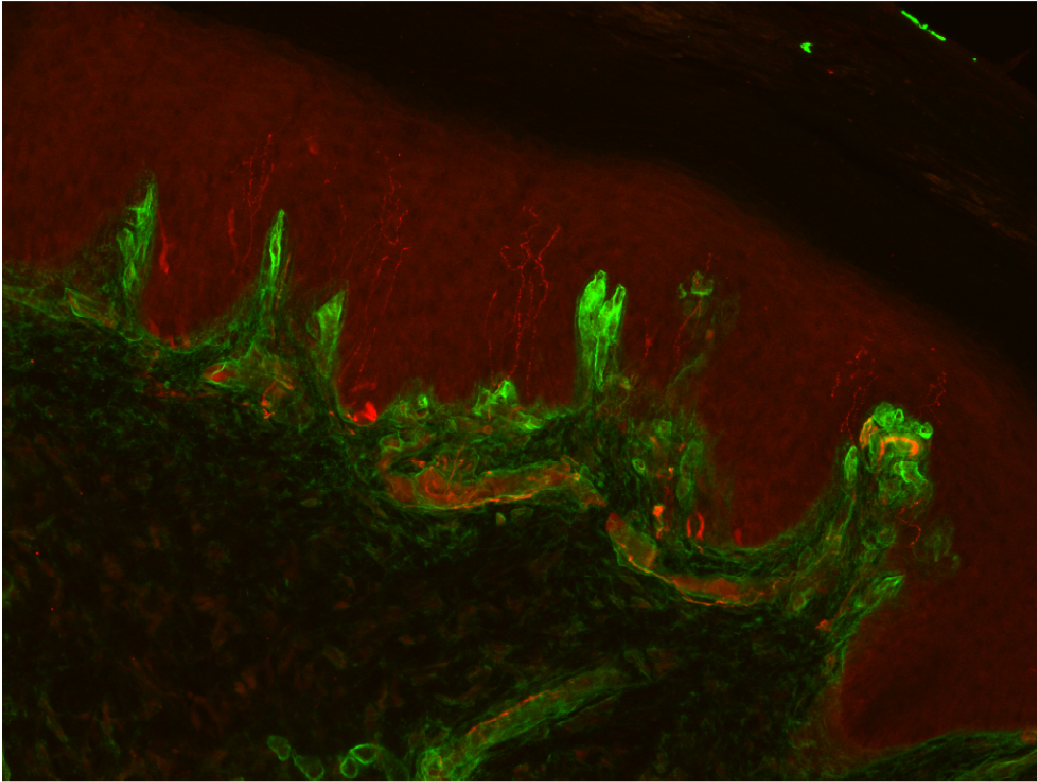


**Figure 27 Intraepidermal Nerve Fibers in Rodent Skin**

In red, IENFs labeled with protein gene product 9.5 (PGP 9.5) and in green, collagen delineating the dermal-epidermal junction in the foot pad of a normal rat.



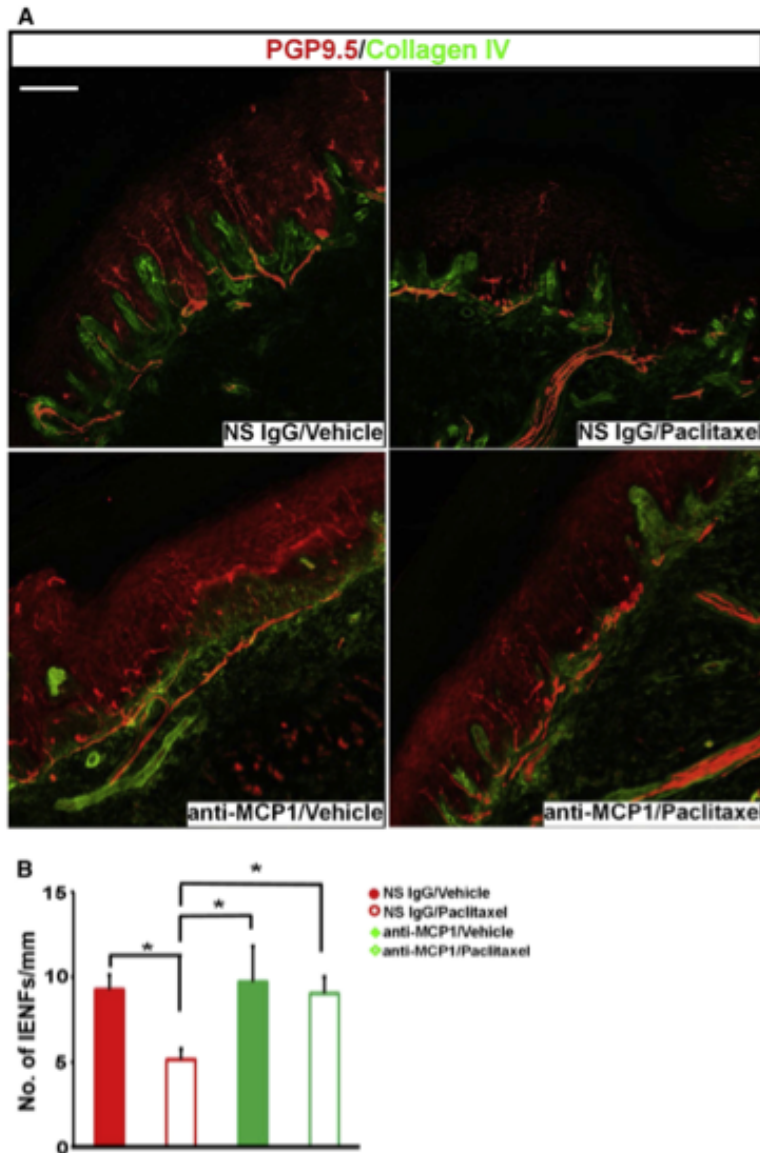


**Figure 28 Blockade of MCP-1 Prevents the Loss of IENFs Induced by Paclitaxel**

(A) Representative images of IENFs (red) in the glabrous hindpaw skin of the rats treated with combinations of nonspecific control peptide IgG (NS/IgG), anti-MCP-1 IgG. Co-treatment with anti-MCP-1 and paclitaxel spared IENFs while control peptide and paclitaxel-treated animals had significantly lower densities of IENFs. (B) The quantification of IENFs in each treatment condition.

Reprinted from Journal of Pain 14(10), Zhang H, Boyette-Davis JA, Kosturakis AK, Li Y, Yoon SY, Walters ET, Dougherty PM, Induction of monocyte chemoattractant protein-1 (MCP-1) and its receptor CCR2 in primary sensory neurons contributes to paclitaxel-induced peripheral neuropathy. Copyright 2013, reprinted with permission from Elsevier.

Quantification of IENFs is performed on slices of skin tissue co-stained with protein gene product 9.5 (PGP 9.5) expressed in the cytoplasm of neurons and collagen. Collagen delineates the dermal epidermal junction and restricts quantification to epidermal fibers. PGP 9.5 is believed to be a pan neuronal marker for IENFs. Other markers such as calcitonin gene-related peptide (CGRP) are thought to label the subset of PGP 9.5 fibers expressing CGRP. Figure 29 shows double staining of PGP 9.5 and CGRP markers and a perfect co-localization of CGRP fibers with PGP. Further experiments, however, show CGRP positive fibers that lack PGP 9.5 staining at concentrations normally used for quantification (1:500 and 1:400, respectively) (Figure 30). This provoked the question: is PGP 9.5 really a pan neuronal marker? The implication of this is that PGP 9.5 may not be a reliable marker for quantifying neuropathy if it is not a pan neuronal marker. Further studies are needed to determine if there are large populations of nerves unlabeled by PGP 9.5.

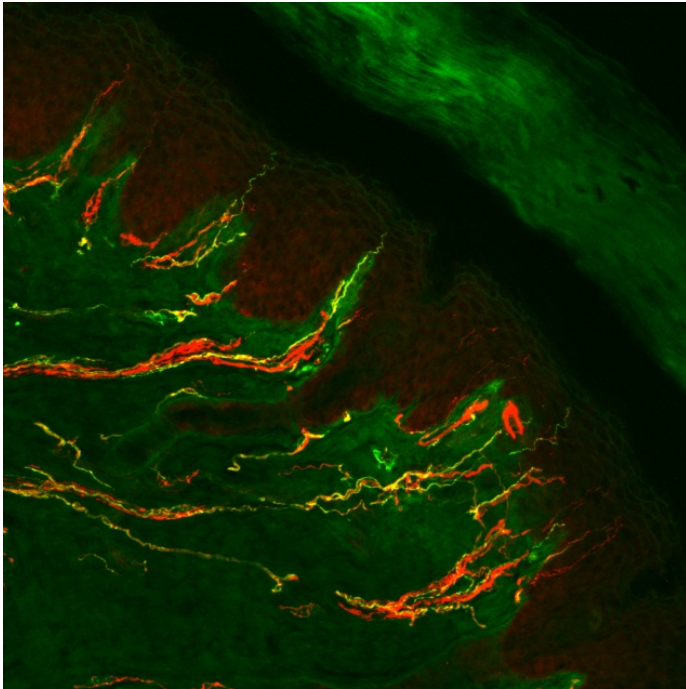


**Figure 29 PGP9.5 and CGRP are Co-Localized in Intraepidermal Nerve Fibers**  
 CGRP (green) IENFs co-localize (yellow) with PGP 9.5 (red) in the epidermis of rodent hindpaw footpad.

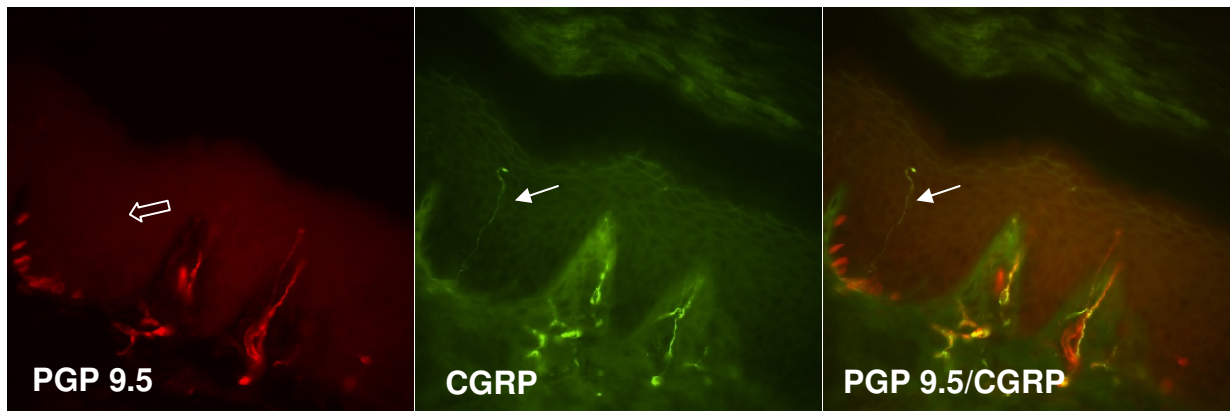


**Figure 30 Some CGRP Positive Fibers Do Not Appear to Express PGP9.5**  
 CGRP-expressing fibers in green and PGP 9.5-expressing fibers in red. Some CGRP positive fibers (solid arrow) do not co-localize with PGP 9.5. The unfilled arrow points to the location where the CGRP positive fiber should have been present.

As described in the discussion of Chapter 2, various cytokines, which include chemokines, are implicated in various inflammatory and pain states<sup>180,181</sup>. The following study was performed in pre-clinical models to investigate the contribution of the chemokine, monocyte chemoattractant protein 1 (MCP-1) and its cognate receptor, CCR2, in several inflammatory and neuropathic pain models. To investigate the role of CCR2 in pain, the painful-behavioral phenotypes of CCR2 knockout (CCR2-KO) mouse were compared to those of wildtype mice. Intraplantar injection of formalin and complete Freund's adjuvant (CFA) served as acute and chronic inflammatory pain models, respectively. The neuropathic pain models used were spared nerve injury (SNI) and chemotherapy (paclitaxel and oxaliplatin).

1% Formalin (10 µl) was unilaterally injected to the hindpaw and licking time was measured. CCR2-KO mice showed no difference in phase 1 (0-10 minutes) or phase 2 (10-45 minutes) of formalin-induced spontaneous pain (Figure 31).

Complete Freund's Adjuvant (CFA) was injected unilaterally into the hindpaws of wildtype and CCR2-KO mice and mechanical testing was performed on days 1, 3, 7, 15, 20, and 27 after injection. CCR2-KO mice and wildtype mice showed similar mechanical allodynia after intraplantar CFA that resolved by Day 27 (Figure 32).

Sural and common peroneal branches of left sciatic nerve were ligated and transected as described<sup>182</sup>. CCR2-KO mice showed similar withdrawal thresholds as sham mice and significantly less mechanical sensitivity compared to wildtype mice on post-operative days 7 and 14 (Figure 33).

Paclitaxel (2 mg/kg) was injected intraperitoneally on days 1, 3, 5, 7. Mechanical withdrawal thresholds were tested at Days 7, 14, and 21. CCR2-KO mice treated with

paclitaxel showed less mechanical hypersensitivity compared with wildtype mice (Figure 34).

Oxaliplatin (3mg/kg) was injected intraperitoneally every day for 5 days. CCR2-KO mice and wildtype mice showed similar decreases in withdrawal thresholds after oxaliplatin injection (Figure 35).

Taken together, these data suggest that CCR2 contributes to neuropathic, but not inflammatory pain. Furthermore, CCR2 is involved in neuropathic pain induced by spared nerve injury and paclitaxel, but not oxaliplatin. Further studies could investigate the reasons CCR2 is involved in paclitaxel, but not oxaliplatin-induced neuropathy.

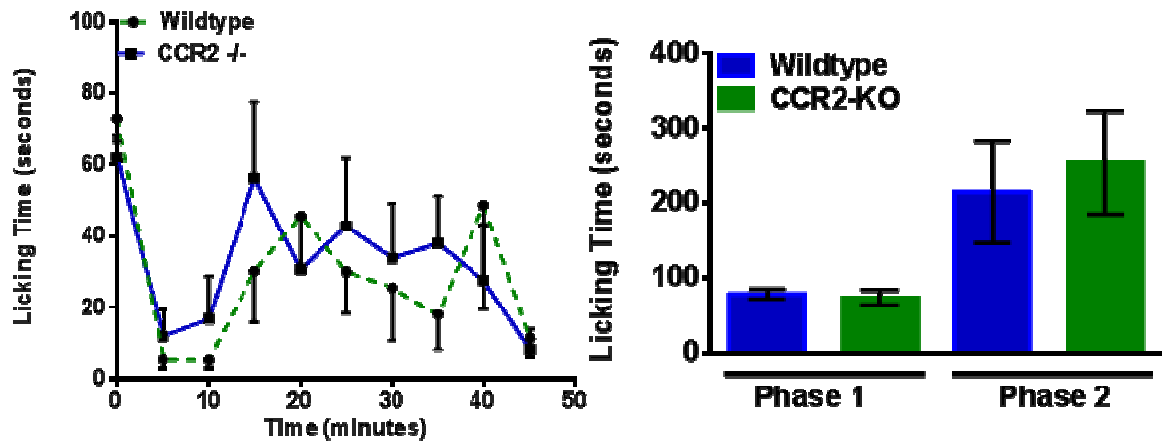


**Figure 31 CCR2-KO Mice Showed No Difference in Formalin-Induced Spontaneous Pain**

Duration of licking time in both phase 1 and phase 2 is similar between wildtype and CCR2-KO mice after intraplantar formalin injection.

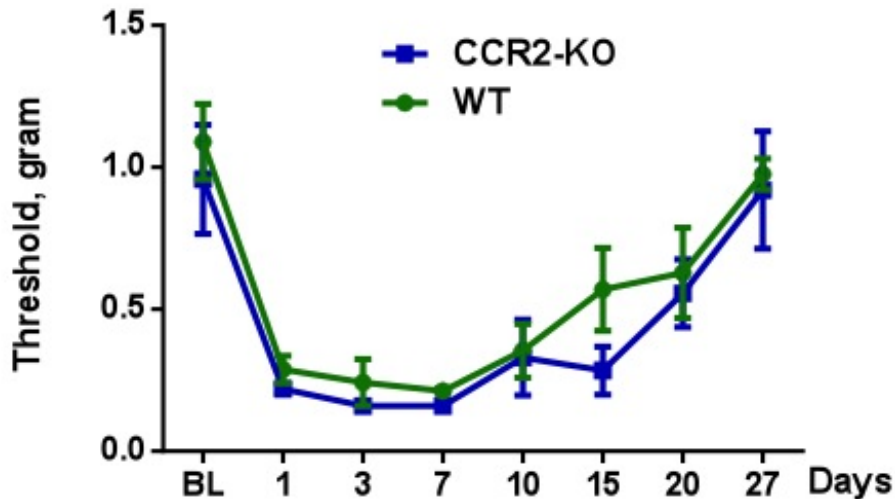


**Figure 32 CCR2-KO Mice Showed No Difference in CFA-Induced Allodynia**

CCR2-KO mice showed similar mechanical withdrawal thresholds after intraplantar CFA injection.

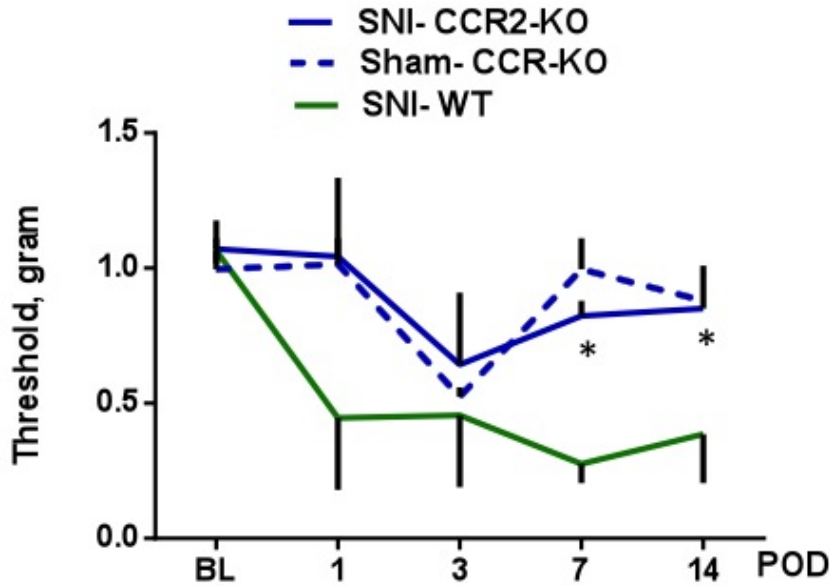


**Figure 33 CCR2-KO Mice Showed Less Mechanical Hypersensitivity after Spared Nerve Injury**

Mechanical allodynia was significantly reduced in CCR2-KO mice after spared nerve injury. \*  $P < 0.05$ , Two-Way ANOVA with Tukey's post hoc test.

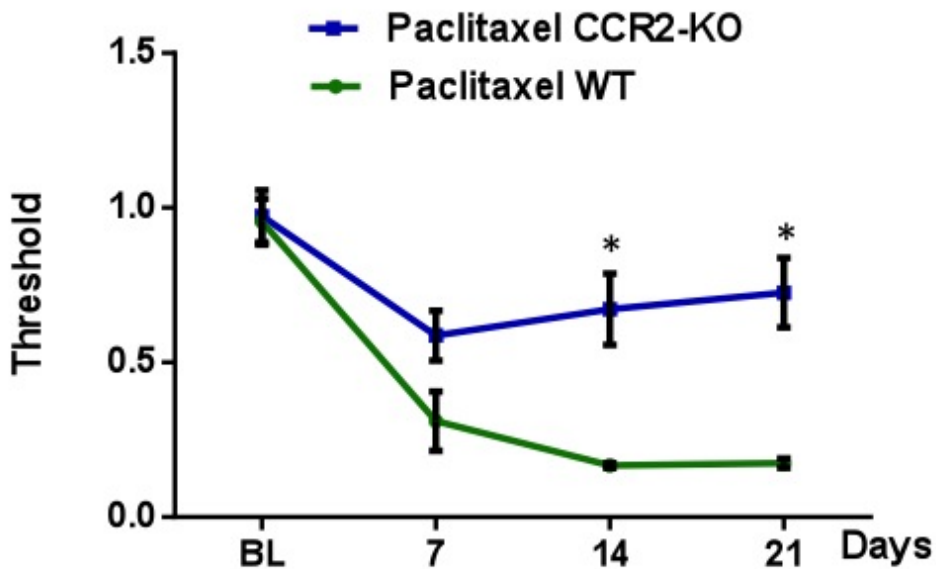


**Figure 34 CCR2- KO Mice Showed Less Mechanical Hypersensitivity after Paclitaxel Treatment**

\* $P < 0.05$ , Multiple  $t$ -test

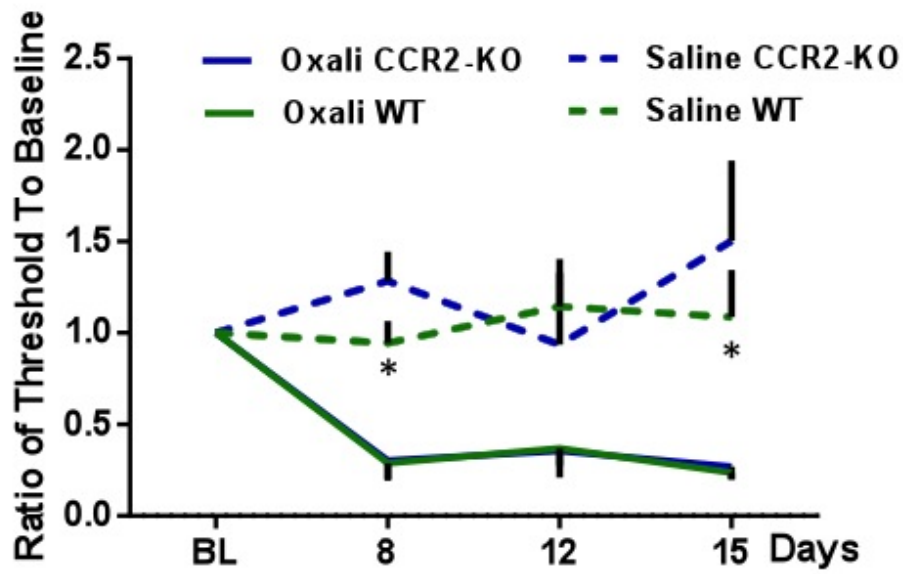


**Figure 35 CCR2-KO Mice Showed No Reduction in Oxaliplatin-Induced Mechanical Hypersensitivity**

\* $P < 0.01$ , Saline CCR2 vs. Oxaliplatin CCR2-KO, Two-Way ANOVA with Tukey's post hoc test.



## References

1. Smith BD, Smith GL, Hurria A, Hortobagyi GN, Buchholz TA. Future of cancer incidence in the United States: burdens upon an aging, changing nation. *Journal of Clinical Oncology*. 2009;27(17):2758–2765. doi:10.1200/JCO.2008.20.8983.
2. *American Cancer Society*.
3. American Society of Clinical Oncology. The state of cancer care in america, 2014: a report by the american society of clinical oncology. *J Oncol Pract*. 2014;10(2):119–142. doi:10.1200/JOP.2014.001386.
4. de Moor JS, Mariotto AB, Parry C, et al. Cancer survivors in the United States: prevalence across the survivorship trajectory and implications for care. *Cancer Epidemiology Biomarkers & Prevention*. 2013;22(4):561–570. doi:10.1158/1055-9965.EPI-12-1356.
5. National Cancer Institute. Chemotherapy Side Effects Sheets. <http://www.cancer.gov/cancertopics/coping/physicaleffects/chemo-side-effects>. 2014:1–2. Available at: <http://www.cancer.gov/cancertopics/coping/physicaleffects/chemo-side-effects>. Accessed May 2, 2014.
6. Polomano RC, Bennett GJ. Chemotherapy-evoked Painful Peripheral Neuropathy. *Pain Med*. 2001;2(1):8–14. doi:10.1046/j.1526-4637.2001.002001008.x.
7. Hershman DL, Lacchetti C, Dworkin RH, et al. Prevention and Management of Chemotherapy-Induced Peripheral Neuropathy in Survivors of Adult Cancers: American Society of Clinical Oncology Clinical Practice Guideline. *Journal of Clinical Oncology*. 2014. doi:10.1200/JCO.2013.54.0914.
8. Gardner EP, Martin JH, Jessell TM. The Bodily Senses. In: *Principles of Neural Science*. 4 ed.; 2000:430–450.
9. Rice RL, Albrecht PJ. Cutaneous Mechanisms of Tactile Perception Morphological and Chemical Organization of the Innervation to the Skin. In: *The Senses A Comprehensive Reference*. Vol 6. 2008:1–31.
10. Gold MS, Gebhart GF. 531E0F73-92CA-4E07-AD9D-0343B63ADD85. *Nature Publishing Group*. 2010;16(11):1248–1257. doi:10.1038/nm.2235.
11. Djouhri L, Lawson SN. A $\beta$ -fiber nociceptive primary afferent neurons: a review of incidence and properties in relation to other afferent A-fiber neurons in mammals. *Brain Research Reviews*. 2004;46(2):131–145. doi:10.1016/j.brainresrev.2004.07.015.
12. Julius D, McCleskey EW. *Cellular and molecular properties of primary afferent neurons*. Wall and Melzack's Textbook of Pain (5th ed); 2006.

13. Basbaum AI, Jessell TM. Principles of Neural Science. In: *Principles of Neural Science*. 4 ed.; 2000:472–491.
14. Meyer RA, Davis KD, Cohen RH, Treede R-D, Campbell JN. Mechanically insensitive afferents (MIAs) in cutaneous nerves of monkey. *Brain Res*. 1991;561(2):252–261.
15. Lynn B, Carpenter SE. Primary afferent units from the hairy skin of the rat hind limb. *Brain Res*. 1982;238(1):29–43. doi:10.1016/0006-8993(82)90768-5.
16. Leem JW, Willis WD, Chung JM. Cutaneous sensory receptors in the rat foot. *J Neurophysiol*. 1993;69(5):1684–1699.
17. Delmas P, Hao J, Rodat-Despoix L. Molecular mechanisms of mechanotransduction in mammalian sensory neurons. *Nat Rev Neurosci*. 2011;12(3):139–153. doi:10.1038/nrn2993.
18. Dubin AE, Patapoutian A. Nociceptors: the sensors of the pain pathway. *J Clin Invest*. 2010;120(11):3760–3772. doi:10.1172/JCI42843.
19. Schaible HG, Schmidt RF. Responses of fine medial articular nerve afferents to passive movements of knee joints. *J Neurophysiol*. 1983.
20. Hunt SP, Mantyh PW. The molecular dynamics of pain control. *Nat Rev Neurosci*. 2001;2(2):83–91. doi:10.1038/35053509.
21. McGrath JA, Eady R, Pope FM. Anatomy and organization of human skin. *Rook's textbook of ....* 2010.
22. Paré M, Smith AM, Rice FL. Distribution and terminal arborizations of cutaneous mechanoreceptors in the glabrous finger pads of the monkey. *J Comp Neurol*. 2002;445(4):347–359. doi:10.1002/cne.10196.
23. Johnson KO. The roles and functions of cutaneous mechanoreceptors. *Current opinion in neurobiology*. 2001;11(4):455–461. doi:10.1016/S0959-4388(00)00234-8.
24. Lucarz A, Brand G. Current considerations about Merkel cells. *European Journal of Cell Biology*. 2007;86(5):243–251. doi:10.1016/j.ejcb.2007.02.001.
25. Chambers MR, Andres KH, Duering von M, Iggo A. The structure and function of slowly adapting type II mechanoreceptor in hairy skin. *Exp Physiol*. 1972;57(4):417–445. doi:10.1111/(ISSN)1469445X/homepage/Permissions.html.
26. Wheat HE, Goodwin AW. Physiological Responses of Sensory Afferents in Glabrous and Hairy Skin of Humans and Monkeys. In: *The senses: A Comprehensive Reference*. Vol 6. 2008:39–54.
27. Dubovů P. Restoration of lamellar structures in adult rat Pacinian corpuscles

- following their simultaneous freezing injury and denervation. *Anat Embryol.* 2000;202(3):235–245. doi:10.1007/s004290000105.
28. Bolanowski SJ, Zwislocki JJ. Intensity and frequency characteristics of pacinian corpuscles. I. Action potentials. *J Neurophysiol.* 1984;51(4):793–811.
  29. Olausson H, Lamarre Y, Backlund H, et al. Unmyelinated tactile afferents signal touch and project to insular cortex. *Nat Neurosci.* 2002;5(9):900–904. doi:10.1038/nn896.
  30. Lumpkin EA, Caterina MJ. Mechanisms of sensory transduction in the skin. *Nature.* 2007;445(7130):858–865. doi:10.1038/nature05662.
  31. Reichling DB, Levine JD. Heat transduction in rat sensory neurons by calcium-dependent activation of a cation channel. *Proc Natl Acad Sci USA.* 1997;94(13):7006–7011.
  32. Caterina MJ, Schumacher MA, Tominaga M, Rosen TA. The capsaicin receptor: a heat-activated ion channel in the pain pathway. *Nature.* 1997;389(6653):816–824. doi:10.1038/39807.
  33. Caterina MJ, Leffler A, Malmberg AB, et al. Impaired nociception and pain sensation in mice lacking the capsaicin receptor. *Science.* 2000;288(5464):306–313. doi:10.1126/science.288.5464.306.
  34. Caterina MJ, Rosen TA, Tominaga M, Brake AJ, Julius D. A capsaicin-receptor homologue with a high threshold for noxious heat. *Nature.* 1999;398(6726):436–441. doi:10.1038/18906.
  35. Peier AM, Moqrich A, Hergarden AC, et al. A TRP channel that senses cold stimuli and menthol. *Cell.* 2002;108(5):705–715. doi:10.1016/S0092-8674(02)00652-9.
  36. Story GM, Peier AM, Reeve AJ, et al. ANKTM1, a TRP-like channel expressed in nociceptive neurons, is activated by cold temperatures. *Cell.* 2003;112(6):819–829.
  37. Merskey H, Bogduk N, eds. Part III Pain Terms. In: *Classification of Chronic Pain*. Second. A Current List with Definitions and Notes on Usage. Seattle: IASP Press; 1994:209–214. Available at: <http://www.iasp-pain.org/Education/Content.aspx?ItemNumber=1698&navItemNumber=576>.
  38. Burgess PR, Perl ER. Myelinated afferent fibres responding specifically to noxious stimulation of the skin. *J Physiol (Lond).* 1967;190(3):541–562.
  39. Basbaum AI, Bautista DM, Scherrer G, Julius D. Cellular and Molecular Mechanisms of Pain. *Cell.* 2009;139(2):267–284. doi:10.1016/j.cell.2009.09.028.
  40. Belkouch M, Dansereau M-A, treault PT, et al. Functional up-regulation of Na.

- Journal of Neuroinflammation*. 2014;11(1):1–17. doi:10.1186/1742-2094-11-45.
41. Woolf CJ. What is this thing called pain? *J Clin Invest*. 2010;120(11):3742–3744. doi:10.1172/JCI45178.
  42. Ricciotti E, FitzGerald GA. Prostaglandins and inflammation. *Arteriosclerosis, Thrombosis, and Vascular Biology*. 2011;31(5):986–1000. doi:10.1161/ATVBAHA.110.207449.
  43. Kidd BL, Urban LA. Mechanisms of inflammatory pain. *British Journal of Anaesthesia*. 2001;87(1):3–11. doi:10.1093/bja/87.1.3.
  44. Treede R-D, Jensen TS, Campbell JN, et al. Neuropathic pain: redefinition and a grading system for clinical and research purposes. In: Vol 70. Lippincott Williams & Wilkins; 2008:1630–1635. doi:10.1212/01.wnl.0000282763.29778.59.
  45. Baron R. Mechanisms of Disease: neuropathic pain—a clinical perspective. *Nat Clin Pract Neurol*. 2006;2(2):95–106. doi:10.1038/ncpneuro0113.
  46. Waxman SG, Zamponi GW. Regulating excitability of peripheral afferents: emerging ion channel targets. *Nat Neurosci*. 2014;17(2):153–163. doi:10.1038/nn.3602.
  47. Yang Y, Wang Y, Li S, et al. Mutations in SCN9A, encoding a sodium channel alpha subunit, in patients with primary erythralgia. *Journal of medical ....* 2004. doi:10.1136/jmg.2003.012153.
  48. Shorer Z, Wajsbrot E, Liran T-H, Levy J, Parvari R. A novel mutation in SCN9A in a child with congenital insensitivity to pain. *Pediatr Neurol*. 2014;50(1):73–76. doi:10.1016/j.pediatrneurol.2013.09.007.
  49. Choi J-S, Boralevi F, Brissaud O, et al. nrneuro1.2010.162. *Nature Publishing Group*. 2010;7(1):51–55. doi:10.1038/nrneuro1.2010.162.
  50. Faber CG, Lauria G, Merkies I. Gain-of-function Nav1. 8 mutations in painful neuropathy. ... *of the National ....* 2012. doi:10.1073/pnas.1216080109/-/DCSupplemental.
  51. Craner MJ, Klein JP, Renganathan M, Black JA, Waxman SG. Changes of sodium channel expression in experimental painful diabetic neuropathy. *Ann Neurol*. 2002;52(6):786–792. doi:10.1002/ana.10364.
  52. Alessandri-Haber N. Transient Receptor Potential Vanilloid 4 Is Essential in Chemotherapy-Induced Neuropathic Pain in the Rat. *Journal of Neuroscience*. 2004;24(18):4444–4452. doi:10.1523/JNEUROSCI.0242-04.2004.
  53. Wu Z, Yang Q, Crook RJ, O’Neil RG, Walters ET. TRPV1 channels make major contributions to behavioral hypersensitivity and spontaneous activity in nociceptors after spinal cord injury. *Pain*. 2013;154(10):2130–2141.

doi:10.1016/j.pain.2013.06.040.

54. Xing H, Chen M, Ling J, Tan W, Gu JG. TRPM8 mechanism of cold allodynia after chronic nerve injury. *Journal of Neuroscience*. 2007;27(50):13680–13690. doi:10.1523/JNEUROSCI.2203-07.2007.
55. Hudson LJ, Bevan S, Wotherspoon G, Gentry C, Fox A, Winter J. VR1 protein expression increases in undamaged DRG neurons after partial nerve injury. *Eur J Neurosci*. 2001;13(11):2105–2114.
56. Herrero JF, Laird J, Lopez-Garcia JA. Wind-up of spinal cord neurones and pain sensation: much ado about something? *Prog Neurobiol*. 2000;61(2):169–203. doi:10.1016/S0301-0082(99)00051-9.
57. Luo ZD, Chaplan SR, Higuera ES, et al. Upregulation of Dorsal Root Ganglion  $\alpha 2\delta$  Calcium Channel Subunit and Its Correlation with Allodynia in Spinal Nerve-Injured Rats. *Journal of Neuroscience*. 2001;21(6):1868–1875.
58. Hains BC, Saab CY, Klein JP, Craner MJ, Waxman SG. Altered sodium channel expression in second-order spinal sensory neurons contributes to pain after peripheral nerve injury. *Journal of Neuroscience*. 2004;24(20):4832–4839. doi:10.1523/JNEUROSCI.0300-04.2004.
59. Moore KA, Kohno T, Karchewski LA, Scholz J, Baba H, Woolf CJ. Partial peripheral nerve injury promotes a selective loss of GABAergic inhibition in the superficial dorsal horn of the spinal cord. *Journal of Neuroscience*. 2002;22(15):6724–6731.
60. Coull JAM, Boudreau D, Bachand K, et al. Trans-synaptic shift in anion gradient in spinal lamina I neurons as a mechanism of neuropathic pain. *Nature*. 2003;424(6951):938–942. doi:10.1038/nature01868.
61. Fields HL. Is there a facilitating component to central pain modulation? *APS Journal*. 1992;1(2):71–78. doi:10.1016/1058-9139(92)90030-G.
62. Dray A. Inflammatory mediators of pain. *British Journal of Anaesthesia*. 1995;75(2):125–131. doi:10.1093/bja/75.2.125.
63. Gaudet AD, Popovich PG, Ramer MS. Wallerian degeneration: Gaining perspective on inflammatory events after peripheral nerve injury. *Journal of Neuroinflammation*. 2011;8(1):110. doi:10.1186/1742-2094-8-110.
64. Myers RR, Campana WM, Shubayev VI. The role of neuroinflammation in neuropathic pain: mechanisms and therapeutic targets. *Drug Discov Today*. 2006;11(1-2):8–20. doi:10.1016/S1359-6446(05)03637-8.
65. Brück W, Friede RL. The role of complement in myelin phagocytosis during PNS wallerian degeneration. *J Neurol Sci*. 1991;103(2):182–187. doi:10.1016/0022-510X(91)90162-Z.

66. De Jongh RF, Vissers KC, Meert TF, Booij LHDJ, De Deyne CS, Heylen RJ. The Role of Interleukin-6 in Nociception and Pain. *Anesthesia & Analgesia*. 2003;1096–1103. doi:10.1213/01.ANE.0000055362.56604.78.
67. Sommer C, Petrusch S, Lindenlaub T, Toyka KV. Neutralizing antibodies to interleukin 1-receptor reduce pain associated behavior in mice with experimental neuropathy. *Neuroscience Letters*. 1999;270(1):25–28. doi:10.1016/S0304-3940(99)00450-4.
68. White FA, Wilson NM. Chemokines as pain mediators and modulators. *Current Opinion in Anaesthesiology*. 2008;21(5):580–585. doi:10.1097/ACO.0b013e32830eb69d.
69. Ji R-R, Berta T, Nedergaard M. Glia and pain: Is chronic pain a gliopathy? *Pain*. 2013;154(S1):S10–S28. doi:10.1016/j.pain.2013.06.022.
70. Ludwig H, Miguel JS, Dimopoulos MA, et al. International Myeloma Working Group recommendations for global myeloma care. *Leukemia*. 2013:1–12. doi:10.1038/leu.2013.293.
71. Wols HM. Plasma cells. In: *Encyclopedia of Life Sciences*. eLS; 2005. doi:10.1038/npg.els.0004030.
72. Cyster JG. Homing of antibody secreting cells. *Immunological Reviews*. 2003;194(1):48–60. doi:10.1034/j.1600-065X.2003.00041.x.
73. Surveillance, Epidemiology, and End Results Program. SEER Program Stat Fact Sheets: Myeloma. *seercancer.gov/statfacts/html/mulmyhtml*. 2014:1–26.
74. Martin NH. The immunoglobulins: a review. *J Clin Pathol*. 1969;22(2):117–131.
75. Raje N, Hideshima T, Anderson KC. Plasma Cell Tumors. In: *Cancer Medicine*. 8 ed. Shelton; 2010:1668–1684.
76. Rajkumar SV, Fonseca R, Lacy MQ, et al. Plasmablastic morphology is an independent predictor of poor survival after autologous stem-cell transplantation for multiple myeloma. *J Clin Oncol*. 1999;17(5):1551–1557.
77. Tricot G, Barlogie B, Jagannath S, et al. Poor prognosis in multiple myeloma is associated only with partial or complete deletions of chromosome 13 or abnormalities involving 11q and not with other karyotype abnormalities. *Blood*. 1995;86(11):4250–4256.
78. Durie-SalmonSS. 2010:1. Available at: <http://myeloma.org/pdfs/Durie-SalmonSS.pdf>.
79. International Staging System. 2008:1–2. Available at: [http://myeloma.org/pdfs/iss%20card2008\\_e3.pdf](http://myeloma.org/pdfs/iss%20card2008_e3.pdf).
80. Cavaletti G, Nobile-Orazio E. Bortezomib-induced peripheral neurotoxicity: still

- far from a painless gain. *Haematologica*. 2007;92(10):1308–1310. doi:10.3324/haematol.11752.
81. Richardson PG, Barlogie B, Berenson J, et al. A phase 2 study of bortezomib in relapsed, refractory myeloma. *N Engl J Med*. 2003;348(26):2609–2617. doi:10.1056/NEJMoa030288.
  82. Garber K. Taking Garbage In, Tossing Cancer Out? *Science*. 2002;295(5555):612–613. doi:10.1126/science.295.5555.612.
  83. Landowski TH, Megli CJ, Nullmeyer KD, Lynch RM, Dorr RT. Mitochondrial-Mediated Disregulation of Ca<sup>2+</sup> Is a Critical Determinant of Velcade (PS-341/Bortezomib) Cytotoxicity in Myeloma Cell Lines. *Cancer Research*. 2005;65(9):3828–3836. doi:10.1158/0008-5472.CAN-04-3684.
  84. Lonial S, Waller EK, Richardson PG, et al. Risk factors and kinetics of thrombocytopenia associated with bortezomib for relapsed, refractory multiple myeloma. *Blood*. 2005;106(12):3777–3784. doi:10.1182/blood-2005-03-1173.
  85. Richardson PG. Frequency, Characteristics, and Reversibility of Peripheral Neuropathy During Treatment of Advanced Multiple Myeloma With Bortezomib. *Journal of Clinical Oncology*. 2006;24(19):3113–3120. doi:10.1200/JCO.2005.04.7779.
  86. Richardson PG, Delforge M, Beksac M, et al. Management of treatment-emergent peripheral neuropathy in multiple myeloma. *Leukemia*. 2012;26(4):595–608. doi:10.1038/leu.2011.346.
  87. Mohty B, El-Cheikh J, Yakoub-Agha I, Moreau P, Harousseau JL, Mohty M. Peripheral neuropathy and new treatments for multiple myeloma: background and practical recommendations. *Haematologica*. 2010;95(2):311–319. doi:10.3324/haematol.2009.012674.
  88. Dimopoulos MA, Mateos M-V, Richardson PG, et al. Risk factors for, and reversibility of, peripheral neuropathy associated with bortezomib-melphalan-prednisone in newly diagnosed patients with multiple myeloma: subanalysis of the phase 3 VISTA study. *European Journal of Haematology*. 2010;86(1):23–31. doi:10.1111/j.1600-0609.2010.01533.x.
  89. Boyette-Davis JA, Cata JP, Zhang H, et al. Follow-Up Psychophysical Studies in Bortezomib-Related Chemoneuropathy Patients. *The Journal of Pain*. 2011;12(9):1017–1024. doi:10.1016/j.jpain.2011.04.008.
  90. Cavaletti G, Gilardini A, Canta A, et al. Bortezomib-induced peripheral neurotoxicity: A neurophysiological and pathological study in the rat. *Experimental Neurology*. 2007;204(1):317–325. doi:10.1016/j.expneurol.2006.11.010.
  91. Casafont I, Berciano MT, Lafarga M. Bortezomib induces the formation of nuclear poly(A) RNA granules enriched in Sam68 and PABPN1 in sensory

- ganglia neurons. *Neurotox Res.* 2010;17(2):167–178. doi:10.1007/s12640-009-9086-1.
92. Windebank AJ, Grisold W. Chemotherapy-induced neuropathy. *J Peripher Nerv Syst.* 2008;13(1):27–46. doi:10.1111/j.1529-8027.2008.00156.x.
93. Kyle RA, Rajkumar SV. Multiple myeloma. *N Engl J Med.* 2004;351(18):1860–1873. doi:10.1056/NEJMra041875.
94. Scott K, Kothari MJ. Evaluating the patient with peripheral nervous system complaints. *J Am Osteopath Assoc.* 2005;105(2):71–83.
95. Millennium Pharmaceuticals, Inc. Velcade Prescribing Information. 2012:1–31. Available at: [http://www.velcade.com/Files/PDFs/VELCADE\\_PRESCRIBING\\_INFORMATION.pdf](http://www.velcade.com/Files/PDFs/VELCADE_PRESCRIBING_INFORMATION.pdf). Accessed March 20, 2014.
96. Cavaletti G, Marmiroli P. Chemotherapy-induced peripheral neurotoxicity. *Nature Reviews Neurology.* 2010. doi:10.1038/nrneurol.2010.160.
97. Wickham R. Chemotherapy-Induced Peripheral Neuropathy: A Review and Implications for Oncology Nursing Practice. *Clinical Journal of Oncology Nursing.* 2007;11(3):361–376. doi:10.1188/07.CJON.361-376.
98. Postma TJ, Heimans JJ. Grading of chemotherapy-induced peripheral neuropathy. *Ann Oncol.* 2000;11(5):509–513.
99. Cornblath DR, Chaudhry V, Carter K, et al. Total neuropathy score: validation and reliability study. *Neurology.* 1999;53(8):1660–1664.
100. Maier C, Baron R, Tölle TR, et al. Quantitative sensory testing in the German Research Network on Neuropathic Pain (DFNS): Somatosensory abnormalities in 1236 patients with different neuropathic pain syndromes. *Pain.* 2010;150(3):439–450. doi:10.1016/j.pain.2010.05.002.
101. Talamo G, Farooq U, Zangari M, et al. Beyond the CRAB Symptoms: A Study of Presenting Clinical Manifestations of Multiple Myeloma. *Clinical Lymphoma, Myeloma & Leukemia.* 2011;10(6):464–468. doi:10.3816/CLML.2010.n.080.
102. Silverstein A, Doninger DE. Neurologic Complications of Myelomatosis. *Arch Neurol.* 1963;9(5):534–544. doi:10.1001/archneur.1963.00460110102011.
103. Silverstein A. Neurological complications of anticoagulation therapy: a neurologist's review. *Arch Intern Med.* 1979;139(2):217–220. doi:10.1001/archinte.1979.03630390069025.
104. Plasmati R, Pastorelli F, Cavo M, Petracci E. Neuropathy in multiple myeloma treated with thalidomide: a prospective study. *Neurology.* 2007.
105. Richardson PG, Xie W, Mitsiades C, et al. Single-Agent Bortezomib in



- Previously Untreated Multiple Myeloma: Efficacy, Characterization of Peripheral Neuropathy, and Molecular Correlations With Response and Neuropathy. *Journal of Clinical Oncology*. 2009;27(21):3518–3525. doi:10.1200/JCO.2008.18.3087.
106. Delforge M, Bladé J, Dimopoulos MA, Facon T. Treatment-related peripheral neuropathy in multiple myeloma: the challenge continues. *Lancet Oncol*. 2010. doi:10.1016/S1470-2045(10)70068-1.
  107. Vichaya EG, Wang XS, Boyette-Davis JA, et al. Subclinical pretreatment sensory deficits appear to predict the development of pain and numbness in patients with multiple myeloma undergoing chemotherapy. *Cancer Chemother Pharmacol*. 2013;71(6):1531–1540. doi:10.1007/s00280-013-2152-7.
  108. Herrmann DN, Boger JN, Jansen C, Alessi-Fox C. In vivo confocal microscopy of Meissner corpuscles as a measure of sensory neuropathy. *Neurology*. 2007;69(23):2121–2127. doi:10.1212/01.wnl.0000282762.34274.94.
  109. Cata JP, Weng H-R, Burton AW, Villareal H, Giralt S, Dougherty PM. Quantitative Sensory Findings in Patients With Bortezomib-Induced Pain. *The Journal of Pain*. 2007;8(4):296–306. doi:10.1016/j.jpain.2006.09.014.
  110. Lee MWL, McPhee RW, Stringer MD. An evidence-based approach to human dermatomes. *Clin Anat*. 2008;21(5):363–373. doi:10.1002/ca.20636.
  111. Kennedy WR, Selim MM, Brink TS, et al. A new device to quantify tactile sensation in neuropathy. *Neurology*. 2011;76(19):1642–1649. doi:10.1212/WNL.0b013e318219fadd.
  112. Ruff RM, Parker SB. Gender- and age-specific changes in motor speed and eye-hand coordination in adults: normative values for the Finger Tapping and Grooved Pegboard Tests. *Percept Mot Skills*. 1993;76(3 Pt 2):1219–1230.
  113. Fuchs PN, Campbell JN, Meyer RA. Secondary hyperalgesia persists in capsaicin desensitized skin. *Pain*. 2000;84(2-3):141–149.
  114. Frustorfer H, Lindblom U, Schmidt WG. Method for quantitative estimation of thermal threshold in patients. *Journal of Neurology, Neurosurgery, and Psychiatry*. 1976;39:1071–1075.
  115. Cata JP, Cordella JV, Burton AW, Hassenbusch SJ, Weng H-R, Dougherty PM. Spinal cord stimulation relieves chemotherapy-induced pain: a clinical case report. *Journal of Pain and Symptom Management*. 2004;27(1):72–78. doi:10.1016/j.jpainsymman.2003.05.007.
  116. Dougherty PM, Cata JP, Cordella JV, Burton A, Weng H-R. Taxol-induced sensory disturbance is characterized by preferential impairment of myelinated fiber function in cancer patients. *Pain*. 2004;109(1-2):132–142. doi:10.1016/j.pain.2004.01.021.

117. Voorhees PM, Dees EC, O'Neil B, Orlowski RZ. The proteasome as a target for cancer therapy. *Clin Cancer Res.* 2003;9(17):6316–6325.
118. Fruhstorfer H, Zenz M, Nolte H, Hensel H. Dissociated loss of cold and warm sensibility during regional anaesthesia. *Pflugers Arch.* 1974;349(1):73–82. doi:10.1007/BF00587918.
119. Konietzny F, Hensel H. Warm fiber activity in human skin nerves. *Pflugers Arch.* 1975;359(3):265–267. doi:10.1007/BF00587384.
120. Torebjörk HE. Afferent G Units Responding to Mechanical, Thermal and Chemical Stimuli in Human Non-Glabrous Skin. *Acta Physiologica Scandinavica.* 1974;92(3):374–390. doi:10.1111/j.1748-1716.1974.tb05755.x.
121. Silberman J, Lonial S. Review of peripheral neuropathy in plasma cell disorders. *Hematol Oncol.* 2008;26(2):55–65. doi:10.1002/hon.845.
122. Richardson PG, Laubach JP, Schlossman RL, Mitsiades C, Anderson K. Complications of Multiple Myeloma Therapy, Part 1: Risk Reduction and Management of Peripheral Neuropathy and Asthenia. *J Natl Compr Canc Netw.* 2010;8(Suppl 1):S–4–S–12.
123. Sonneveld P, Jongen JLM. Dealing with neuropathy in plasma-cell dyscrasias. *Hematology Am Soc Hematol Educ Program.* 2010;2010(1):423–430. doi:10.1182/asheducation-2010.1.423.
124. Palumbo A, Anderson K. Multiple myeloma. *N Engl J Med.* 2011;364(11):1046–1060. doi:10.1056/NEJMra1011442.
125. Bolton CF, Winkelmann RK, Dyck PJ. A quantitative study of Meissner's corpuscles in man. *Trans Am Neurol Assoc.* 1964;89:190–192.
126. Bolton CF, Winkelmann RK, Dyck PJ. *A quantitative study of Meissner's corpuscles in man.* Neurology; 1966.
127. Denier C, Lozeron P, Adams D, et al. Multifocal neuropathy due to plasma cell infiltration of peripheral nerves in multiple myeloma. *Neurology.* 2006;66(6):917–918. doi:10.1212/01.wnl.0000203345.29020.db.
128. Sanchorawala V. Light-Chain (AL) Amyloidosis: Diagnosis and Treatment. *Clinical Journal of the American Society of Nephrology.* 2006;1(6):1331–1341. doi:10.2215/CJN.02740806.
129. Hsu HL, Liu KL. Osteosclerotic myeloma with POEMS syndrome. *QJM.* 2010;103(12):993–994. doi:10.1093/qjmed/hcp183.
130. Dispenzieri A, Kyle RA, Lacy MQ, et al. POEMS syndrome: definitions and long-term outcome. *Blood.* 2003;101(7):2496–2506. doi:10.1182/blood-2002-07-2299.

131. Nakayama-Ichihama S, Yokote T, Hirata Y, et al. Multiple cytokine-producing plasmablastic solitary plasmacytoma of bone with polyneuropathy, organomegaly, endocrinology, monoclonal protein, and skin changes syndrome. *Journal of Clinical Oncology*. 2012;30(7):e91–4. doi:10.1200/JCO.2011.38.9288.
132. Kuku I, Bayraktar MR, Kaya E, et al. Serum Proinflammatory Mediators at Different Periods of Therapy in Patients With Multiple Myeloma. *Mediators of Inflammation*. 2005;2005(3):171–174. doi:10.1155/MI.2005.171.
133. Tsirakis G, Pappa CA, Kaparou M, et al. Assessment of proliferating cell nuclear antigen and its relationship with proinflammatory cytokines and parameters of disease activity in multiple myeloma patients. *Eur J Histochem*. 2011;55(3):e21. doi:10.4081/ejh.2011.e21.
134. Schäfers M, Sorkin LS, Geis C, Shubayev VI. Spinal nerve ligation induces transient upregulation of tumor necrosis factor receptors 1 and 2 in injured and adjacent uninjured dorsal root ganglia in the rat. *Neuroscience Letters*. 2003;347(3):179–182. doi:10.1016/S0304-3940(03)00695-5.
135. Schäfers M, Sorkin LS, Sommer C. Intramuscular injection of tumor necrosis factor-alpha induces muscle hyperalgesia in rats. *Pain*. 2003;104(3):579–588. doi:10.1016/S0304-3959(03)00115-5.
136. Verri WA Jr., Cunha TM, Parada CA, Poole S, Cunha FQ, Ferreira SH. Hypernociceptive role of cytokines and chemokines: Targets for analgesic drug development? *Pharmacology & Therapeutics*. 2006;112(1):116–138. doi:10.1016/j.pharmthera.2006.04.001.
137. Woolf CJ, Allchorne A, Safieh-Garabedian B, Poole S. Cytokines, nerve growth factor and inflammatory hyperalgesia: the contribution of tumour necrosis factor alpha. *Br J Pharmacol*. 1997;121(3):417–424. doi:10.1038/sj.bjp.0701148.
138. Cui JG, Holmin S, Mathiesen T, Meyerson BA, Linderöth B. Possible role of inflammatory mediators in tactile hypersensitivity in rat models of mononeuropathy. *Pain*. 2000;88(3):239–248.
139. Okamoto K, Martin DP, Schmelzer JD, Mitsui Y, Low PA. Pro- and Anti-inflammatory Cytokine Gene Expression in Rat Sciatic Nerve Chronic Constriction Injury Model of Neuropathic Pain. *Experimental Neurology*. 2001;169(2):386–391. doi:10.1006/exnr.2001.7677.
140. Shubayev VI, Myers RR. Upregulation and interaction of TNFalpha and gelatinases A and B in painful peripheral nerve injury. *Brain Res*. 2000;855(1):83–89.
141. Sommer C, Lindenlaub T, Teuteberg P, Schäfers M, Hartung T, Toyka KV. Anti-TNF-neutralizing antibodies reduce pain-related behavior in two different

- mouse models of painful mononeuropathy. *Brain Res.* 2001;913(1):86–89.
142. Sommer C, Marziniak M, Myers RR. The effect of thalidomide treatment on vascular pathology and hyperalgesia caused by chronic constriction injury of rat nerve. *Pain.* 1998;74(1):83–91. doi:10.1016/S0304-3959(97)00154-1.
  143. Sommer C, Schäfers M, Marziniak M, Toyka KV. Etanercept reduces hyperalgesia in experimental painful neuropathy. *J Peripher Nerv Syst.* 2001;6(2):67–72.
  144. Sommer C, Schmidt C, George A. Hyperalgesia in experimental neuropathy is dependent on the TNF receptor 1. *Experimental Neurology.* 1998;151(1):138–142. doi:10.1006/exnr.1998.6797.
  145. Sorkin LS, Doom CM. Epineurial application of TNF elicits an acute mechanical hyperalgesia in the awake rat. *J Peripher Nerv Syst.* 2000;5(2):96–100. doi:10.1046/j.1529-8027.2000.00012.x.
  146. Junger H, Sorkin LS. Nociceptive and inflammatory effects of subcutaneous TNF  $\alpha$ . *Pain.* 2000;85(1-2):145–151. doi:10.1016/S0304-3959(99)00262-6.
  147. Oprée A, Kress M. Involvement of the proinflammatory cytokines tumor necrosis factor- $\alpha$ , IL-1  $\beta$ , and IL-6 but not IL-8 in the development of heat hyperalgesia: effects on heat-evoked calcitonin gene-related peptide release from rat skin. *J Neurosci.* 2000;20(16):6289–6293.
  148. Schäfers M, Lee DH, Brors D, Yaksh TL, Sorkin LS. Increased sensitivity of injured and adjacent uninjured rat primary sensory neurons to exogenous tumor necrosis factor- $\alpha$  after spinal nerve ligation. *Journal of Neuroscience.* 2003;23(7):3028–3038.
  149. Jin S-X, Zhuang Z-Y, Woolf CJ, Ji R-R. p38 Mitogen-Activated Protein Kinase Is Activated after a Spinal Nerve Ligation in Spinal Cord Microglia and Dorsal Root Ganglion Neurons and Contributes to the Generation of Neuropathic Pain. *Journal of Neuroscience.* 2003;23(10):4017–4022.
  150. Eliav E, Benoliel R, Herzberg U, Kalladka M, Tal M. The role of IL-6 and IL-1 $\beta$  in painful perineural inflammatory neuritis. *Brain Behavior and Immunity.* 2009;23(4):474–484. doi:10.1016/j.bbi.2009.01.012.
  151. Kelly JJ, Kyle RA, Miles JM, O'Brien PC, Dyck PJ. The spectrum of peripheral neuropathy in myeloma. *Neurology.* 1981;31(1):24–31.
  152. Ropper AH, Gorson KC. Neuropathies associated with paraproteinemia. *New England Journal of Medicine.* 1998;338(22):1601–1607. doi:10.1056/NEJM199805283382207.
  153. Boyette-Davis JA, Eng C, Wang XS, et al. Subclinical Peripheral Neuropathy Is a Common Finding in Colorectal Cancer Patients Prior to Chemotherapy. *Clinical Cancer Research.* 2012;18(11):3180–3187. doi:10.1158/1078-

0432.CCR-12-0205.

154. Cianfrocca M, Flatters SJL, Bennett GJ, et al. Peripheral neuropathy in a woman with breast cancer. *J Pain*. 2006;7(1):2–10. doi:10.1016/j.jpain.2005.10.001.
155. Garrido-Mesa N, Zarzuelo A, Gálvez J. Minocycline: far beyond an antibiotic. *Br J Pharmacol*. 2013;169(2):337–352. doi:10.1111/bph.12139.
156. Agwuh KN, MacGowan A. Pharmacokinetics and pharmacodynamics of the tetracyclines including glycylicyclines. *J Antimicrob Chemother*. 2006;58(2):256–265. doi:10.1093/jac/dkl224.
157. Plane JM, Shen Y, Pleasure DE, Deng W. Prospects for Minocycline Neuroprotection. *Arch Neurol*. 2010;67(12). doi:10.1001/archneurol.2010.191.
158. Metz LM, Zhang Y, Yeung M, et al. Minocycline reduces gadolinium-enhancing magnetic resonance imaging lesions in multiple sclerosis. *Ann Neurol*. 2004;55(5):756–756. doi:10.1002/ana.20111.
159. Zhang Y, Metz LM, Yong VW, et al. Pilot study of minocycline in relapsing-remitting multiple sclerosis. *Can J Neurol Sci*. 2008;35(2):185–191.
160. Casha S, Zygun D, McGowan MD, Bains I, Yong VW, John Hurlbert R. Results of a phase II placebo-controlled randomized trial of minocycline in acute spinal cord injury. *Brain*. 2012;135(Pt 4):1224–1236. doi:10.1093/brain/aws072.
161. Mei X-P, Xu H, Xie C, et al. Neuroscience Research. *Neuroscience Research*. 2011;70(3):305–312. doi:10.1016/j.neures.2011.03.012.
162. Boyette-Davis J, Dougherty PM. Protection against oxaliplatin-induced mechanical hyperalgesia and intraepidermal nerve fiber loss by minocycline. *Experimental Neurology*. 2011;229(2):353–357. doi:10.1016/j.expneurol.2011.02.019.
163. Boyette-Davis J, Xin W, Zhang H, Dougherty PM. Intraepidermal nerve fiber loss corresponds to the development of Taxol-induced hyperalgesia and can be prevented by treatment with minocycline. *Pain*. 2011;152(2):308–313. doi:10.1016/j.pain.2010.10.030.
164. Palanca A, Casafont I, Berciano MT, Lafarga M. Reactive nucleolar and Cajal body responses to proteasome inhibition in sensory ganglion neurons. *BBA - Molecular Basis of Disease*. 2014;1842(6):848–859. doi:10.1016/j.bbadis.2013.11.016.
165. Badros A, Goloubeva O, Dalal JS, et al. Neurotoxicity of bortezomib therapy in multiple myeloma: A single-center experience and review of the literature. *Cancer*. 2007;110(5):1042–1049. doi:10.1002/cncr.22921.
166. Investigators NN-P. A pilot clinical trial of creatine and minocycline in early

- Parkinson disease: 18-month results. *Clinical Neuropharmacology*. 2008. doi:10.1097/WNF.0b013e3181342f32.
167. Pradat P-F, Delanian S. Peripheral Nerve Disorders. In: *Handbook of Clinical Neurology*. Vol 115 (3rd series). Late radiation injury to peripheral nerves. Elsevier B.V.; 2013:743–758. doi:10.1016/b978-0-444-52902-2.00043-6.
  168. Shaffer SW, Harrison AL. Aging of the somatosensory system: a translational perspective. *Physical Therapy*. 2007;87(2):193–207. doi:10.2522/ptj.20060083.
  169. Cleeland CS, Farrar JT, Hausheer FH. Assessment of cancer-related neuropathy and neuropathic pain. *The Oncologist*. 2010;15 Suppl 2(Supplement 2):13–18. doi:10.1634/theoncologist.2009-S501.
  170. Raghavendra V. Inhibition of Microglial Activation Attenuates the Development but Not Existing Hypersensitivity in a Rat Model of Neuropathy. *Journal of Pharmacology and Experimental Therapeutics*. 2003;306(2):624–630. doi:10.1124/jpet.103.052407.
  171. Zhang H, Yoon S-Y, Zhang H, Dougherty PM. Evidence That Spinal Astrocytes but Not Microglia Contribute to the Pathogenesis of Paclitaxel-Induced Painful Neuropathy. *The Journal of Pain*. 2012;13(3):293–303. doi:10.1016/j.jpain.2011.12.002.
  172. Argyriou AA, Iconomou G, Kalofonos HP. Bortezomib-induced peripheral neuropathy in multiple myeloma: a comprehensive review of the literature. *Blood*. 2008;112(5):1593–1599. doi:10.1182/blood-2008-04-149385.
  173. Dispenzieri A, Kyle RA. Neurological aspects of multiple myeloma and related disorders. *Best Practice & Research Clinical Haematology*. 2005;18(4):673–688. doi:10.1016/j.beha.2005.01.024.
  174. Simmons Z. Paraproteinemia and neuropathy. *Current Opinion in Neurology*. 1999;12(5):589–595.
  175. Schneider SP, Perl ER. Comparison of primary afferent and glutamate excitation of neurons in the mammalian spinal dorsal horn. *J Neurosci*. 1988;8(6):2062–2073.
  176. Holzer P. Neurogenic vasodilatation and plasma leakage in the skin. *Gen Pharmacol*. 1998;30(1):5–11. doi:10.1016/S0306-3623(97)00078-5.
  177. Schmelz M, Michael K, Weidner C, Schmidt R, orebjörk HE, Handwerker HO. Which nerve fibers mediate the axon reflex flare in human skin? *NeuroReport*. 2000;11(3):645.
  178. Millan MJ. Descending control of pain. *Prog Neurobiol*. 2002;66(6):355–474. doi:10.1016/S0301-0082(02)00009-6.
  179. Tavee J, Zhou L. Small fiber neuropathy: A burning problem. *Cleveland Clinic*

*Journal of Medicine*. 2009;76(5):297–305. doi:10.3949/ccjm.76a.08070.

180. Abbadie C, Lindia JA, Cumiskey AM, et al. Impaired neuropathic pain responses in mice lacking the chemokine receptor CCR2. *Proc Natl Acad Sci USA*. 2003;100(13):7947–7952. doi:10.1073/pnas.1331358100.
181. Zhang H, Boyette-Davis JA, Kosturakis AK, et al. Induction of Monocyte Chemoattractant Protein-1 (MCP-1) and Its Receptor CCR2 in Primary Sensory Neurons Contributes to Paclitaxel-Induced Peripheral Neuropathy. *The Journal of Pain*. 2013:1–14. doi:10.1016/j.jpain.2013.03.012.
182. Shields SD, Eckert WA, Basbaum AI. Spared nerve injury model of neuropathic pain in the mouse: a behavioral and anatomic analysis. *J Pain*. 2003;4(8):465–470. doi:10.1016/S1526-5900(03)00781-8.

## **Vita**

Alyssa Kosturakis was born in Houston, Texas on January 24, 1988, to Irene Kosturakis and Robert Rodriguez. After completing her work at the John Cooper High School, The Woodlands, TX in 2006 she entered the University of Pennsylvania, Philadelphia, PA. She received the degree of Bachelor of Arts with a major in the Biological Basis of Behavior and a minor in Spanish in May 2010. For the next 2 years she worked as a Research Assistant in the Department of Anesthesiology and Critical Care at the UT MD Anderson Cancer Center. In September 2012 she entered the University of Texas Graduate School of Biomedical Sciences.

Permanent Address:

2114 Park Street

Houston, TX 77019